Scuola Internazionale Superiore di Studi Avanzati - Trieste

SISSA, International School for Advanced Studies

PhD course in Statistical Physics

Academic Year 2012/2013

Pre-Thermalization in Quantum Spin Chains

Thesis submitted for the degree of

Doctor Philosophiae

Supervisor:

Dr. Alessandro Silva

Candidate:

Jamir Marino

October 30th, 2013

SISSA - Via Bonomea 265 - 34136 TRIESTE - ITALY

SISSA, International School for Advanced Studies

PhD course in Statistical Physics

Academic Year 2012/2013

Pre-Thermalization in Quantum Spin Chains

Thesis submitted for the degree of

Doctor Philosophiae

Supervisor:

Dr.Alessandro Silva

Candidate:

Jamir Marino

October 30th, 2013

All you need in this life is ignorance and confidence; then success is sure.

Mark Twain

Acknowledgements

First of all I would like to thank my parents for their lovely, human and generous support during this experience in Trieste.

I would like to express my gratitude to Matteo Marcuzzi for having shared with me the daily challenges of quantum quenches with unprecedented patience and toughness.

I am also glad to mention in this section Andrea Gambassi for all the time he spent listening to my speculations and '*rowdy*' arguments.

A special thank is for the SISSA Director, Guido Marintelli, for the years together in the Govering Board of SISSA. He taught me how to handle with people which is a special gift for a physicist.

It is really difficult to summarize here my gratitude towards my advisor, Alessandro Silva. He taught me how to see physics behind each single equation and how to overcome my limits, he shared with me his own personal way to look at physics and to do this job. I will be forever indebted with him.

My last word is to Gaia, who taught me to live.

Contents

Chapter 1

Introduction

1.1 Non-Equilibrium Dynamics of Quantum Many Body systems

Since the experiment of Kinoshita *et al.* [1] in 2006, where the lack of thermalization in a 1D Bose gas was clearly observed, the interest in non-equilibrium dynamics of closed interacting quantum many body systems exploded in the community of condensed matter physics. The impressive progress in realizing experimental realizations of isolated, tunable quantum many body systems with cold gases changed completely the way in which theory and experiments look at each other. Prototypical models of theoretical physics, which provided in the last fifty years an effective low energy description of quantum many body systems, are today realizable in experiments with cold atoms. The Hubbard, Bose-Hubbard, Luttinger, Kondo, Ising model and many others today are not anymore just textbooks hamiltonians but represent the experimental playground to test many theoretical issues in a field essentially unexplored: quantum non-equilibrium dynamics. The possibility of realizing isolated quantum systems decoupled from any source of decoherence, dissipation and interaction with the environment calls for a theoretical investigation of quantum ergodicity, quantum thermalization and the mechanisms behind relaxation, when the only driving force is quantum unitary dynamics.

Despite the countless number of possibilities for driving a system out-of-equilibrium, the interest in the last few years focused on a class of physically interesting protocols, the so called *quantum quenches*, which consist in preparing the system in the ground state of a given hamiltonian and to sudden change an internal parameter initiating the out-of-equilibrium dynamics. Quantum quenches can be both studied theoretically and easily realized in laboratory, displaying very rich physics, such as the interplay between dimensionality, integrability and thermalization or the emergence of long-lived non-equilibrium quasi-stationary states, or the out-of-equilibrium dynamics

arising from quenches between two quantum phases. Moreover, the tantalizing possibility to study non-equilibrium dynamics generalizing the broad range of tools, used for equilibrium physics, such as mean-field theory or the renormalization group, is attracting the interest of many physicists in the broad area of condensed matter and statistical physics.

The first studies of quantum quenches focused on the properties attained by the asymptotic states attained at long times after a quench. If, on one hand, the naive expectation that generic quantum many body systems thermalize at long time scales, has been confirmed by a series of pioneering works in the field (see [2] for a review on the subject), on the other hand, the mechanism behind quantum thermalization remains unknown, and a heated debate on the origin of such quantum thermal behavior and on quatum ergodicity, quantum chaos and their relationships with the corresponding classical behavior, literally exploded. A notable exception are integrable quantum many body systems, where the existence of many conserved charges highly constrains the scattering processes which are expected to redistribute the energy among the elementary degrees of freedom and to cause thermalization; indeed, in this case the system approaches an asymptotic non-thermal steady state which bears strong memory of the initial state, the so called Generalized Gibbs Ensemble (GGE). This is, roughly speaking, a sort of grandcanonical ensemble accounting for all the conserved quantities of the theory. The GGE has been tested and verified both numerically and analytically in a very broad class of models and protocols [2].

The GGE and the thermal state usually are looked at as two mutual exclusive possibilities. However in 2011, a new ground-breaking experiment [3] changed the way in which people looked at the GGE and the thermal state. J. Schmiedmayer's group, in Vienna, investigated experimentally the out-of-equilibrium dynamics of a coherent splitted one dimensional Bose gas, finding clear evidence that for long intermediate times the system approaches a non-thermal metastable state well described by a Generalized Gibbs ensemble based on a Luttinger model. Only at later times, the system departs from the pre-thermal state possibly towards true thermal equilibrium. This phenomenology was already encountered ten years ago in the theoretical study of non-equilibrium quantum field theories and discussed under the name of *pre-thermalization* [4]. This experiment revived the interest of theoretical physicists who developed a modern way to look at thermalization dynamics in integrable models. A weakly non-integrable quantum many body system driven away from equilibrium will first approach an intermediate quasi-steady state described by a GGE, built perturbatively starting from the non-integrable hamiltonian, and only for longer times, when perturbation theory breaks down and inelastic scattering processes become leading in the dynamics of the system, a thermal behaviour will possibly occur [5].

Pre-thermalization is the first step towards an unified description of out-of-equilibrium dynamics, which aims at merging together our current understanding of relaxation dynamics in integrable and non-integrable systems. This PhD Thesis is devoted to deepen our physical comprehension and physical intuition on pre-thermalization dynamics in quantum many body systems.

1.2 Thesis Abstract

The results presented in this PhD Thesis aim at understanding thermalization dynamics and, strictly speaking, pre-thermalization in both open and closed quantum spin chains driven out-of-equilibrium. In order to make analytical progress, we consider perturbations of the Quantum Ising Chain (QIC), one of the simplest integrable models, whose non-equilibrium dynamics has been studied in great details in the last few years. In Chapter 2 we introduce for the non-technical reader the main recent ideas behind quantum thermalization and relaxation in integrable and non-integrable quantum many body systems, while Chapter 3 contains an introduction to the current understanding of pre-thermalization.

In Chapter 4 we start our study considering a QIC perturbed by a time-dependent noise in the direction of the transverse magnetic field [6] [7]. We generalize the concept of pre-thermalization to a noisy quantum many body system driven away from equilibrium simultaneously by a quantum quench of the transverse field and by the noise, highlighting the mechanism behind pre-thermalization and the subsequent relaxation towards the thermal state in a wide class of physically relevant observables. Our main achievement is to show that pre-thermalization occurs quite generally up to time scales where the noise is dominated by the non-equilibrium dynamics induced by the quench of the transverse field, while for longer times pre-thermal plateaux disappear and the noise leaves different signatures in different observables.

In Chapter 5 we consider the more challenging problem of pre-thermalizat--ion in a closed non-integrable quantum spin chain [8]. We show using a mapping of a weakly non-integrable spin chain into a hard core boson model, that pre-thermalization is successfully captured by a low-density description of the theory, which results in a integrable, bosonic model, that constitutes an excellent description for the out-of-equilibrium dynamics up to intermediate time scales. On the other hand, in order to investigate the late time dynamics we resort to a diagrammatic approach, which serves for a two-fold scope. First, we focus on the effect of the leading inelastic processes, realizing that they constitute only a sub-leading correction to the pre-thermal

plateau, found within the effective low-energy description; and secondly, we show from a Quantum Boltzmann equation perspective how inelastic processes are the fundamental ingredient in order to have thermalization in the late time dynamics.

The main technical tool used to derive the results in Chapter 4 and 5 is the Keldysh contour technique which is reviewed in the Appendix.

This PhD Thesis is based on the following works:

- J. Marino, A. Silva, Relaxation, pre-thermalization and diffusion in a noisy Quantum Ising Chain, Phys. Rev. B 86, 060408 (*Rapid Communications*) (2012).
- M. Marcuzzi, J. Marino, A. Gambassi, A. Silva, Pre-thermalization in a non-integrable quantum spin chain after a quench, arXiv:1307.3738 (2013) (submitted to Phys. Rev. Lett.).
- J. Marino, A. Silva, Non-Equilibrium Dynamics of a Noisy Quantum Ising Chain: statistics of the work and prethermalization after a sudden quench of the transverse field, arXiv:1309.7595 (2013) (submitted to Phys. Rev. B).

Chapter 2

Quenches and Thermalization

In this chapter we introduce in a non-technical fashion the physics of the simplest protocol to study non-equilibrium dynamics of quantum many body systems, the *quantum quench*, and we discuss the definition of equilibration for a closed interacting quantum system. After a comprehensive summary of groundbreaking experiments which in the last decade renewed the interest in out-of-equilibrium dynamics of quantum many body systems, we review the most popular proposals for the mechanism behind quantum thermalization. In the last part of the chapter, we address, in particular, the case of relaxation dynamics in integrable models, highlighting, in particular, the quench dynamics of the Transverse Field Quantum Ising Chain (QIC), which constitutes the playground for our theoretical studies of *pre-thermalization* in this PhD Thesis.

2.1 Quantum Quenches

As we stressed in the Introduction, quantum gases can exhibit an unprecedented degree of isolation from dissipation and environmental decoherence. Therefore, to a very good approximation, their dynamics is unitary and quantum many body coherence is preserved during the time scales of the experiments. This remarkable fact stimulated the focus in out-of-equilibrium dynamics of *closed* quantum many body systems. The simplest protocol in this context is the so called *quantum quench*, which consists in preparing the system in the ground state of a quantum many body hamiltonian $H(g_0)$, characterized by an internal parameter g_0, and suddenly switch this parameter to a different value $g_0 \to g$, letting the system evolve under the new Hamiltonian $H(g)$. The ground state of the *pre-quench* Hamiltonian, $|\psi_0^{g_0}\rangle$, is in general not an eigenstate of the new Hamiltonian, and it will have a finite overlap with all the new eigenstates ($|\psi_n^g\rangle$), making the subsequent quantum evolution in general not trivial (see Fig. 2.1).

Quantum quenches became very popular in the last decade for the broad range of possibilities they allow to explore; for instance, one may study the

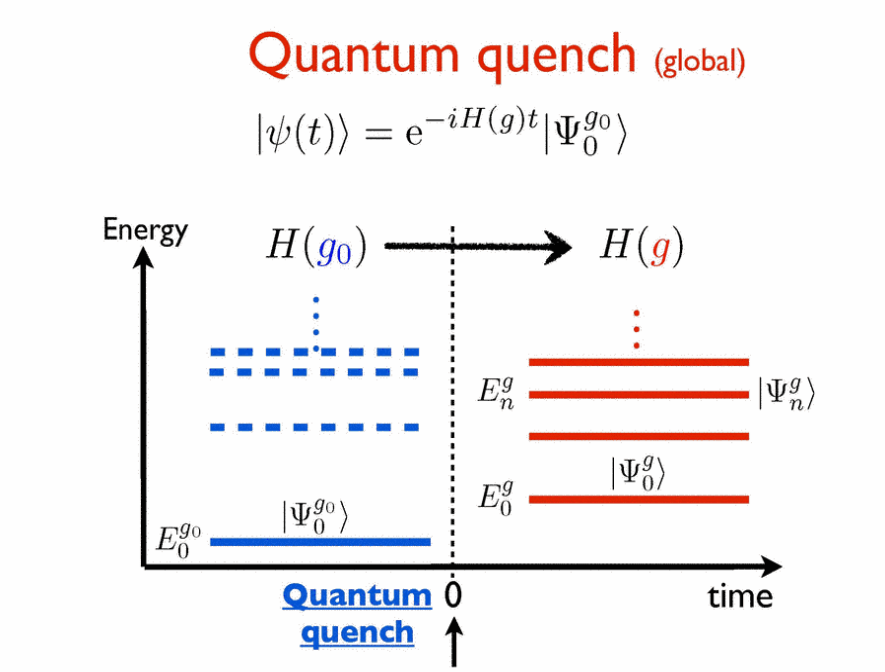

Figure 2.1: A schematic representation of the Hilbert space before and after a quantum quench of the control parameter g. [Courtesy of A. Gambassi]

abrupt change of a control parameter across quantum phase transitions or the sudden switching on of interactions, quenches can affect only a small subregion of the system (local quenches) or the whole system (global quenches), moreover, they can be easily reproduced in cold atoms experiments, allowing for a natural merging between theoretical and experimental studies.

Before reviewing the impressive experimental progress of the last ten years in manipulating and controlling quantum gases, and consequently to explore the out of equilibrium dynamics of quantum many body systems, let us first clarify in which sense a quantum system can relax and - if the case - thermalize.

2.2 Quantum Thermalization

The underlying concept behind classical thermalization is *ergodicity*, which requires equivalence between the phase space average and the time average for every almost initial condition of the dynamics, with fixed energy E.

Generalizing the notion of ergodicity to the quantum realm is hard as it was realized in the early days of quantum mechanics [9]. Let us see how a trivial attempt in doing so would fail. Consider an Hamiltonian with eigenstates $|\psi_\alpha\rangle$ and energies E_α and let us organize the spectrum on energy shells of width δE, sufficiently large to contain many states but small on macroscopic scales and let us denote the set of eigenstates of the hamiltonian lying in the energy window $(E,\, E+\delta E)$ by $\mathcal{H}(E)$. A natural definition of microcanonical density matrix in this case would be

$$\rho_{mic}(E) = \sum_{\alpha\in\mathcal{H}(E)} \frac{1}{\mathcal{N}} |\psi_\alpha\rangle\langle\psi_\alpha|, \tag{2.1}$$

where $\mathcal{N}$ is the total number of eigenstates in the microcanonical shell above defined. In order to fullfill the ergodicity requirement, we should ask whether, for a generic initial condition made out of states in a microcanonical shell $|\psi_0\rangle = \sum_{\alpha\in\mathcal{H}(E)} c_\alpha |\psi_\alpha\rangle$, the long-time average of the density matrix of the system will equal the microcanonical density matrix. It is immediate to realize that the time average

$$\overline{|\psi(t)\rangle\langle\psi(t)|} = \sum_\alpha |c_\alpha|^2 |\psi_\alpha\rangle\langle\psi_\alpha| \tag{2.2}$$

can be equal to the microcanonical average (2.1) only if $|c_\alpha|^2 = 1/\mathcal{N}$, which is a very special condition, satisfied by a very restricted class of initial states.

Another simple argument, showing how a naive approach to quantum thermalization is not enough to fully understand the problem, consists in recalling the basic fact that the trace of the density matrix is constant during unitary quantum evolution, hence, starting from a pure state, the system will remain pure during the whole dynamics, $Tr(\rho(t)^2) = 1$ for all times t. On the other hand, if thermalization is expected to occur, the systems should relax towards a Gibbs thermal ensemble $\rho_{can}(T)$, characterized by a temperature T, determined according to conservation of energy, but such ensemble is a mixed state $Tr(\rho_{can}(T)^2) < 1$. In other words, imagine to prepare the system in the ground state $|\psi_0\rangle$ of a given hamiltonian H_0 and to sudden switch the hamiltonian into a new one H and let evolve the system, $|\psi(t)\rangle = \exp(-iHt)|\psi_0\rangle$. As we said before the system is in a pure state and it will never approach neither the Gibbs ensemble neither any other asymptotic stationary state, described by a mixed state. This can be easily realized considering a simple example, which consists in studying the evolution of the hermitian operators

$$O^{(m,n)} = |n\rangle\langle m| + |m\rangle\langle n| \tag{2.3}$$

built using the eigenstates $|m\rangle$ and $|n\rangle$ with energies E_m and E_n of the post-quench hamiltonian, H. The time-dependent expectation value

$$\langle\psi_t|O^{(m,n)}|\psi_t\rangle = \langle\psi_0|n\rangle\langle m|\psi_0\rangle e^{i(E_n-E_m)t} + h.c \tag{2.4}$$

is oscillating in time and will never become stationary.

These simple but important facts lead us to consider a more precise definition of thermalization for quantum systems, which requires to focus on reduced density matrices of a subsystem and local observables therein defined [10], instead on quantum states.

Generally speaking, physical properties of quantum many body systems are accessed through the experimental measurement of local observables, hence an intuitive definition of thermalization would require to focus on local properties of a given system in the thermodynamic limit, or, in other words, to ask questions about thermalization only for observables defined in a finite subsystem A. The crucial point in looking at a given subsystem A is that the complement $\overline{A}$ can act as an effective bath and consequently the reduced density matrix of A can be described by a mixed state. Given the density matrix of the total system $\rho(t) = |\psi_t\rangle\langle\psi_t|$, the reduced density matrix of A can be easily defined as

$$\rho_A(t) = Tr_{\overline{A}}[\rho(t)]. \tag{2.5}$$

In this framework, the question about thermalization of quantum many body systems can be rephrased in these terms, asking whether for any finite subsystem A

$$\lim_{t\to\infty} \rho_A(t) =^{?} \rho_{stat,A} \equiv Tr_{\overline{A}}[\rho_{stat}], \tag{2.6}$$

i.e. whether the long time limit of the reduced density matrix will approach in the thermodynamic limit a time independent reduced density matrix defined by the last equality of (2.6); Eq. (2.6) implies that for any local observable O_A, the asymptotic expectation value can be predicted by ρ_{stat}

$$\lim_{t\to\infty} \langle\psi_t|O_A|\psi_t\rangle = Tr[\rho_{stat}O_A]. \tag{2.7}$$

In this sense it is meaningfull to say that a quantum many body system driven out of equilibrium relaxes to a stationary distribution, given by the density matrix ρ_{stat}.

The common and naive expectation that generic quantum many body systems relax towards a canonical Gibbs ensemble can be violated in some notable cases; for instance, when integrability plays a major role, the existence of many local integrals of motion I_n prevents relaxation towards the thermal state, because an infinite amount of information about the initial state is retained. Since the expectation values of the integrals of motion over the initial state, $\langle\psi_0|I_n|\psi_0\rangle$, is conserved during the dynamics. In this case the density matrix of the entire system is expected to be in the form of the so called Generalized Gibbs Ensemble (GGE) [11]

$$\rho_{stat} = \rho_{GGE} = \frac{1}{Z} e^{-\sum_n \lambda_n I_n} \tag{2.8}$$

where $Z = Tr[e^{-\sum_n \lambda_n I_n}]$ is a generalized partition function, and I_n are the local conserved quantities of the integrable model, i.e. local operators

satisfying

$$[I_n, I_m] = 0 = [I_n, H]. \tag{2.9}$$

The Lagrange multipliers are fixed by the requirements

$$\langle \psi_0 | I_n | \psi_0 \rangle = Tr[\rho_{GGE} I_n], \tag{2.10}$$

which account for the fact that the asymptotic steady state store an infinite amount of information about the initial state. It is worthwhile to stress at this point that the only assumption behind the GGE is the standard prescription of statistical mechanics, requiring to maximize the many body entropy subject to the constraints of the integrals of motion [12]. More about the choice of the integrals of motion in (2.8) and the predictive power of the GGE will come in a subsequent paragraph; let us now turn our attention to the fascinating issue of the recent experimental progress in realizing in laboratories the relaxation dynamics discussed in these first few paragraphs.

2.3 Thermalization and Dynamics in the Laboratory

The theoretical interest in studying non-equilibrium dynamics of quantum many body systems is mainly due to the recent outburst in the experimental realization and manipulation of quantum many body hamiltonians with cold gases [13]. First of all, the dilute nature of cold atoms and the extremely low temperatures of the experiments allow for the observation of dynamical effects which can last for very long times of the order of milliseconds; considering that the typical lifetime of ultracold systems is of the order of few seconds, non-equilibrium dynamics and quantum many-body coherent effect are fully accessible in this kind of experiments. In order to appreciate these numbers, they should be compared with the typical time scales of equilibration in conventional solid state physics experiments, usually extremely fast, of the order of picoseconds. Furthermore, all the usual mechanisms of relaxation for electrons in solid state physics are absent in the ultracold context: there are no phonons that can transfer energy into the lattice, no impurities to allow momentum to dissipate, and no spin-orbit interaction to mediate spin relaxation. This is precisely the desired scenario for studying coherent non-equilibrium dynamics as it was brilliantly demonstrated in the observation of collapse and revival of the quantum many body wave function after a quench across a superfluid-to-Mott insulator quantum phase transition [14] and in the study of the formation of topological defects during a quench of trapped spinor Bose gases through a critical point [15].

Another remarkable feature in cold atoms experiments consists in the possibility of tuning the internal parameters governing hamiltonian dynamics with an unprecedented control and accuracy via Feshbach resonance [16] and

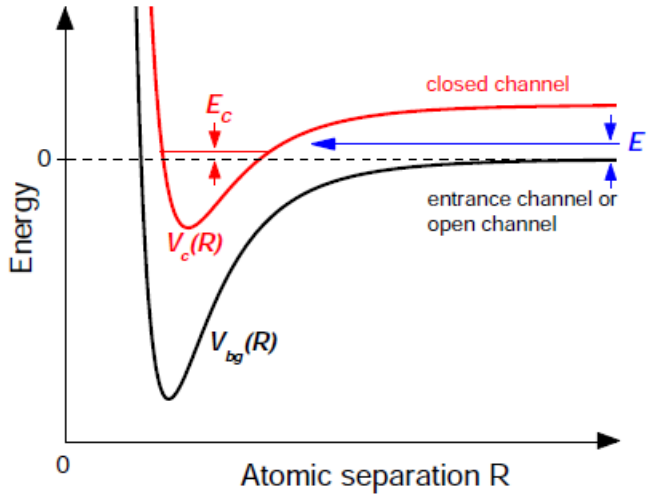

Figure 2.2: Basic two-channel model for a Feshbach resonance. (Taken from [13].)

realizing a large class of prototypical non-equilibrium protocols, like quantum quenches.

Feshbach resonances are quantum mechanical scattering resonances, which occur at very low scattering energies in the domain of ultracold gases. This resonance takes place when the state of two free colliding atoms couples to a molecular bound state, and it can be induced by an external magnetic field, easily tunable in the laboratory. The physics behind Feshbach resonance can be understood looking at the picture 2.2. We consider two molecular potential curves $V_{bg}(R)$ and $V_c(R)$; for large intermolecular distances R, the background potential $V_{bg}(R)$ asymptotically connects two free atoms in the ultracold gas, while $V_c(R)$ can support a bound state. If a given low energy collision state ($\sim E$), having the V_{bg} potential as open channel, approaches the bound molecular state in the closed channel of $V_c(R)$, a Feshbach resonance occurs with a strong mixing between the two states, even if the coupling is weak. Empirically this resonant effect can be quantified by this simple expression for the s-wave scattering length

$$a(B) = a_{bg}\Big(1 - \frac{\Delta}{B - B_0}\Big), \tag{2.11}$$

where the back-ground scattering length a_{bg} represents the off-resonant value, and B_0 is the location of the resonance position, where the scattering length diverges $a \to \infty$, with a resonance width parametrized by Δ.

Last but not least, many archetypical models of theoretical condensed matter physics, which in the past were only textbooks hamiltonians, can be realized experimentally through cold gases, allowing the possibility to explore the interplay of dimensionality, interactions, fluctuations during the quantum coherent dynamics, as it will be elucidated in the forthcoming examples. Before reviewing and citing the most relevant experiments for realization and control of quantum many body dynamics out-of-equilibrium, it could be useful to summarize the simple but striking physical idea behind the realization of quantum hamiltonians with cold atoms, as it was first conceived in the pioneering paper by Jaksch *et al.* [17]. The authors of [17] essentially realized that a quantum many body hamiltonian of bosons in optical lattices interacting via a delta-potential characterized by an s-wave scattering length a and trapped in an external potential, can be mapped into a Bose-Hubbard model, where the ratio between the hopping and on-site repulsion of two atoms can be controlled by the scattering length a and the energy offset of each lattice site can be tuned via the external trapping potential, e.g. a magnetic trap. This seminal paper has been considered the cornerstone for more sophisticated realizations in laboratory of quantum many body hamiltonians using cold atoms [13].

Let us now review the most relevant experiments of the last ten years, which shed new light on the realization of quantum non-equilibrium dynamics and which rise the problem of quantum thermalization at the edge of experimental interest.

The first ground-breaking experiments which initiated the theoretical quest for relation between thermalization in isolated quantum systems and quantum integrability are the pioneering studies on thermalization in 1D Bose gases.

In the experiment by Kinoshita *et al.* [1], arrays of tightly confined tubes of ultracold ^{87}Rb atoms were prepared in a superposition of states of opposite momentum. The imparted kinetic energy was small compared to the energy required to excite the atoms to the higher transverse states and the gases remained effectively one dimensional along the z direction. The system was then allowed to evolve for variable durations before the momentum distribution was sampled. The initial momentum distributions exhibited some dephasing due to trap anharmonicities, but, even after thousands of collisions, the dephased distribution remained non-Gaussian, signaling that the non-equilibrium Bose gas did not equilibrate on the time scales of the experiment (see Fig. 2.3).

The popular explanation of this experiment refers to the fact that the experimental realization of this system is close to the Lieb-Liniger gas with pointlike collisional interactions [18], which is a notable example of integrable quantum many body system. This experiment revived the theoretical interest on the effects of dimensionality and integrability in the relaxation dynamics of

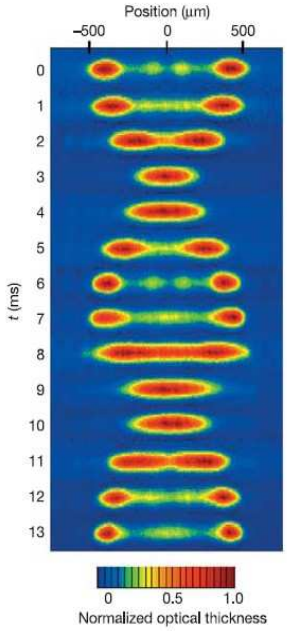

Figure 2.3: Absorption image in the first oscillation cycle in the experiment of Kinoshita *et al.*, showing the absence of relaxation towards a steady state. (Taken from [1].)

quantum many body systems, highlighting the role of non-trivial conservation laws in preventing relaxation towards the usual canonical Gibbs ensemble and triggering the interest of theoreticians on asymptotic non-thermal steady states approached after a quantum quench.

Another representative experiment addressing the issue of quantum quen--ches in many-body systems was performed the last year and focuses on the spreading of quantum correlations after a sudden quench of a one-dimensional quantum gas in an optical lattice [19]. The mechanism of spreading of correlations in a quantum many body systems driven out of equilibrium is of paramount importance. Since the early days of quantum quenches the seminal work by Calabrese and Cardy on quenches in Conformal Field Theories showed that correlations spread at finite velocity, given by the Lieb-Robinson velocity [20], which had already found a number of applications in condensed matter theory in the past. More specifically, Calabrese and Cardy [21] argued that quantum-entangled quasiparticles emerge from the initially highly excited state and propagate ballistically, carrying correlations across the system, as we are going to discuss better in the following sections. Even if the existence of such a 'speed of light' in solid state physics has profound

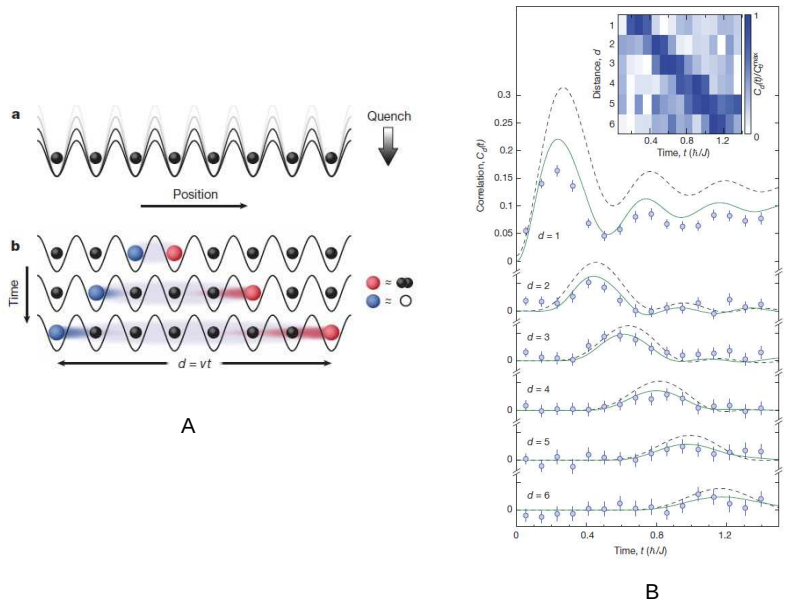

Figure 2.4: **A**: Quench protocol realized in the experiment [19]: red balls are doublons, blue balls are holons. The picture shows the propagation in opposite direction of the holon/doublon pairs, created after the quench, with velocity v. **B**: Time evolution of the two-point parity correlations for a quench from effective effective interaction strength $U/J = 40$ to $U/J = 9$ (with the geometry realized in the experiment the critical point of the transition is located at $(U/J)_c \simeq 3.4$.) (Taken from [19].)

theoretical implications, it had never been observed experimentally. The experimental setup of [19] consists in preparing an ultracold bosonic gas of rubidium in an optical lattice deep in the Mott regime and to sudden quench the interaction strength to a final value closer to the critical point of the Bose-Hubbard model. The system is described by the hamiltonian $H = -J\sum_{\langle i,j\rangle} b_i^\dagger b_j + b_j^\dagger b_i + \frac{U}{2}\sum_i n_i(n_i-1)$, and the initial many body sate is an highly excited respect to the new hamiltonian. Right after the quench, it acts as a source of quasiparticles; more precisely, it can be written as a sum of entangled quasiparticles pairs of a doublon with momentum k and energy ϵ_k^d and a holon with momentum $-k$ and energy ϵ_{-k}^h propagating in opposites directions

$$|\psi(t)\rangle \simeq |\psi_0\rangle + i\sqrt{8}\frac{J}{U}\sum_k \sin(ka)\Big[1 - e^{-i[\epsilon_k^d+\epsilon_{-k}^h]t/\hbar}\Big] d_k^\dagger h_{-k}^\dagger |\psi_0\rangle. \qquad (2.12)$$

The propagation of quasi-particle pairs is reflected in the two point parity

correlation functions for sites separated by a distance d

$$C_d(t) = \langle s_j(t) s_{j+d}(t) \rangle - \langle s_j(t) \rangle \langle s_{j+d}(t) \rangle, \tag{2.13}$$

where $s_j(t) = e^{i\pi[n_j(t)-\overline{n}]}$ measures the parity of the occupation number $n_j(t)$. The main result of the experiment can be summarized in Fig.2.4 and it shows clearly a positive correlation signal between pairs separated by a distance d and propagating with velocity v, spreading with increasing time to larger distances.

Another recent interesting experiment, [22], concerning the time scales of relaxation in quenched quantum many body systems concerns the direct observation of the relaxation dynamics of a Bose-Hubbard model using ultracold atoms in an optical lattice. The experiment can be summarized in three steps: (1) at $t = 0$ the system is initiated in the state $|\psi(t = 0)\rangle = |..., 1, 0, 1, 0, 1, ...\rangle$ such that only lattice sites with an even site index are occupied and no tunnel coupling is present along the chain; (2) the quench dynamics is initiated by the sudden variation of a distinct set of parameters J and U and the system follows the non-equilibrium dynamics according to the Bose-Hubbard model; (3) finally, the tunnel coupling is suppressed again and the properties of the evolved state are read out. The result for the odd-site density are reported in Fig. 2.5, where it can be clearly seen an approach towards the equilibrium value which follows a power law decay, as discussed by the authors in their work [22].

Finally, while the relevance of this experiment and of the previous one lies on the possibility of a detailed experimental study of the time scales of equilibration and of the dynamical mechanism behind thermalization, let us now focus on experiments connected more directly to this Thesis, in particular on experimental realizations of Quantum Ising Chains.

The experimental group in Innsbruck [23] as well as the Greiner's group in Harvard [24], using a titled Bose-Hubbard model $H = -J \sum_{\langle i,j \rangle} b_i^\dagger b_j + b_j^\dagger b_i + \frac{U}{2} \sum_i n_i(n_i - 1) + E \sum_i i n_i + \sum_i \epsilon_i n_i$, where the linear energy shift from site to site is denoted by E, and ϵ_i accounts for a weak external confinement, have been able to simulate the QIC paramagnetic/ferromagnetic transition, controlling the tilt E. For sufficiently small tilt ($E \ll U$) and sufficiently strong interactions ($U \gg J$) the ground state of the system is a Mott insulator with exactly one atom per site. When the tilt is ramped adiabatically from $E < U$ to $E > U$ across $E \simeq U$ at finite J, the system establishes a regular periodic pattern of dipole states, showing double occupied states with empty states in between (see 2.6). This system can be mapped onto an effective Ising spin model [24] [25], where the two distinct ground states, (with PM (paramagnetic) and AFM (anti-ferromagnetic) order respectively) are connected via a quantum phase transition at the quantum critical point $E_c = U + 1.85J$. Quench dynamics of the QIC can be simulated, ramping

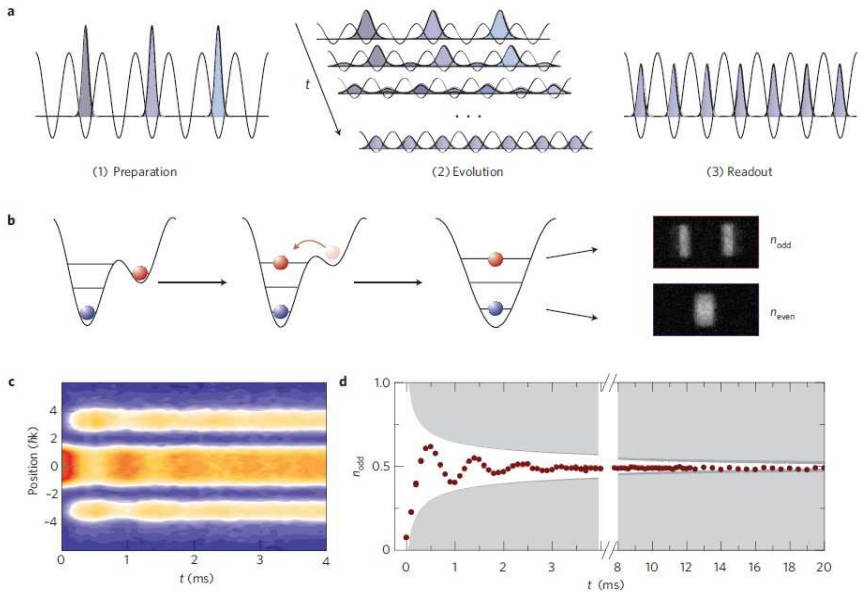

Figure 2.5: The upper pictures summarize the quench protocol performed in experiment [22]. The (**d**) plot shows the relaxation dynamics of the odd-site density versus time. (Taken from [22].)

suddenly the tilt towards the critical point and measuring the doublons produced as a function of time. In Fig. 2.7 it is shown how a quench close to the transition (blue line) displays strong oscillations, which damp out to an equilibrium value over time scales of the order of milliseconds.

2.4 A mechanism for Quantum Thermalization?

As we anticipated in the section 2.2. it is not obvious what feature of many-body quantum mechanics makes quantum thermalization possible in a sense analogous to the way in which dynamical chaos makes classical thermalization possible. The quest for a mechanism underlying quantum thermalization is one of the most debated issues of the last years in the domain of quantum quenches [2]. At the present time, one of the most celebrated conjectures regarding the approach towards a thermal state in generic isolated quantum systems is the Eigenstate Thermalization Hypothesis (ETH). In a nutshell,

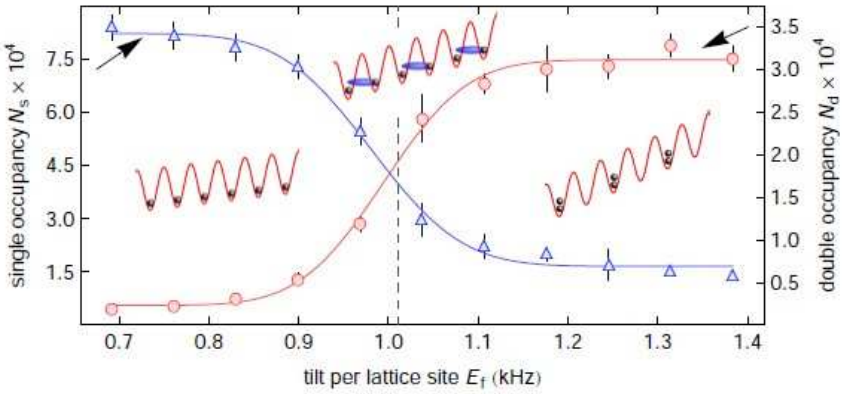

Figure 2.6: The number of doublons N_d (circles) and the number of singly occupied sites N_s(triangles) are plotted versus the tilt at the end of the ramp. The insets show a schematic of the Ising phase transition for a 1D Mott-insulator chain from the PM (left) to the AFM (right) ground state. (Taken from [23].)

thermalization should happen at the level of individual eigenstates and time evolution plays just a mere auxiliary role, with the consequence that to compute thermal averages it is enough to average over a single many-body eigenstate in the microcanonical energy window.

The pillar of ETH is the Berry conjecture, as it was firstly shown by Srednicki in '94 [26]. For a system of N hard spheres, each of radius a, the energy eigenfunctions of this quantum many body systems can be decomposed in plane waves in the usual way

$$\psi_\alpha(\mathbf{X}) = N_\alpha \int d^{3N}\mathbf{P} A_\alpha(\mathbf{P})\delta(\mathbf{P}^2 - 2mU_\alpha)\exp[i\mathbf{P}\cdot\mathbf{X}/\hbar]. \tag{2.14}$$

The Berry conjecture assumes that the coefficients $A_\alpha(\mathbf{P})$ are random gaussian variables with a delta correlated two point function in α and in $\mathbf{P}$. If we consider an eigenstate of the energy and compute the fraction of atoms with momentum in a range d^3p around p ($f_{QM}(p,t)d^3p$), i.e. the momentum distribution function, this is expected to reproduce the Maxwell-Boltzmann

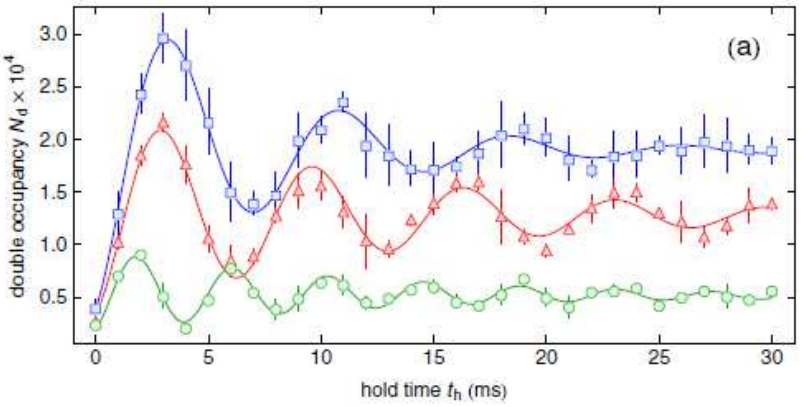

Figure 2.7: Dynamic response for a quench to the resonance point $E \simeq U$ with $U = 1.019kHz$, for $E = 1.038$ (blue line), $E = 0.973$ (red line), $E = 0.865kHz$ (green line). (Taken from [23].)

distribution at a temperature T_α, after averaging over the distribution function of the coefficients A_α [26]. Moreover, fluctuations around this distribution are negligible: an eigenstate which satisfies Berry's conjecture predicts a thermal distribution for the momentum distribution function of a single constituent particle. Besides the specific example of this quantum gas, the conjecture has been shown to hold for integrable hamiltonian weakly perturbed by a single matrix taken from a random gaussian ensemble [27] and for quantum systems, which have a chaotic classical counterpart [26]. In general, it is expected to hold for generic non-integrable quantum many body systems as it was reported in a celebrated numerical work by Rigol *et al.* [28].

Considering that ETH is the only hypothesis for quantum thermalization tested for a broad class of systems (for a comprehensive review on this subject see [2]), we are going now to discuss in more detail how it is expected to work. Let us prepare the gas of N hard spheres in an initial state, given by the superposition of the many body eigenfunctions, $\widetilde{\psi}_\alpha(\mathbf{P})$, in momentum

representation ($\mathbf{P} = \{\mathbf{p}_1, \mathbf{p}_2, ..., \mathbf{p}_N\}$), with certain coefficients, C_α,

$$\widetilde{\psi}(\mathbf{P}, 0) = \sum_\alpha C_\alpha \widetilde{\psi}_\alpha(\mathbf{P}), \tag{2.15}$$

and consider the subsequent unitary evolution

$$\widetilde{\psi}(\mathbf{P}, t) = \sum_\alpha C_\alpha \exp(-iU_\alpha t/\hbar)\widetilde{\psi}_\alpha(\mathbf{P}). \tag{2.16}$$

The momentum distribution function is given at time t by the following expression

$$f_{QM}(\mathbf{p}_1, t) = \int d^3p_2...d^3p_N |\widetilde{\psi}(\mathbf{P}, t)|^2 = \sum_{\alpha,\beta} C^*_\alpha C_\beta e^{i(U_\alpha - U_\beta)t/\hbar} \Phi_{\alpha\beta}(\mathbf{p}_1), \tag{2.17}$$

where C_α are the coefficients set by the initial condition and

$$\Phi_{\alpha\beta}(\mathbf{p}_1) = \int d^3p_2...d^3p_N \widetilde{\psi^*_\alpha(\mathbf{P})}\widetilde{\psi^*_\beta(\mathbf{P})} \tag{2.18}$$

is the overlap between the many-body eigenstates α and β.

If the system is prepared in a non thermal initial state, nonthermal features will dephase after a time $t \gg \hbar/\Delta$ and we get

$$\langle f_{QM}(\mathbf{p}_1, t)\rangle = \sum_\alpha |C_\alpha|^2 \langle \Phi_{\alpha\alpha}(\mathbf{p}_1)\rangle, \tag{2.19}$$

where the average is intended over the gaussian ensemble postulated in Berry's conjecture and Δ is the uncertainty in the energy

$$\Delta^2 = \sum_\alpha |C_\alpha|^2 (U_\alpha - \overline{U})^2. \tag{2.20}$$

If the initial condition is sufficiently narrow in the microcanonical energy shell, the average energy $\overline{U}$ can replace all the U_α under the hypothesis $\Delta \ll \overline{U}$ and we can extract $\langle \Phi_{\alpha\alpha}(\mathbf{p}_1)\rangle$ from (2.19), ending up with $\langle f_{QM}(\mathbf{p}_1, t)\rangle \simeq \langle \Phi_{\alpha\alpha}(\mathbf{p}_1)\rangle$. $\langle \Phi_{\alpha\alpha}(\mathbf{p}_1)\rangle$ can be shown to be equal to $f_{MB}(\mathbf{p}_1, \overline{T})$, which is the Maxwell-Boltzmann distribution, using Berry's conjecture (2.14) and after some simple algebra (see for details Eq. (3.8)-(3.11) of [26]).

In a nutshell the importance of ETH lies in the fact that states very different in structure but narrow in energy give all the same thermal expectation value, if they have the shape predicted by Berry conjecture; moreover, the role of time evolution is just to dephase and kill off-diagonal matrix elements, leaving behind only the diagonal ones, which already contain the expected thermal behaviour.

Even if the ETH works in many cases, the actual explanation of quantum thermalization could be more involved, as some interesting works suggest. For instance, a seminal work on quench dynamics of the Bose-Hubbard model showed that for large values of the final interaction strength the system approached a nonequilibrium steady state with strong memory of the initial conditions, and only when the post-quench interaction strength was comparable to the hopping, thermal correlations were restored in the long time limit [29]. The explanation behind this counter-intuitive behavior was given in terms of the ineffectiveness of quasi-particles interactions deep in the Mott regime, with a suppression of thermalization, because of the impossibility of redistributing the non-equilibrium quasiparticle distribution imposed on the system by the initial conditions. Moreover, strict dependence on the initial state was observed in a numerical study of integrability breaking in a one dimensional quantum Ising chain [30]

$$H = -\sum_i \sigma_i^x \sigma_{i+1}^x - g\sum_i \sigma_i^z - B\sum_i \sigma_i^x \tag{2.21}$$

Numerical results for the three-sites reduced density matrix available for this system show that if the initial state has all spins aligned along the positive y direction, then the reduced density matrix approaches the thermal canonical ensemble, while for states pointing along the positive z direction persistent oscillations occur at large times with a very slow diffusive relaxation towards the thermal state, requiring to time average in order to see the appearance of a canonical distribution. Remarkably, for initial states pointing along the x direction relaxation is fast, but the distance between the evolved state and the thermal one is remarkably different from zero even in the long time limit.

This large variety of possible scenarios calls for a deeper understanding of the mechanism behind quantum thermalization. Though subject is currently a matter of active research a complementary point of view to ETH is provided by the connection between quantum thermalization and the many-body localization transition. This direction received some recent interest in the comunity of quantum quenches [31] [32], but it remains essentially unexplored and calls for a more sophisticated understanding. The idea can be summarized noticing that the quasi-particle space can be thought as a multidimensional lattice where each point is identified by the occupations $n(k)$ of the various quasiparticle modes $|\psi_\alpha\rangle = |n_\alpha(k)\rangle$. As long as states are localized in quasi-particle space, the system behaves as integrable: any initial condition spreads into few sites, maintaining strong memory of the initial state, and the system will not thermalize, because the basic requirement of ergodicity cannot be satisfied. On the other hand, when a strong enough integrability-breaking perturbation hybridizing the various states $|n_\alpha(k)\rangle$ is applied, the consequent delocalization in quasi-particle space will lead to thermalization (see fig. 2.8). The operatorial nature of the integrability-breaking term can lead to different de-localized phases: if the initial state is

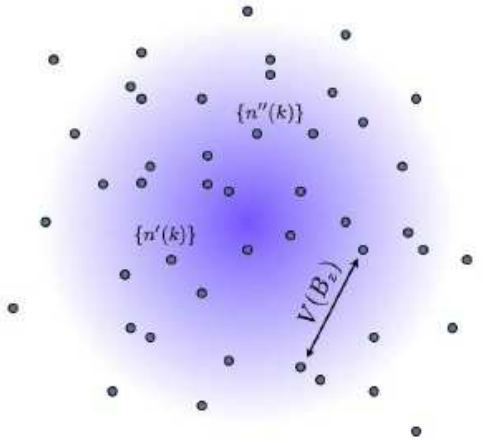

Figure 2.8: An integrability breaking perturbation introduces hopping matrix elements $\widehat{V}$ among different sites, which hybridize, and for enough strong perturbations this may lead to de-localization of wave functions among all points in quasiparticle space in a microcanonical energy shell, leading to thermalization. (Taken from [31].)

allowed to diffuse into all states in a micro-canonical energy shell generating a cascade of all possible lower energy excitations, then real thermalization will occur; on the other hand, if an homogeneous redistribution of energy among the states $|n_\alpha(k)\rangle$ is prevented by selection rules, a delocalized non-ergodic phase can emerge, inhibiting full thermalization.

2.5 Quenches in Integrable Models: the GGE

Before discussing the state of art concerning quantum quenches in integrable models, it should be clarified which is the exact notion of *quantum integrability*. In classical mechanics a system with n degrees of freedom is integrable if possesses n independent integrals of motion in involution, i.e. Poisson-commuting. Integrability means in this case that the differential equations describing time evolution can be explicitly integrated by the use of action-angle variables. The relevance for such definition in the classical domain lies in the fact that solutions of equations of motion in the integrable case display

only periodic motion on tori in the phase space (or loosely speaking the trajectory covers only a small portion of the phase space), while non-integrable models explore the phase space densely in the course of dynamics.

Pitfalls are encountered when this definition is naively extendend to the quantum realm. For instance, it is not clear what is the number of degrees of freedom in a system with a finite dimensional Hilbert space, like a quantum spin chain, whether the number of spins, which is proportional to the size of the system, L, or instead the dimension of the Hilbert space which scale exponentially with L. Moreover, the criterion of a maximal independent set of commuting operators is too naive in the quantum domain, since, for instance, the projectors on the eigenstates diagonalizing the haimiltonian would fullfill formally this requirement, but it would not discriminate among the various possible hamiltonians. The quest for a proper definition of quantum integrability is still going on, and the interested reader could find a complete review on the subject in [33]; in the following we will adopt the definition given by Sutherland in [34] which seems at the present time the most suited and which is stimulating promising lines of research in establishing a relation between integrability and thermalization [35]. In a nutshell, a quantum system is said integrable if any multi-body scattering process can be decomposed in a sequence of binary collisions, which in 1+1 dimensions would not allow for redistribution of energy and momentum (in the absence of internal quasi-particle indices), hence, loosely speaking, the required condition is that the potential supports only elastic scattering among its elementary excitations. This is a very special condition which finds its formal encoding in the Yang-Baxter equation of integrable field theories, where it can be proved that the existence of many integrals of motion prevent dissipation or production of particles during interactions, with the consequence that particles maintain their identity upon scattering [36]. As a matter of fact, the Bethe ansatz solution is exactly the non-diffractive expression for the N particle wavefunction and for this precise reason it constitutes the foundation for the study of integrable systems in one dimension.

As briefly anticipated in Section 2.2, relaxation dynamics in integrable systems should lead to an asymptotic steady state, called the GGE (Generalized Gibbs Ensemble), as conjectured by Rigol *et al.* [11], which is a sort of grand-canonical ensemble accounting for all the conserved quantities of the theory, in the form

$$\rho_G = \frac{e^{-\sum_\alpha \lambda_\alpha I_\alpha}}{Z}, \tag{2.22}$$

where I_α are the mutually commuting integrals of motion of the theory. In statistical physics the ordinary Gibbs ensemble emerges for small subsystems from the assumption of statistical independence between sufficiently big subsystems, this requires that the I_α in the GGE should be local integrals of motion in terms of the basic degrees of freedom of the theory.

Let us start considering a simple example, the quench dynamics of the Quantum Ising Chain

$$H = -\sum_i \sigma_i^x \sigma_{i+1}^x + g\sigma_i^z, \tag{2.23}$$

which can be diagonalized after a Jordan Wigner transformation and a Bogolyubov rotation into a sum of free fermionic modes, $H = \sum_k \epsilon_k \gamma_k^\dagger \gamma_k$, where ϵ_k is the quasi-particle energy. It has been shown [37] that the proper integrals of motion for the GGE are the fermonic occupation numbers $I_k = \gamma_k^\dagger \gamma_k$ diagonalizing the theory; the same authors showed in [38] that the GGE density matrix can be also expressed in terms of a family of local integrals of motion, $\{\mathcal{I}_n\}$, involving only spins on $\sim n$ neighboring sites. The two formulations are equivalent since the I_k can be expressed as a linear combination of the $\{\mathcal{I}_n\}$. Concerning the important question about the connection between locality of conservation laws and its relevance for a GGE description of the asymptotic steady state, the authors of [38] showed that in order to obtain a good description of the stationary state reduced-density-matrix of a subsystem of size l, we need to retain all local conservation laws, $\{\mathcal{I}_n\}$, whose densities involve at most $l + n_0$ neighboring spins, where n_0 is a constant depending on the pre-quench and post-quench values of the transverse field. Leaving out highly local conservation laws generally provides a very poor description of the stationary state.

On the other hand, in continuum integrable systems, like integrable field theories, it is natural to associate the I_α to the occupation numbers of the quasiparticles diagonalizing the theory $A(\theta)$, where θ is the rapidity. Fioretto and Mussardo [39] conjectured that for a specific class of translationally invariant initial states

$$|\psi_0\rangle \sim e^{-\int d\theta K(\theta) A^\dagger(\theta) A^\dagger(-\theta)} |0\rangle \tag{2.24}$$

(which naturally emerge in the quench of the transverse field of the QIC or in the coherent split of 1d-quasi-condensates), the long-time limit of the average of local operators can be predicted by a continuum version of the GGE

$$\rho_{GGE} = \frac{e^{-\int d\theta \lambda(\theta) A^\dagger(\theta) A(\theta)}}{Z}. \tag{2.25}$$

The GGE conjecture [11] has been tested in a broad range of quench protocols, ranging from the seminal work by Cazalilla [40] on the study of correlation functions in the Luttinger Model after a sudden switch-on of interactions to the recent studies of quench dynamics in the XXZ chain [41], and it has been rigorously proved by Barthel and Schollwock [42] for quadratic hamiltonians of fermions or bosons, highlighting remarkably that the mechanism of relaxation in integrable systems is usually an algebraic decay arising

from inhomogeneous dephasing of the off-diagonal elements of the reduced density matrix, when they are employed to evaluate expectation values of physical observables.

All the analytical evidence for a GGE description of quenches in integrable models is based on free theories in which the pre- and post- quench eigenmodes are linearly related, usually by a Bogolyubov transformation. Very recently Kormos *et al.* [45] have considered the interesting experimental situation (see [1]) where a one-dimensional Bose gas is quenched from zero to infinite interaction. In a nutshell, they considered the Lieb-Liniger (LL) model on a ring $H = \int_0^L dx \Big[\partial_x \phi(x)^\dagger \partial \phi(x) + c\phi(x)^\dagger \phi(x)^\dagger \phi(x)\phi(x)\Big]$ and prepared the many-body system in the ground state with $c = 0$, letting it evolve under the LL hamiltonian with infinite interaction ($c = \infty$), equivalent to a system of free hard-core bosons. Although this is a quench among free theories, the pre- and post- quench eigenmodes are not linearly related, and remarkably the GGE still characterizes the asymptotic steady state of the system, predicting the stationary value of the dynamical density-density correlation function for instance.

Before concluding this section, it is important to stress that at the current level of understanding the GGE lacks of predictive power in some peculiar but physically relevant situations. For instance, in the QIC correlation functions of different eigenmodes are predicted to be zero by the GGE, $\langle n_k n'_k \rangle = 0$, or correlators of the type $\langle \gamma_k^\dagger(t)\gamma_{-k}(t)\rangle$ are expected to be zero as well; these statements are not true for initial states where translational invariance is broken, which violates the above mentioned conditions already at the level of the initial state [43]. Moreover, expectation values of global operators, like the global transverse magnetization, $M^z = \sum_i \sigma_i^z$, in the QIC, are not correctly predicted by the GGE, because in the thermodynamic limit correlations between k and $-k$ modes, $\langle n_k n_{-k}\rangle \neq 0$, which are present for translationally invariant states like (2.24), are not negligible, as instead happens for expectation values of local operators after a quantum quench [44].

2.5.1 Quench Dynamics of the Quantum Ising Chain

Finally, we would like to briefly review in a bit more of detail the quench dynamics in a transverse field Quantum Ising Chain (QIC), which has been studied in detail as a benchmark for many interesting ideas concerning the GGE and relaxation dynamics in integrable models in the last few years [46] [37] [47], and which will be our starting point for studying pre-thermalization in this PhD Thesis.

The Quantum Ising Chain (QIC) is described by the hamiltonian

$$H = -J \sum_i \sigma_i^x \sigma_{i+1}^x + g\sigma_i^z \tag{2.26}$$

where $\widehat{\sigma}_i^{x,z}$ are the longitudinal and transverse spin operators at site i and g is the strength of the transverse field. The Quantum Ising Chain (QIC) is among the simplest, yet non-trivial integrable many-body system, whose static properties [48] are to a great extent known. The QIC is characterized by two dual gapped phases, a quantum paramagnetic ($g > 1$) and ferromagnetic one ($g < 1$) separated by a quantum critical point located at $g = 1$.

The spin hamiltonian is unitarily equivalent to spinless fermions, as can be shown performing the Jordan-Wigner transformation [48], introducing c_i, through the relation $\widehat{\sigma}_i^z = 1 - 2c_i^\dagger c_i$ and $\widehat{\sigma}_i^+ = -\prod_{j<i}(1 - 2c_j^\dagger c_j)c_i^\dagger$. The Hamiltonian takes in Fourier space, $c_k = \sum_j c_j e^{ikj}$, the simple form

$$H = 2\sum_{k>0} \widehat{\psi}_k^\dagger \widehat{H_k} \widehat{\psi}_k \tag{2.27}$$

where

$$\widehat{H_k} = (g - \cos k)\sigma_z - (\sin k)\sigma_y \tag{2.28}$$

and $\widehat{\psi}_k$ is the Nambu spinor $\binom{c_k}{c_{-k}^\dagger}$ and σ_y, σ_z are the Pauli matrices in the 2×2 Nambu space. The diagonal form $H = \sum_{k>0} E_k(\gamma_k^\dagger \gamma_k - \gamma_{-k}\gamma_{-k}^\dagger)$, with energies $E_k = \sqrt{(g - \cos k)^2 + \sin^2 k}$, is achieved after a Bogoliubov rotation $c_k = u_k(g)\gamma_k - iv_k(g)\gamma_{-k}^\dagger$ and $c_{-k}^\dagger = u_k(g)\gamma_{-k}^\dagger - iv_k(g)\gamma_k$; the coefficients are given by

$$u_k(g) = \cos(\theta_k(g)) \qquad v_k(g) = \sin(\theta_k(g)) \tag{2.29}$$

where $\tan(2\theta_k(g)) = \sin(k)/(g - \cos(k))$, which shows that the QIC is equivalent to free fermions, whose mass is the gap of the theory $\Delta = |g - 1|$ [48].

The canonical quench protocol for the QIC consists in preparing the system in the ground state of $H(g_0)$, to sudden switch the transverse field to a different value g and to study the subsequent time evolution. This initial state, expressed in terms of Bogolyubov fermions diagonalizing the post-quench hamiltonian, has a similar form to the initial state of the experiment by Cheneau [19] (see for instance (2.12)) and it has also the same form of the so-called integrable boundary states in statistical field theory [49],

$$|\psi(g_0)\rangle_{GS} \sim \exp\Big[\sum_{k>0} i\tan(\Delta\theta_k)\gamma_k^\dagger(g)\gamma_{-k}^\dagger(g)\Big]|\psi(g)\rangle_{GS}, \tag{2.30}$$

where $\Delta\theta_k = \theta_k(g) - \theta_k(g_0)$ is the difference of the Bogolyubov angle before and after the quench.

The quench dynamics of the QIC will be reviewed in this Section, distinguishing between *local* and *non-local* operators in terms of the Jordan-Wigner fermions. As it should be clear from the previous introduction to the QIC, 1pt or 2pt functions of the transverse magnetization are local operators in the fermionic degrees of freedom and their out-of-equilibrium dynamics after

a quench can be easily evaluated with a trivial computation, for instance, the expectation value of the on-site transverse magnetization

$$\langle \sigma_l^z \rangle = -\int_0^\pi \frac{dk}{\pi} \Big(\cos\theta_k \cos\Delta\theta_k + \sin\theta_k \sin\Delta\theta_k \cos(2\epsilon_k t) \Big) \tag{2.31}$$

displays a constant term, which is the asymptotic value described by the GGE, and an oscillating term, describing the coherent evolution due to pairs of quasiparticles propagating after the quench from the initial state (2.30), decaying to zero in the long time limit $Jt \gg 1$, as a power law $1/(Jt)^{3/2}$. This is consistent with the general argument provided by Barthel and Schollowock [42] for the relaxation dynamics of observables in integrable models occurring through inhomogeneous dephasing, i.e. the sum of many oscillating factors with slightly different phases, like in Eq. (2.31).

The notion that the GGE predicts the asymptotic value of observables in the QIC can be understood better looking at the infinite limit of the connected transverse magnetization two points function

$$\rho_c^{zz}(l,\infty) = -\int_{-\pi}^{\pi} \frac{dk}{2\pi} e^{ilk} e^{i\theta_k} \cos\Delta\theta_k \int_{-\pi}^{\pi} \frac{dp}{2\pi} e^{ilp} e^{-i\theta_p} \cos\Delta\theta_p; \tag{2.32}$$

this result resembles the finite temperature correlation function

$$\rho_c^{zz}(l,\infty) = -\int_{-\pi}^{\pi} \frac{dk}{2\pi} e^{ilk} e^{i\theta_k} \tanh\Big(\frac{\beta\epsilon_k}{2}\Big) \int \frac{dp}{2\pi} e^{ilp} e^{-i\theta_p} \tanh\Big(\frac{\beta\epsilon_p}{2}\Big), \tag{2.33}$$

where the temperature β can be replaced by a mode-dependent inverse temperature, defined by

$$\beta\epsilon_k \to \beta_k\epsilon_k = 2\tanh^{-1}\Big(\cos(\Delta\theta_k)\Big) \tag{2.34}$$

and derived assuming that the Lagrange multipliers, β_k, of the GGE

$$\rho \sim e^{-\sum_k \beta_k \epsilon_k \gamma_k^\dagger \gamma_k} \tag{2.35}$$

are fixed by the initial condition

$$Tr[\rho_{GGE} n_k] = \langle \psi_0 | n_k | \psi_0 \rangle. \tag{2.36}$$

The emergence of mode-dependent temperatures from the GGE are a consequence of integrability, since in this case the elementary degrees of freedom do not interact among them, and so each single Bogolyubov fermion will thermalize at its own temperature, imposed by the energy injected with the initial quench. The asymptotic value of $\rho^{zz}(l,\infty)$ is in general exponential in space separation $\sim e^{-l/\xi}$ (for quenches not ending into the critical point), with a correlation length ξ dependent from the initial and final value of the

quench protocol; this value is approached following a power law, which immediately implies that in order to see the stationary value predicted by the GGE it is required a time exponentially large in the separation l.

Computations involving the order parameter are more difficult, since it is a non-local observable in the fermionic representation. In general, they require the re-summation of infrared divergences in a form-factor expansion or the evaluation of the determinant representation of correlation functions characteristic of a free-fermionic theory [37]. For instance, for quenches within the ferromagnetic phase, the order parameter relaxes towards zero exponentially

$$\langle \sigma_l^x(t) \rangle \propto \exp\Big[t \int_0^\pi \frac{dk}{\pi} \epsilon'_k \log(\cos \Delta\theta_k) \Big], \tag{2.37}$$

where $\epsilon'_k = \frac{d}{dk}\epsilon_k$, while the two-point functions exhibit decay both in time and space

$$\begin{aligned} \rho^{xx}(l,t) \propto \exp\Big[l \int_0^\pi \frac{dk}{\pi} \theta(2\epsilon'_k t - l) \log|\cos \Delta\theta_k| \Big] \times \\ \times \exp\Big[2t \int_0^\pi \frac{dk}{\pi} \theta(l - 2\epsilon'_k t) \epsilon'_k \log|\cos \Delta\theta_k| \Big] \end{aligned} \tag{2.38}$$

with a correlation length

$$\xi^{-1} = \int_{-\pi}^{\pi} \frac{dk}{2\pi} \xi^{-1}(k) = -\int_{-\pi}^{\pi} \frac{dk}{2\pi} \log|\cos \Delta\theta_k| \tag{2.39}$$

which can be predicted again in a GGE framework, as a thermal correlation length with a mode-dependent temperature β_k, as discussed above. It is important to stress at this point that for small quenches (up to second order in $(g - g_0)^2$) the GGE correlation length and a true thermal correlation length coincide, making difficult to distinguish, for this observable, the GGE prediction from the thermal expectation value. Concerning relaxation dynamics of observables, it should be observed that the two-points correlation function can be expressed as

$$\frac{\rho^{xx}(l,t)}{\Big(\rho^x(t)\Big)^2} \sim \exp\Big[\int_0^\pi \frac{dk}{\pi} \Big[\frac{l}{\xi(k)} - \frac{2t}{\tau(k)} \Big] \theta(2\epsilon'_k t - l) \Big] \tag{2.40}$$

where $\tau(k) = \xi_k/\epsilon'_k$, is the average mode-dependent decay time obtained by multiplying the mode-dependent inverse correlation length by the velocity. The theta function expresses the fact that a given mode contributes to the relaxation dynamics if the distance, l, lies within its forward light cone, indicating that quasiparticles injected by the initial quench propagate in the system ballistically, as discussed in experiment [65] of Section 2.3.

Chapter 3

Pre-Thermalization

Pre-thermalization is the present way to understand the Generalized Gibbs Ensemble. The word pre-thermalization, generally speaking, refers to the possibility for a system driven out-of-equilibrium to approach an intermediate quasi-steady state, before drifting towards the final stationary state of the dynamics. This word has been employed in a variety of contexts ranging from condensed matter physics to elementary particle physics; the aim of this introductory paragraph is to explain the way in which pre-thermalization has been introduced in the context of quantum quenches, how it is shaping our understanding of non-equilibrium dynamics and how it makes possible to merge in the same context both the GGE and the thermal Gibbs ensemble.

The idea is mainly due to Kollar *et al.* and it emerged from combined numerical and analytical evidences coming from a series of works on the subject, summarized in Ref. [5]. A quantum many body system prepared in the ground state of an integrable hamiltonian and weakly quenched away from the integrable point would first approach a intermediate quasi-steady state predicted by a GGE, built perturbatively from the pre-quench hamiltonian, and only later on, when inelastic scattering becomes relevant, the system will depart from the GGE plateau approaching eventually the thermal state, which is the true final asymptotic steady state of the system. In this sense, the GGE expectation value of observables after a quench in an integrable systems is just a close relative to this pre-thermal plateau found in thermalization dynamics of weakly non-integrable quantum many body systems. This idea is extremely appealing from the point of view of experiments, since a realization of integrable systems in laboratory is always an approximation, and for longer times deviation from an experimental integral setup could arise, leading in principle to thermalization. This last point will be addressed in the last section of this Chapter; let us now go into the details of Kollar *et al.*.

As it is clear from Fig. 3.1 thermalization dynamics in an integrable model ends in a GGE, which is immortal for long times, on the other hand, a small interaction quench in a non-integrable system results in a more sophisticated

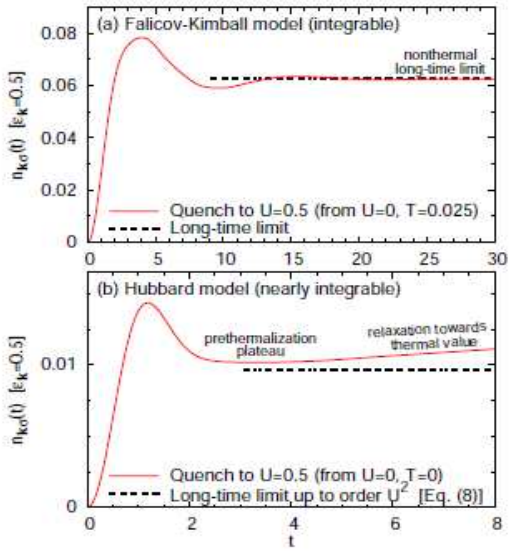

Figure 3.1: The plot shows the time evolution of the momentum occupation distribution function $n_{k\sigma}$ for small interaction quenches in the Falicov-Kimball model, $H = \sum_{ij} V_{ij} c_i^\dagger c_j + E_f \sum_i f_i^\dagger f_i + U \sum_i f_i^\dagger f_i c_i^\dagger c_i$, which is a close relative to the Hubbard model except from the fact that only the itinerant electrons c_i can hop between lattice sites while the f_i electrons are fixed [integrable case] (a) and in the Hubbard model ($d > 1$) [non-integrable case] (b). (Taken from [5].)

thermalization scenario: first observables approach a pre-thermal plateau, which is a strong relative of the GGE, but this state is just a metastable state of the dynamics because at later times inelastic processes drift the expectation value of observables towards the real thermal value.

The argument of [5] considers as a starting point an integrable hamiltonian $H_0(t = 0) = \sum_\alpha \epsilon_\alpha I_\alpha$, and to sudden turn on a small integrability breaking term $H(t > 0) = H_0 + gH_1$, $g \ll 1$. The basic concept is to obtain perturbed constants of motion, $\tilde{I}_\alpha$, starting from the set I_α; these new constants of motion are derived in perturbation theory and are approximately conserved in the sense that they commute among them and with the total hamiltonian up to a given order in perturbation theory. To be more specific, the authors of [5] employ a unitary transformation to cast the hamiltonian

in the following form

$$H = \sum_{\alpha} \epsilon_{\alpha} \tilde{I}_{\alpha} + \sum_{\tilde{n}} |\tilde{n}\rangle (g E_n^{(1)} + g^2 E_n^{(2)}) \langle \tilde{n}| + O(g^3) \tag{3.1}$$

where $\tilde{I}_{\alpha}$ are the approximated constants of motion which commute among them and with the full hamiltonian up to the second order, while $|\tilde{n}\rangle$, $E_n^{(1,2)}$ are the the perturbed eigenvectors and eigenvalues in the sense of Rayleigh-Schrodinger. Kollar *et al.* show that the pre-thermalization plateau can be predicted by a GGE, which includes the $\tilde{I}_{\alpha}$ as constants of motion, disregarding the projectors appearing in (3.1), which in general are not linear combinations of the $\tilde{I}_{\alpha}$. In other words, non-thermal steady states can be understood as pre-thermal states that never decay, and in turn pre-thermal states in non-integrable systems can be put in the form of a Generalized Gibbs Ensemble, closely related to the GGE of the underlying integrable hamiltonian by perturbation theory. The prediction of [5] is clearly expected to hold for intermediate time scales $1/g \ll t \ll 1/g^2$, as a natural limitation coming from perturbative computations, and so the pre-thermal metastable state is expected to be-long lived as much as the integrable point is weakly perturbed. If real thermalization occurs, it is expected on time scales of the order $1/g^3$ and in general triggered by inelastic processes.

There are many open issues in this scenario. First of all, it is not clear which are the time scales of pre-thermalization and for thermalization, which are the physical mechanisms which govern pre-thermalization, and which is the role of the initial state: for instance it would be interesting to understand what happens in the case of composite quenches, i.e. simultaneous switching on of integrable and non-integrable perturbations. In particular, it is not clear at all whether pre-thermalization will always occur; following the above lines of reasoning, pre-thermalization is expected to occur for small perturbations, but how small it should be it is not clear at all. Analogously, understanding how much integrability should be broken in the thermodynamic limit to have real thermalization, i.e. a quantum version of the KAM theorem, is another extremely interesting question to investigate.

In the following, we are going to review the present understanding of the problem and its experimental realizations, highlighting the features relevant to address the original results of this PhD Thesis contained in the next chapters.

3.1 Pre-Thermalization and Non-Equilibrium Dynamics

In order to understand more quantitatively the emergence of *pre-thermalizati--on* in the non-equilibrium dynamics of quenched quantum many body systems we are going to review in this Section two paradigmatic systems that at the present level of understanding constitute the only two cases where pre-thermalization has been explored thoroughly. First of all, we are going to present the quench dynamics of the Hubbard model which has been explored in numerical and analytical detail by Kehrein, Eckstein, Kollar and co-workers, and in the second part of this Section we are going to address pre-thermalization in non-equilibrium quantum field theories starting from the pioneering works by Berges and Wetterich.
The non-equilibrium dynamics of fermionic Hubbard model in $d > 1$ dimensions at half-filling (Fermi energy $\epsilon_F = 0$), following a sudden quench of the interactions ($\Theta(t)$ is the Heaviside Theta and it accounts for the sudden switch-on of interactions)

$$H = \sum_{k,\sigma=\pm} \epsilon_k : c^\dagger_{k\sigma} c_{k\sigma} : + \Theta(t) \sum_i \Big(n_{i,+} - \frac{1}{2}\Big)(n_{i,-} - \frac{1}{2}\Big) \tag{3.2}$$

has been studied analytically by Kehrein and Moeckel [50] using the flow-equation method. This method consists in solving the Heisenberg equations of motion for the operators that one is interested in by performing a unitary transformation to an approximate eigenbasis of the interacting Hamiltonian at a given order in the interaction strength, in this way it is easy to work out the time evolution and then transform back to the original basis. The authors of [50] implement the above diagonalizing transformation by the flow equation method [51]: one uses a continuous sequence of infinitesimal unitary transformations parametrized by a parameter B , that connects the eigenbasis of the free Hamiltonian ($B = 0$) with the energy diagonal basis of the interacting Hamiltonian ($B = \infty$). Each infinitesimal step of the unitary transformation is defined by the canonical generator $\eta(B) = [H_0(B), H_{int}(B)]$, where $H_0(B)$ is the free and $H_{int}(B)$ the interacting part of the Hamiltonian. This generator $\eta(B)$ has the required property of making $H(B)$ increasingly energy diagonal for $B \to \infty$ [51]. All operators $O(B)$ will flow according to the differential equation $\partial O(B)/\partial B = [\eta(B), O(B)]$. Making a suitable ansatz the authors are able to derive and solve flow equations for the momentum distribution function in the limit of infinite dimensions for computational convenience. Three distinct stages of the non-equilibrium dynamics emerge:

- *Initial buildup of correlations for times*[1] $0 < t \simeq \rho_F^{-1} U^{-2}$: a fast reduction of the Fermi-surface discontinuity induced by the initial condition

[1] ρ_F denotes the density of states at the Fermi level.

is observed, with oscillations decaying as $1/t$ in the momentum distribution function. This short-time regime is interpreted by the authors as the formation of quasi-particles from the free electrons of the initial state.

- *Pre-Thermalization*: for times $t >\sim \rho_F^{-1}U^{-2}$ there are no further changes in the momentum distribution function, which is that of a zero temperature Fermi Liquid with a Z factor (the quasi-particle residue) smaller than in equilibrium $1 - Z^{NEQ} = 2(1 - Z^{EQU})$. If this system was integrable, this regime of dynamics would become stable, but the inelastic processes at later times drives this metastable state towards the true equilibrium distribution function.

- *Thermalization* The two previous regimes have been derived within the flow equation approach including all the contributions up to times smaller than $\rho_F^{-3}U^{-4}$. A Boltzmann equation description is expected to hold in the late stages of the dynamics, and imposing this condition the authors of [50] are able to show that starting from the pre-thermal state, the system will approach a Fermi-Dirac distribution function with a temperature $T \sim U$.

Very recently Kollar *et al.* [52] have shown that the full kinetic equation of a quenched Hubbard model can be derived from first principles, i.e. the evolution of the density matrix. It contains both the prethermalization regime and the Quantum Boltzmann equation and moreover it is able to describe the cross-over between these two time scales, employing a numerical solution based on dynamical mean field theory (DMFT) which becomes exact in the limit of infinite dimensions.

Full numerical support to the results of [50] has been provided by Eckstein *et al.* [53] studying the small ($U \ll V$) and large quench ($U \gg V$) regime of the Hubbard model, looking at the time evolution of the double occupation $D(t) = \langle n_{i,+}(t)n_{i,-}(t)\rangle$ and the discontinuity $\Delta n(t) = n(0^-, t) - n(0^+, t)$ of the momentum distribution function at the Fermi energy $\epsilon = 0$ (remember that the initial condition is the ground state of a non-interacting fermionic system, so $n(\epsilon, t)$ is a sharp function, which marks the Fermi surface in the initial state). For small quenches, while the discontinuity remains finite in the pre-thermal regime, some observables, like the double occupation attain their thermal value, even if the system has not reached thermal equilibrium; on the other hand, in the large interaction quench limit collapse-revival oscillations around a quasi-stationary value are observed for both these two quantities, decaying on a time scale proportional to the inverse of the hopping amplitude of the fermions, while thermalization is expected to occur on longer time scales. This suggests a second pre-thermal regime also for large interactions, that can be understood thinking to the potential as the

free part of the hamiltonian and to the hopping as the the perturbation that drives the system eventually towards the equilibrium state. The tantalizing possibility of speculating about a dynamical phase transition in this model is suggested by the fact that at a certain critical interaction thermalization occurs fast both in the momentum distribution function and in the double occupation, without the appearance of a pre-thermal regime which instead delays relaxation in the weak and strong coupling limit, as discussed previously.

An interesting feature stressed by Kehrein [50] concerns re-distribution of energy among elementary degrees of freedom during non-equilibrium dynamics. The initial state is an excited state for the post-quench hamiltonian and its energy in general will be redistributed by the scattering mechanism among the degrees of freedom of the model, keeping constant the total energy of the system. It turns out remarkably that in the pre-thermal stage of dynamics the interaction energy and the kinetic energy already reach their asymptotic value and, even more remarkably, for this kind of system the excitation energy of the initial quantum state with respect to the equilibrium ground state of the quenched hamiltonian is stored into the pre-thermal kinetic energy; hence, the subsequent thermalization dynamics consists in redistributing this excess energy injected through the quench in a such a way that different momenta reach a Fermi-Dirac distribution function, starting from the non-equilibrium pre-thermal state.

This peculiar property of the quenched Hubbard model studied in Ref. [50] strongly resembles to the study of Non-Equilibrium Quantum Field Theories by Berges and collaborators (for a comprehensive review on this subject see [54]). Their approach consists in re-summing numerically all the relevant diagrams contributing to out-of-equilibrium self energies, using the Keldysh formalism for Green's functions out-of-equilibrium. Their main results [4] are similar to the thermalization dynamics scenario discussed by Kehrein [50]. A *dephasing* mechanism due to the sum over oscillating functions with a sufficiently dense frequency spectrum spectrum leads to the equipartition between kinetic energy and potential energy and to the establishment of a time-independent equation of state relating pressure and density $p = p(\epsilon)$, even if the system is still very far from equilibrium. This dephasing phenomenon is very quick and independent from the scattering processes leading to true thermalization; this first stage of thermalization dynamics is called by Berges *pre-thermalization*. It should be noted at this point how this closely resembles the scenario depicted by Kollar *et al.* [5], where first a relaxation towards a perturbative GGE occurs which should be governed by the same dephasing mechanism leading to relaxation in integrable systems, and in principle weakly influenced by non-integrable scattering processes. The second stage of thermalization dynamics for Berges occurs at a damping

time, t_{damp}, controlled by inelastic collisions, and characterized by a relaxation of the mode occupation numbers, $n_p(t)$; information about the initial stage has been lost at this intermediate stage of dynamics, but the momentum distribution function still does not look thermal. Only at later stages, true thermal equilibrium set up with an equilibration time $t \simeq t_{eq}$, which describes the universal rate of approach to the equilibrium values of all the relevant correlation functions.

Instances of pre-thermalization have been also argued to occur in systems of quenched spinor condensates [55] and in the quench dynamics of a quantum sine-Gordon model with the cosine potential representing the underlying commensurate lattice or periodic potential [56].

The challenge for theory is to merge in a unified scenario these results belonging to two very different domains of physics, taking into account also the experimental findings on pre-thermalization in cold atoms systems, which we are going to report now in the last section of this Chapter.

3.2 Pre-Thermalization in the Laboratory

Pre-Thermalization has been successfully observed in experiments involving quasi-1D Bose gases by Jorg Schimedmayer's group in Vienna. The experiment [3] considers a single 1D Bose gas of $2 - 3 \times 10^3$ ^{87}Rb atoms in the quasi-condensate regime, where many longitudinal modes are populated with a consequent rich spatial structure and dynamics of their local phase, in contrast with 3D condensates where the existence of a long-range order allows the characterization of the state with a single global phase. In the experiment a single 1D Bose gas is prepared using standard evaporative cooling in a magnetic microtrap on an atom chip; the strong magnetic field, generated by the current flowing in the atom chip wire, results in a tight longitudinal confinement, forbidding excitations to radial modes (typically $k_B T, \mu \ll \hbar\omega$, where ω is the typical radial trapping). The non-equilibrium protocol is realized deforming in a controllable way the harmonic confinement into a double-well potential by applying radio-frequency radiation via additional wires on the atom chip; the initial state is prepared splitting rapidly and coherently the single 1D gas into two uncoupled 1D Bose gases in the double well potential.

After the splitting, the two gases have almost identical longitudinal phase profile, which reflects the memory that they originally come from a single quasi-condensate, in sharp contrast to two independent 1D Bose gases, which display in general uncorrelated phase profiles.

A good theoretical description for the model is given by two uncoupled Luttinger liquids [57], characterized by the two scalar fields $\phi_{i=1,2}(r,t)$; the

splitting process decouples the phase difference $\phi_s = \phi_1(r,t) - \phi_2(r,t)$ from the sum of the phases $\phi_c = \phi_1(r,t) + \phi_2(r,t)$. The evolution of ϕ_s is described by the Hamiltonian

$$H = \frac{\hbar c_s}{2} \int \Big[\frac{K_s}{\pi} (\nabla \phi_s(r))^2 + \frac{\pi}{K_s} n_s^2(r) \Big] dr, \tag{3.3}$$

where c_s is the sound velocity and K_s is the so called Luttinger parameter which reflects the strength of interactions and correlations. The second-quantization version of this hamiltonian is

$$H_s = \sum_{k \neq 0} \hbar c_s |k| b^\dagger_{s,k} b_{s,k} + \frac{\hbar \pi c_s}{2K_s} n^2_{s,k=0}, \tag{3.4}$$

where a collective mode or sound wave with momentum k modulates the phase difference $\phi_s(r)$ with length scale $1/k$ and time scale of the inverse of the excitation energy $1/c_s\hbar|k|$. The initial state can be written as the coherent superposition of modes propagating with opposite momentum (apart from a normalization),

$$|\psi_0\rangle \simeq \prod_{k \neq 0} (\exp(W_k b^\dagger_{s,k} b^\dagger_{s,-k}))|0\rangle \otimes |\psi_{s,k=0}\rangle, \tag{3.5}$$

where $2W_k = \frac{1-\alpha_k}{1+\alpha_k}$ (with $\alpha_k = \frac{|k|K_s}{\pi\rho}$) and $\langle n_{s,0}|\psi_{s,k=0}\rangle = \exp\left(-\frac{1}{2\rho} n^2_{s,0}\right)$ (where the state $|n_{s,k=0}\rangle$ is the normalized eigenstate of the operator $\widehat{n}_{s,k=0}$ with eigenvalue $n_{s,k=0}$). The fast splitting leads to a strong suppression of fluctuations in the relative phase $\phi_{s,k}$ with a consequent equipartition of energy among each k-mode; for this reason the system looks like thermal at a given temperature $k_B T_{eff} = g\rho/2$, where g is proportional to the scattering length and the transverse confinement ω, while ρ is the density of each half of the system.

The experiment studies how the memory of the initial state evolves and decay in time and whether true thermal equilibrium corresponding to two uncorrelated condensates is reached asymptotically. The protocol consists in letting evolve the system in the double well for some time, and then release the two gases and look at the interference pattern, quantified by the integrated interference contrast

$$C^2(L) = \frac{1}{L} \Big| \int_{-L/2}^{L/2} dz e^{i\phi_s(z,t)} \Big|^2, \tag{3.6}$$

which measures the local phase difference along the longitudinal direction. For the initial state this quantity is large, because there is essentially no difference in the phase profile of the two condensates, later on - taking into

account the integrable nature of the Luttinger Liquid model- only dephasing occurs which in turns modifies the relative phase profile resulting in a decreasing $C(L)$ in time. For instance, it is possible to extract the mean squared contrast $\langle C(L)^2 \rangle$ which is a direct measure of the integrated two points correlation function to infer that, after an initial rapid decay on a time scales of the order of 10ms due to the dephasing mechanism described above, a quasi-steady state emerges that evolves further only on a much longer time scale (see Fig. 3.3). This intermediate steady state has an effective temperature of about 14 nK which turns out to be in strong agreement with the theoretical estimate based on the Luttinger model paradigm, and it is roughly a factor five lower than the initial temperature of the unsplit system ($T \simeq 78$nK), hence the observed steady state cannot be the true thermal equilibrium of the system. Simple estimates provided by the authors show that thermalization could occur in this system on time scales ranging from 200 ms to 4 s, and it may be induced by anharmonic terms which spoil the Luttinger liquid description, namely three body collisions connected with higher radial excitations. Such processes are expected since the experimental realization of a 1D Integrable system is always an approximation, so on longer time scales high body scattering could occur, revealing the non-integrable nature of the gas. The mismatch between the observed temperature and the initial temperature can be understood, noticing that the initial thermal energy remains stored in the common mode fluctuations, $\phi_c(r)$, of the two halves of the system, which are not probed by the interference pattern in the experiment. The emergence of an intermediate steady state different from the thermal equilibrium one is at the present time considered the clearest evidence of a pre-thermalized state. Before concluding, we would like to mention that the light cone effect discussed in the previous sections has been detected also in the out-of-equilibrium dynamics of the coherent split of 1D Bose gases [66]: thermal correlations of a pre-thermalized state emerge locally in their final form and propagate through the system in a light-cone fashion, exactly in the same way discussed for the experiment involving a quench of the Bose Hubbard model in [22].

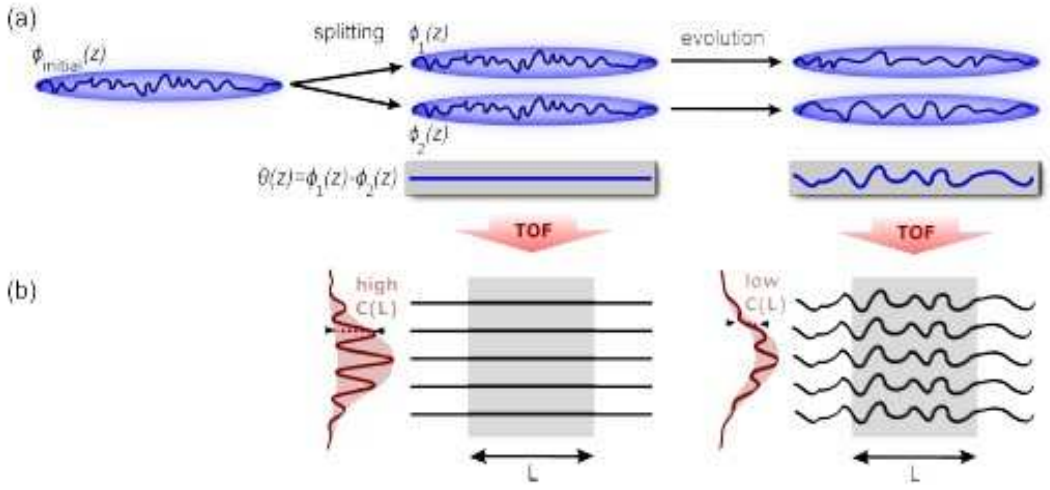

Figure 3.2: Non-equilibrium dynamics of a coherently split 1D Bose gas. In (a) the splitting process and the subsequent evolution are schematically portrayed; in (b) the corresponding patter of the interference contrast is shown. (Taken from [3].)

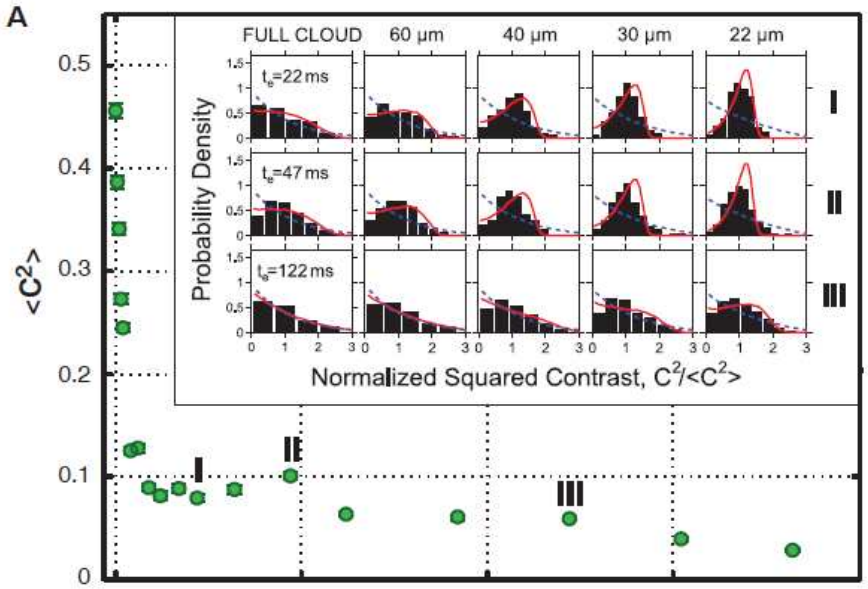

Figure 3.3: Decay of the squared interference contrast versus time. After an initial dephasing (I), the system approach a quasi-steady state (II), and only on much longer time scales the system starts departing from this plateau (III). In the inset the probability density of the normalized square contrast for various system sizes is shown. The same phenomenon can be seen in the main picture from a complementary point of view: the distribution function approaches for long intermediate times a quasi-stationary value and only later it departs towards the eventual thermal state. (Taken from [3].)

Chapter 4

Pre-Thermalization in a Noisy Quantum Ising Chain

In this Chapter we start our study of pre-thermalization in quantum many body systems, considering a Quantum Ising Chain (QIC) perturbed by a time-dependent delta correlated noise in the transverse field direction, and driven out of equilibrium also by a quench of the static component of the transverse field. This system allows for analytic solution of its non-equilibrium dynamics and we elucidate the signature of pre-thermalization and thermalization in observables of physical interest. We find remarkably that pre-thermalization occurs also in noisy quantum many body systems driven out of equilibrium. The work discussed in this Chapter is based on the *Rapid Communication* [6] and on the paper [7].

4.1 The model, the out of equilibrium protocol and the initial state

The focus of this Chapter is in the out of equilibrium dynamics of a perturbed QIC, described by the hamiltonian

$$\begin{aligned} H =& H_0 + V(t), \\ H_0 =& -J\sum_i \sigma_i^x\sigma_{i+1}^x + g\sigma_i^z, \\ V =& \sum_i \delta g(t)\sigma_i^z, \end{aligned} \tag{4.1}$$

where H_0 describes the Integrable Quantum Ising Chain and $V(t)$ is a time-dependent gaussian white noise, with zero average and amplitude Γ,

$$\begin{aligned} \langle \delta g(t)\rangle &= 0, \\ \langle \delta g(t)\delta g(t')\rangle &= \frac{\Gamma}{2}\delta(t-t'). \end{aligned} \tag{4.2}$$

Here $\widehat{\sigma}_i^{x,z}$ are the longitudinal and transverse spin operators at site i and g is the strength of the transverse field. The QIC is among the simplest, yet non-trivial integrable many-body system, whose static properties and quench dynamics are to a great extent known. It is characterized by two dual gapped phases, a quantum paramagnetic ($g > 1$) and ferromagnetic one ($g < 1$) separated by a quantum critical point located at $g = 1$. In the following we assume $J = 1$ and we restore it in the computations only when it is necessary.

We will consider the dynamics for the following out of equilibrium protocol: at time $t < 0$ the system is prepared in the ground state of H_0 with a certain value of the transverse field g_0, $|\psi_0\rangle = |\psi(g_0)\rangle_{GS}$, and $\delta g(t) = 0$. At later time, $t > 0$ the system is evolved according to the full hamiltonian H (see (4.1)) with a different value of the transverse field g, as portrayed in Fig. 4.1.

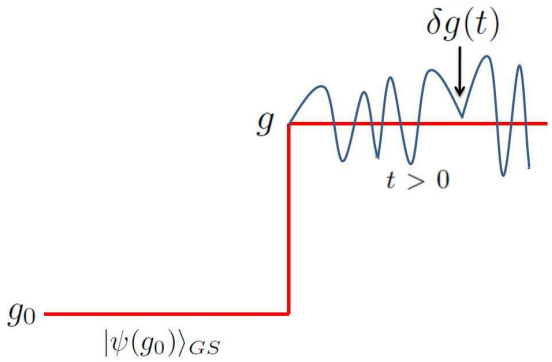

Figure 4.1: Out of equilibrium protocol studied in this paper for the QIC: the system is prepared in the ground state of the Ising chain with $g_0 > 1$ and is evolved according to the Ising Hamiltonian with a different value of the transverse field $g > 1$, plus a gaussian delta-correlated noise on top of it. For simplicity, both g_0 and g are chosen within the paramagnetic phase.

A sudden quench of the transverse field populates all excited states of the system, injecting an extensive ammount of energy; this is easy to understand by looking at the populations and the coherences immediately after the quench. In the basis of the Bogolyubov fermions diagonalizing $H(g)$:

$$\begin{aligned}
\langle\psi_0|\gamma_k^\dagger(g)\gamma_k(g)|\psi_0\rangle &= \sin^2(\theta_k - \theta_k^0) \\
\langle\psi_0|\gamma_k^\dagger(g)\gamma_{-k}^\dagger(g)|\psi_0\rangle &= -i\frac{\sin 2(\theta_k - \theta_k^0)}{2} \\
\langle\psi_0|\gamma_{-k}(g)\gamma_k(g)|\psi_0\rangle &= i\frac{\sin 2(\theta_k - \theta_k^0)}{2} \\
\langle\psi_0|\gamma_{-k}(g)\gamma_{-k}^\dagger(g)|\psi_0\rangle &= \cos^2(\theta_k - \theta_k^0),
\end{aligned} \tag{4.3}$$

where $\theta_k \equiv \theta_k(g)$ and $\theta_k^0 \equiv \theta_k(g_0)$. Moreover, the initial state can be written as a coherent superposition of pairs of quasiparticles created on the vacuum of the theory after the quench ($H(g)$):

$$|\psi(g_0)\rangle_{GS} = N \prod_{k>0} \Big(1 + i \tan(\Delta\theta_k)\gamma_k^\dagger(g)\gamma_{-k}^\dagger(g)\Big)|\psi(g)\rangle_{GS}, \tag{4.4}$$

where

$$\begin{aligned} &\Delta\theta_k = \theta_k - \theta_k^0, \\ &N = \exp\Big[-\frac{1}{2}\sum_{k>0}\log(1+\tan^2\Delta\theta_k)\Big]. \end{aligned} \tag{4.5}$$

Below we will focus on the interplay between the effect of a sudden quench of g and the time dependent noise driving the dynamics of the system.

4.2 Statistics of the work $P(w)$

Let us start our analysis by considering the statistic of the work done on a quantum many body system after a quantum quench, $P(w)$ characterized by a generic non-equilibrium protocol $g(t)$. This quantity requires two energy measurements: one at the initial time, $t = \tau_0$, and one at the final time $t = \tau$ (for a comprehensive review on the subject see [58]). We assume that the final energy is measured with respect to the final hamiltonian, H_τ, and that for each realization of the out-of-equilibrium protocol the work w is given as a difference of the outcomes of the two measures of the energy at initial and final time. The statistics of the work is then defined as

$$P(w) = \sum_{n,m} \delta(w - (E_n(\tau) - E_m(\tau_0)))p(n|m,\tau)p_m, \tag{4.6}$$

with $p(n|m,\tau) \equiv |\langle\psi_n(\tau)|U(\tau,\tau_0)|\psi_m(\tau_0)\rangle|^2$, and $p_m \equiv |\langle\psi_m(\tau_0)|\phi(\tau_0)\rangle|$, where $|\phi(\tau_0)\rangle$ is the initial state of the system, $U(\tau,\tau_0)$ is the evolution operator from τ_0 to τ, and $|\psi_i(\tau)\rangle$ are the instantaneous wave-functions, computed from the equation $H_t|\psi_i(t)\rangle = E_i(t)|\psi_i(t)\rangle$. In Ref. [58], it has been shown that the characteristic function $G(u) = \int dw e^{iuw} P(w)$ contains full information about the statistics of the work w and can be written as a two time correlation function

$$G(u) = \langle e^{iuH^H_{\tau,\tau_0}} e^{-iuH_{\tau_0}}\rangle, \tag{4.7}$$

where $H^H_{\tau,\tau_0} = U^\dagger(\tau,\tau_0)H_{\tau,\tau_0}U(\tau,\tau_0)$ is the final Hamiltonian used in the final measurement in the Heisenberg picture. For a sudden quench it follows immediately that

$$G(u) = \langle e^{iH(g_1)u} e^{-iH(g_0)u}\rangle, \tag{4.8}$$

where $H(g_0)$ and $H(g_1)$ are the initial and final hamiltonian respectively.

One may compute exactly the statistics of the work for a generic time variation of the transverse field in the QIC (see the Appendix of this Chapter and Ref. [60]). For a sudden quench of the transverse field in the QIC, one obtains for $P(w)$, at low w, a peak located at ΔE_0, i.e. the difference in the ground states energies before and after the quench, plus a continuum starting above 2Δ, describing pairs of quasi-particles. This continuum displays an edge singularity with universal features [59, 60]. For sudden quenches within the paramagnetic phase, one may obtain

$$P(\omega) \propto \delta(\omega) + \frac{\sqrt{\pi}}{4}\frac{\Theta(\omega - 2\Delta)}{\delta}\rho_-^2\sqrt{\frac{\omega - 2\Delta}{\Delta}}, \tag{4.9}$$

where $\delta = 4\pi/L$ is the two-particle level spacing, $\omega = w - \Delta E_0$, $\rho_- = \frac{\Delta_0 - \Delta_1}{\Delta_0}$ and Θ is the Heaviside step function [59].

Since the exponents of these singularities are expected to be universal [59] it is natural to start our study of the effect of the noise by clarifying its role on the universal low-energy behaviour of the statistics of the work. We separate two effects: first we consider a quench with a final random value of the transverse field drawn from a gaussian distribution function and then a gaussian time-dependent delta correlated noise acting on the system during its time evolution till the measurement time $t = \tau$.

As a warm up, let us start with the first case, a quench of the QIC with a final value of the transverse field drawn from a gaussian distribution function, corresponding to a value of the final mass, centered in $\overline{\Delta}$ and with variance γ:

$$p(\Delta) = \frac{1}{\gamma\sqrt{2\pi}}e^{-\frac{(\Delta-\overline{\Delta})^2}{2\gamma^2}}. \tag{4.10}$$

We now want to compute $P(\omega)$ averaged over this probability distribution. The average energy injected into the system through this quench is equal to the energy injected in a sudden protocol

$$\begin{aligned}\Delta E_{injected} &\equiv \overline{\langle\psi(g_0)|(H(\overline{g}+\eta) - H(g_0))|\psi(g_0)\rangle} = \\ &= \Delta E_{Quench} \equiv \langle\psi(g_0)|(H(\overline{g}) - H(g_0))|\psi(g_0)\rangle,\end{aligned} \tag{4.11}$$

meaning that the noise affects the statistic of the work, $P(\omega)$, starting from the second and higher order moments. Nevertheless, as shown below, the probability distribution (averaged over disorder) is reshaped in the energy window of interest. We can study the statistics of the work by taking the average of (4.9) over the gaussian distribution (4.10) and assuming $\frac{\gamma}{\overline{\Delta}} \ll 1$, $\frac{\gamma}{|\overline{\Delta}-\Delta_0|} \ll 1$, i.e. the fluctuations of the noise are small compared to the final gap and the amplitude of the quench.

First of all, it is important to notice that the energy difference of the ground states ΔE_0^{noise}, can be expressed as the difference in the ground states

one would have without noise ΔE_0, plus an extensive correction proportional to the fluctuations $\eta = \Delta - \overline{\Delta}$:

$$\begin{aligned} \Delta E_0^{noise} &= E_{GS}(\overline{g}+\eta) - E_{GS}(g_0) \backsimeq \Delta E_0 - f(\overline{g})\eta, \\ \Delta E_0 &= -\Big(\frac{\overline{g}+1}{\pi} E\Big(\frac{4\overline{g}}{(1+\overline{g})^2}\Big) - \frac{g_0+1}{\pi} E\Big(\frac{4g_0}{(1+g_0)^2}\Big)\Big) \end{aligned} \tag{4.12}$$

where we retained only the first order term of the expansion [1] and E is a complete elliptic function. The function $f(\overline{g})$ [2] can be expressed as a combination in the following way

$$f(\overline{g}) = \frac{L}{\pi}\Big[\frac{1}{\pi} E\Big(\frac{4\overline{g}}{(1+\overline{g})^2}\Big) + \frac{\overline{g}-1}{2(\overline{g}+1)^2} \times_2 F_1\Big(\frac{1}{2}, \frac{3}{2}, 2, \frac{4\overline{g}}{(\overline{g}+1)^2}\Big)\Big] \equiv L\Xi(\overline{g}). \tag{4.13}$$

where ${}_2F_1$ is an hypergeometric function.

Below we focus on the *average* statistics of the work

$$\begin{aligned} P(\omega) \propto \int_{-\infty}^{\infty} d\eta \frac{e^{-\frac{\eta^2}{2\gamma^2}}}{\sqrt{2\pi\gamma}} \Big[\delta(\omega + f(\overline{g})\eta) + + \frac{\sqrt{\pi}}{4} \frac{\Theta(\omega + f(\overline{g})\eta - 2\overline{\Delta} - 2\eta)}{\delta} \times \\ \times \Big(\frac{\Delta_0 - \overline{\Delta} - \eta}{\Delta_0}\Big)^2 \sqrt{\frac{\omega + f(\overline{g})\eta - 2\overline{\Delta} - 2\eta}{\overline{\Delta} + \eta}}\Big] \simeq \frac{e^{-\frac{\omega^2}{2(\gamma f(\overline{g}))^2}}}{\sqrt{2\pi}\gamma f(\overline{g})} + \\ + \int_{-\infty}^{\infty} d\eta \frac{e^{-\frac{\eta^2}{2\gamma^2}}}{\sqrt{2\pi\gamma}} \frac{\sqrt{\pi}}{4} \frac{\Theta(\omega + f(\overline{g})\eta - 2\overline{\Delta} - 2\eta)}{\delta} \rho_-^2 \sqrt{\frac{\omega + f(\overline{g})\eta - 2\overline{\Delta} - 2\eta}{\overline{\Delta}}} \end{aligned} \tag{4.14}$$

where in the second line we assumed $\frac{\gamma}{\overline{\Delta}} \ll 1$ and $\frac{\gamma}{|\overline{\Delta} - \Delta_0|} \ll 1$. This formula contains two physical effects, the first one is a global fluctuation involving the shift of the ground state energy (see Eq. (4.12)). This effect is proportional to the system size L and affects in the same way both the delta peak singularity and the continuum starting at $\omega = 2\Delta$. The second effect is associated to the fluctuations affecting the masses of the quasi-particles emitted after the quench and it does not scale with the size of the system. If one is interested in measuring the work with reference to ΔE_0 in an energy window close to $\Delta E_0 + 2\overline{\Delta}$, the first type of fluctuations are obviously dominant and most importantly detrimental. Indeed, the last integral in Eq. (4.14) can be

[1] Expansion (4.12) can be truncated at the first order provided that $\Gamma \ll 2\Big|\frac{\partial_g E_{GS}(g)}{\partial_g^2 E_{GS}(g)}\Big| \equiv \mathcal{F}(g)$. $\mathcal{F}(g)$ is an increasing positive monotonic function that never vanishes in the paramagnetic phase ($g > 1$).

[2] The function $\Xi(g)$ is a monotomic function within the paramagnetic phase ($g > 1$), $0.45 \lesssim \Xi(g) \lesssim 0.50$.

cast in the following form $A\sqrt{\gamma'}\int_{-c}^{\infty} dy e^{-y^2/2}\sqrt{y+c}$ (where $A = \frac{1}{4\sqrt{2}}\frac{1}{\delta}\frac{\rho_-^2}{\sqrt{\overline{\Delta}}}$, $\gamma' = \gamma(f(g)-2)$ and $c = \frac{\omega-2\overline{\Delta}}{\gamma'}$). At energies around $2\overline{\Delta}$ one would observe

$$\overline{P(\omega)} \simeq \frac{1}{\sqrt{2\pi}\gamma'} + C\frac{\rho_-^2}{\delta}\sqrt{\frac{\gamma'}{\overline{\Delta}}}\Big(\frac{1}{\Gamma(\frac{5}{4})} + \frac{\sqrt{2}}{\Gamma(\frac{3}{4})}\frac{\omega-2\overline{\Delta}}{\gamma'} + ...\Big) \tag{4.15}$$

where C is a numerical prefactor and Γ is the Euler Gamma function.

It could be interesting to subtract these fluctuations by some means. In order to to so there are in principle two possibilities: the first one is to measure for each realization only the energy differences with respect to the threshold, subtracting the extensive shift of the ground state energy due to the noise (see Eq.(4.12)); the second one consists in rescaling the noise amplitude by the system size, $\gamma \to \frac{\gamma}{L}$. In both ways Eq. (4.14) can be properly averaged in the energy range of interest. For $\omega - 2\overline{\Delta} \gg \gamma'$

$$P(\omega) \propto P_{quench}(\omega)\Big(1 + O\Big(\frac{\gamma\Xi(g)}{(\omega-2\overline{\Delta})}\Big)^2\Big), \tag{4.16}$$

which essentially means that well above the energy threshold for the production of pairs of quasi-particles in a sudden quench, the statistics of the work is left unchanged. On the other hand, for $\omega \ll 2\overline{\Delta} - \gamma'$, the statistics of the work displays a gaussian tail controlled by the renormalized noise amplitude γ',

$$P(\omega) \propto \frac{\rho_-^2}{\delta}\sqrt{\frac{\gamma'}{\overline{\Delta}}}\Big(\frac{\gamma'}{|\omega-2\overline{\Delta}|}\Big)^{3/2} e^{-\frac{(\omega-2\overline{\Delta})^2}{2\gamma'^2}}. \tag{4.17}$$

Let us now proceed our analysis considering more complicated effects. We prepare the system in the ground state of the Ising chain in the paramagnetic phase, with $g_0 > 1$ and we let evolve the system under the generic time-dependent hamiltonian $H_0 + V(t)$. In the following we assume that we have subtracted the shift of the ground state energy and that the amplitude of the noise has been rescaled.

It is a remarkable fact that for each realization of the noise the square root singularity at the lower energy threshold is independent from the out-of equilibrium protocol performed on the QIC [60]; what changes is the spectral weight of the singularity in $P(w)$, which in general will depend on the details of the time dependent quench, as discussed in the Appendix of this Chapter. The expression of the statistics of the work in this case is

$$P(\omega,\tau) \simeq \delta(\omega) + \frac{\sqrt{\pi}}{4}\frac{\Theta(\omega-2\Delta(\tau))}{\delta}|\rho(\tau)|^2\sqrt{\frac{\omega-2\Delta(\tau)}{\Delta(\tau)}}, \tag{4.18}$$

where

$$
\begin{aligned}
|\rho(\tau)|^2 &\equiv \Delta^2(\tau)\Big|\rho - \int_0^\tau \frac{e^{2i\int_0^t dt'\Delta(t')}}{\Delta(t)^2}\dot{\Delta}(t)dt\Big|^2 \\
&= \Delta^2\Big(\rho^2 - 2\rho Re\Big[\int_0^\tau \frac{e^{2i\int_0^t dt'\Delta(t')}}{\Delta(t)^2}\dot{\Delta}(t)dt\Big] + \\
&+ \Big|\int_0^\tau \frac{e^{2i\int_0^t dt'\Delta(t')}}{\Delta(t)^2}\dot{\Delta}(t)dt\Big|^2\Big)
\end{aligned}
\tag{4.19}
$$

and $\rho = \frac{\Delta_0 - \Delta(0)}{\Delta_0\Delta(0)}$, where in general $\Delta(0)$ is different from Δ_0.

The derivation of Eq. (4.18) is postponed in the Appendix of this Chapter. Using integration by parts, it is easy to show that

$$
\int_0^\tau \frac{e^{2i\int_0^t dt'\Delta(t')}}{\Delta(t)^2}\dot{\Delta}(t)dt = \frac{1}{\Delta(0)} - \frac{1}{\Delta(\tau)}e^{2i\int_0^\tau dt'\Delta(t')} + 2i\int_0^\tau dt e^{2i\int_0^t dt'\Delta(t')},
\tag{4.20}
$$

When taking the noise average of these expressions there are going to be two separate effects. The first will consist in fluctuations of Δ at the initial and final point of the trajectory which will produce consequences similar to the ones discussed above in the static case. If we think to the statistics of $\Delta(t)$ as being Gaussian with:

$$
\langle\Delta(t)\Delta(t')\rangle \simeq \frac{\Gamma}{2}\delta_{\tau_c}(t-t'),
\tag{4.21}
$$

where τ_c is a correlation time [3], the fluctuations at the endpoints have amplitude $\gamma = \sqrt{\frac{\Gamma}{\tau_c}}$. Now in the limit, $\frac{\gamma}{\Delta}$, $\frac{\gamma}{|\Delta-\Delta_0|} \ll 1$ we argue that to the leading order the various terms in Eq. (4.18) can be averaged separately:

$$
P(\omega,\tau) \simeq \delta(\omega) + \frac{\sqrt{\pi}}{4}\frac{\Theta(\omega-2\Delta(\tau))}{\delta}\overline{|\rho(\tau)|^2}\overline{\sqrt{\frac{\omega-2\Delta(\tau)}{\Delta(\tau)}}}.
\tag{4.22}
$$

While the average of the square root singularity will produce the smearing of the singularity described above, the average of the spectral weight will produce a time dependent prefactor that appears to describe the heating of the system under the influence of the noise. In order to average $\overline{|\rho(\tau)|^2}$, we first notice that for $\frac{\gamma}{\Delta}$, $\frac{\Gamma}{\Delta} \ll 1$, we have

$$
\overline{\frac{1}{\Delta(\tau)}e^{2i\int_0^\tau dt'\Delta(t')}} \simeq \frac{1}{\overline{\Delta(\tau)}}\overline{e^{2i\int_0^\tau dt'\Delta(t')}} \simeq \frac{1}{\Delta}e^{-\Gamma\tau}e^{2i\Delta\tau},
\tag{4.23}
$$

[3] This can be easily seen introducing a finite correlation time τ_c, $\langle\eta(t)\eta(t')\rangle = \frac{\Gamma}{2}\frac{1}{\sqrt{2\pi\tau_c^2}}e^{-\frac{(t-t')^2}{2\tau_c^2}}$; taking the limit $t \to t'$, from the two-time correlation function we need to recover $\langle\eta^2(t)\rangle \sim \gamma^2$, and so $\gamma \sim \sqrt{\frac{\Gamma}{\tau_c}}$. If the condition $\tau \gg \tau_c$ is properly taken into account, a gaussian correlated noise gives the same result of a delta correlated noise.

where crossed correlations with the boundary term proportional to $\Delta(\tau)$ can be neglected. Indeed, expanding in Taylor series the left hand side, we get

$$\frac{e^{2i\Delta\tau}}{\Delta}\Big(1-\frac{\eta(\tau)}{\Delta}+\frac{\eta(\tau)^2}{\Delta^2}+...\Big)\Big(1+2i\int_0^\tau dt'\eta(t')+\frac{1}{2}(2i)^2\int_0^\tau dt'dt''\eta(t')\eta(t'')+...\Big) \tag{4.24}$$

and, taking the average over the noise, we finally have

$$\frac{e^{2i\Delta\tau}}{\Delta}e^{-\Gamma\tau}\Big(1-i\frac{\Gamma}{\Delta}+\Big(\frac{\gamma}{\Delta}\Big)^2-\Big(\frac{\Gamma}{\Delta}\Big)^2-i\Big(\frac{\gamma}{\Delta}\Big)^2\frac{\Gamma}{\Delta}+i\Big(\frac{\Gamma}{\Delta}\Big)^3+...\Big) \tag{4.25}$$

It should be clear that in the limit $\frac{\gamma}{\Delta}\ll 1$, $\frac{\Gamma}{\Delta}\ll 1$, only the first term can be kept in the right hand side of (4.25).

Using Eq. (4.20), Eq. (4.21), and neglecting correlations coming from boundary terms, it is now straightforward to average over the noise; for instance, for the second term in Eq. (4.19) we get

$$\begin{aligned}&\overline{Re\Big[\int_0^\tau\frac{e^{2i\int_0^t dt'\Delta(t')}}{\Delta(t)^2}\dot{\Delta}(t)dt\Big]}=\frac{1}{\Delta}\Big(1-e^{-2\Gamma\tau}\cos(2\Delta\tau)\Big)+\\&+\frac{1}{\Delta^2+\Gamma^2}\Big[\Delta\Big(e^{-2\Gamma\tau}\cos(2\Delta\tau)-1\Big)+\Gamma e^{-2\Gamma\tau}\sin(2\Delta\tau)\Big]\simeq\\&\overset{\simeq}{\frac{\Gamma}{\Delta}\ll 1}\frac{\Gamma}{\Delta^2}e^{-2\Gamma\tau}\sin(2\Delta\tau).\end{aligned} \tag{4.26}$$

which is of order $\frac{\Gamma}{\Delta}$ when reinserted in (4.19).

The third contribution can be written as

$$\begin{aligned}&\Big|\int_0^\tau\frac{e^{2i\int_0^t dt'\Delta(t')}}{\Delta(t)^2}\dot{\Delta}(t)dt\Big|^2\equiv\Big(\frac{1}{\Delta(0)}-\frac{1}{\Delta(\tau)}e^{2i\int_0^\tau dt'\Delta(t')}+2i\int_0^\tau dte^{2i\int_0^t dt'\Delta(t')}\Big)\times\\&\times\Big(\frac{1}{\Delta(0)}-\frac{1}{\Delta(\tau)}e^{-2i\int_0^\tau dt'\Delta(t')}-2i\int_0^\tau dte^{-2i\int_0^t dt'\Delta(t')}\Big)=\\&=\Big|\frac{1}{\Delta(0)}-\frac{1}{\Delta(\tau)}e^{2i\int_0^\tau dt'\Delta(t')}\Big|^2+2Re\Big[2i\Big(\frac{1}{\Delta(0)}-\frac{1}{\Delta(\tau)}e^{-2i\int_0^\tau dt'\Delta(t')}\Big)\times\\&\times\int_0^\tau dte^{2i\int_0^t dt'\Delta(t')}\Big]+4\int_0^\tau dte^{2i\int_0^t dt'\Delta(t')}\times\int_0^\tau dte^{-2i\int_0^t dt'\Delta(t')}.\end{aligned} \tag{4.27}$$

Under the same approximations stated above and using again (4.20), it is possible to average (4.27) over the time-dependent noise (4.21), disregarding noise fluctuations in the boundary terms proportional to $\Delta(0)$ and $\Delta(\tau)$. To compute the average of (4.27), we need to average products of two noise dependent quantities; for instance, it is easy to derive

$$\overline{4\int_0^\tau dte^{2i\int_0^t dt'\Delta(t')}\times\int_0^\tau dte^{2i\int_0^t dt'\Delta(t')}}\overset{\simeq}{\frac{\Gamma}{\Delta}\ll 1}4\frac{\Gamma\tau}{\Delta^2}+O\Big(\frac{\Gamma}{\Delta}\Big) \tag{4.28}$$

while all the other terms in (4.27) are subleading in the limit $\frac{\Gamma}{\Delta} \ll 1$ and $\frac{\gamma}{\Delta} \ll 1$.

Hence, our result on the statistics of the work, $P(\omega, \tau)$, can be summarized in the following expression which contains a transparent physical meaning

$$P(\omega, \tau) \simeq \delta(\omega) + (\rho_-^2 + 4\Gamma\tau)Q(\omega) \tag{4.29}$$

where

$$Q(\omega) = \frac{\sqrt{\pi}}{4}\overline{\frac{\Theta(\omega - 2\Delta)}{\delta}\sqrt{\frac{\omega - 2\Delta}{\Delta}}}. \tag{4.30}$$

The long time growth of the spectral weight appears to indicate the continuous heating of the system (it resembles the time dependence of the energy absorbed by the system at the early stages of the dynamics, as it will be clear from Eq.(4.52)). Notice indeed that the energy absorbed by the system during the time-dependent protocol $g(t)$ is non zero, in sharp contrast to the static case, as we will show in the next Section. In the following we will study in more sophisticated quantities the interplay between dynamical noise and coherent effects due to a quantum quench of the Ising Chain.

4.3 Kinetic equations

In this section we are going to study the kinetics of local observables and their correlation functions in the QIC. In order to accomplish this task, we are interested in deriving a kinetic equation for the equal time non-equilibrium Green's function for the protocol discussed in the previous Section. We will do so by deriving a master equation, using the Keldysh contour technique, in order to obtain analytically an expression for the 2-point functions of Bogolyubov fermions at equal time. These equations will then be used to compute all the observables of interest and their the out-of-equilibrium dynamics.

We start recalling the definition of the statistical Green function on the Keldysh contour [62]

$$G^c = -i\langle T_c \psi_{ki}(\tau)\psi^\dagger_{kj}(\tau')\rangle, \tag{4.31}$$

where T_c is the time ordering operator on the Keldysh contour, τ and i and j are indices in the Nambu space; we define the lesser Green function as

$$G^<(t, t') = \left[G^<_k(t, t')\right]_{i,j} = i\langle \psi^\dagger_{k,j}(t')\psi_{k,i}(t)\rangle, \tag{4.32}$$

which is a matrix in the Nambu space (here t and t' are real times).
Using the standard approach [62], we first write the equation for the statistical Green function with the noise as a perturbation and we resum the Dyson

series (Fig. 4.2)

$$G^c_{\tau,\tau'} = G^c_{0_{\tau,\tau'}} + G^c_{0_{\tau,\tau''}} \otimes \Sigma^c_{\tau'',\tau'''} \otimes G^c_{\tau''',\tau'} \tag{4.33}$$

where $G^c_{0_{\tau,\tau'}}$ is the unperturbed Green function and $\Sigma^c_{\tau,\tau'}$ is the self energy; in right hand side the symbol $\otimes$ is understood as a convolution product, all the quantities are evaluated along the Keldysh contour.

In the following we will neglect noise crossed diagrams, computing the self-energy within the so called *self-consistent Born approximation* [62], controlled by the small parameter $\frac{\Gamma}{\Delta}$, as illustrated in Fig. 4.2.

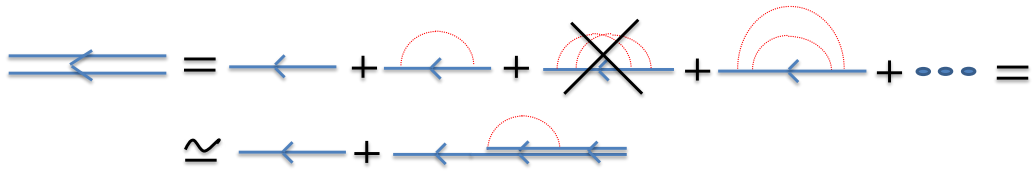

Figure 4.2: A diagraatic representation of the Dyson series (4.33). Crossed dyagrams are neglected according to the *self-consistent Born approximation*.

The Dyson equation for the statistical Green function is then

$$\begin{aligned} i\partial_t G^<(t,t') =& H_k G^<(t,t') + \int dt''[\Sigma^<(t,t'')G^a(t'',t')+ \\ &+ \Sigma^r(t,t'')G^<(t'',t')], \\ -i\partial_{t'} G^<(t,t') =& G^<(t,t')H_k + \int dt''[G^r(t,t'')\Sigma^<(t'',t')+ \\ &+ G^<(t,t'')\Sigma^a(t'',t')]. \end{aligned} \tag{4.34}$$

Within the self consistent Born approximation, we obtain for the self energies in (4.34):

$$\begin{aligned} \Sigma^<_{t,t'} &= \frac{\Gamma}{2}\delta(t-t')\sigma_z G^<_{t,t'}\sigma_z \\ \Sigma^{r,a}_{t,t'} &= \mp i\frac{\Gamma}{4}\delta(t-t'). \end{aligned} \tag{4.35}$$

We substitute (4.35) in (4.34), subtract the two resulting equations and take the limit $t \to t'$; defining the density matrix

$$\rho_k(t) = -iG^<_k(t,t) \tag{4.36}$$

we finally obtain the master equation

$$\delta_t \rho_k = -i[H_k, \rho_k] + \frac{\Gamma}{2}(\sigma_z \rho_k \sigma_z - \rho_k), \tag{4.37}$$

where $[H_k, \rho_k]$ is responsible for the free dynamics and the second term on the right hand side contain information about the dissipation due to the noise.

We now apply to (4.37) a Bogolyubov rotation $U(\theta_k) = \exp(-i\theta_k\sigma_x)$ with $\theta_k = 1/2 \arctan[(\sin k)/(g-\cos k)]$, which diagonalizes the Ising model in the basis of the Bogoliubov fermions γ_k. We get

$$\partial_t \rho_k = -i[\widetilde{H_k}, \rho_k] + \frac{\Gamma}{2}(\sigma'\rho_k\sigma' - \rho_k), \tag{4.38}$$

where $\sigma' = U^\dagger(\theta_k)\sigma_z U(\theta_k) = \cos 2\theta_k\sigma_z + \sin 2\theta_k\sigma_y$ and the density matrix is expressed in the basis of the Bogoliubov fermions.

Before solving Eq. (4.38), let us comment on the properties of the noise. In the base diagonalizing the final hamiltonian, H_k appears as

$$\begin{aligned} H_k =& E_k\sigma_z + \delta g(t)(\sigma_z \cos 2\theta_k + \sigma_y \sin 2\theta_k) = \\ & E_k\sigma_z + \delta g_k^z(t)\sigma_z + \delta g_k^y(t)\sigma_y, \end{aligned} \tag{4.39}$$

where $\delta g_k^z(t)$ and $\delta g_k^y(t)$ statisfy

$$\begin{aligned} \langle \delta g_k^z(t)\delta g_k^z(t')\rangle &= \frac{\Gamma}{2}(\cos 2\theta_k)^2\delta(t-t'), \\ \langle \delta g_k^y(t)\delta g_k^y(t')\rangle &= \frac{\Gamma}{2}(\sin 2\theta_k)^2\delta(t-t'), \end{aligned} \tag{4.40}$$

where it should be easy to see that our model is equivalent to the QIC perturbed by two k-dependent delta correlated noises, one along the z direction and the other one along y. Moreover the noise along the y direction is correlated to the noise along the z direction

$$\langle \delta g_k^z(t)\delta g_k^y(t')\rangle = \frac{\Gamma}{2}\sin 2\theta_k \cos 2\theta_k \delta(t-t'). \tag{4.41}$$

The usual way to solve a master equation like (4.38) is to decompose the density matrix in the basis of the Pauli matrices

$$\rho_k = \frac{1}{2}\mathbf{1} + \delta f_k\sigma_z + x_k\sigma_x + y_k\sigma_y. \tag{4.42}$$

Plugging this decomposition in the master equation (4.38) we end up with a system of differential equations for the coefficients of the density matrix (4.42)

$$\begin{aligned} \partial_t(\delta f_k) &= -\Gamma \sin^2 2\theta_k \delta f_k + \frac{\Gamma}{2} y_k \sin 4\theta_k \\ \partial_t x_k &= -\Gamma x_k - 2E_k y_k \\ \partial_t y_k &= \frac{\Gamma}{2}\sin 4\theta_k \delta f_K + 2E_k x_k - \Gamma \cos^2 2\theta_k y_k. \end{aligned} \tag{4.43}$$

We will in the following solve this system of equations in the limit $\frac{\Gamma}{\Delta} \ll 1$, which allows to neglect y-z correlations; we checked this approximation

numerically for different values of k in the Brillouin zone. Taking into account the different initial conditions (4.3), corresponding to an extensive amount of energy injected in the system by the quench of the transverse field, we immediately obtain

$$\delta f_k(t) = (\sin^2(\Delta\theta_k) - 1/2)e^{-\Gamma t \sin^2 2\theta_k}. \tag{4.44}$$

For the coherences $z_k = x_k - iy_k$ we instead obtain

$$\partial_t z_k = (2E_k i - \Gamma)z_k + \frac{\Gamma}{2}(1 - \cos^2(2\theta_k))\frac{z_k - z_k*}{2}; \tag{4.45}$$

from this equation we see that the coherences decay exponentially fast as $\Gamma t \gg 1$, as one can see close to $k \simeq 0, \pi$:

$$z_k \simeq z_k^0 e^{2iE_k t} e^{-\Gamma t}. \tag{4.46}$$

On the other hand, from equation (4.44), we see that while most of the modes relax fast to their thermal occupation ($n_k \simeq 1/2$) on time scales of the order of $1/\Gamma$, the relaxation rates tend to vanish close to the band edges ($k = 0, \pm\pi$) (see Fig. 4.3).

We give the expression for δf_k and z_k for $k \simeq 0$, as they will be useful to compute the leading behaviour of physical observables during thermalization dynamics, as it will be more clear in the next sections:

$$\begin{aligned} \langle \gamma_k^\dagger \gamma_k \rangle &= \frac{1}{2} + \frac{1}{2}\Big(\frac{k^2}{2\Delta^2}\rho_-^2 - 1\Big)e^{\frac{-\Gamma k^2 t}{\Delta^2}} \\ \langle \gamma_k^\dagger \gamma_{-k}^\dagger \rangle &= -\frac{ik}{2\Delta}\rho_- e^{-\alpha t - i\beta t}, \end{aligned} \tag{4.47}$$

where $\rho_- \equiv \frac{\Delta_0 - \Delta}{\Delta_0}$ and

$$\begin{aligned} \alpha &= \Gamma\Big(1 - \frac{1}{2}\Big(\frac{k}{\Delta}\Big)^2\Big) \\ \beta &= 2\Delta\Big(1 + \frac{1}{2}\Big(\frac{k}{\Delta}\Big)^2\Big). \end{aligned} \tag{4.48}$$

4.4 Thermalization Dynamics of Observables

Let us start now the study of the interplay between quench and noise in the time evolution of observables of interest, studying their dynamics from the intial state towards the asymptotic steady state, which is the infinite temperature state, where all fermion modes are equally occupied, $n_k = 1/2$, for all k in the Brillouin zone. We shall start computing the energy absorbed by the system. We will then be concerned with the study of thermalization dynamics of the transverse magnetization correlator and, finally, we are going to look for signatures of the noise in the time evolution of the order parameter correlations.

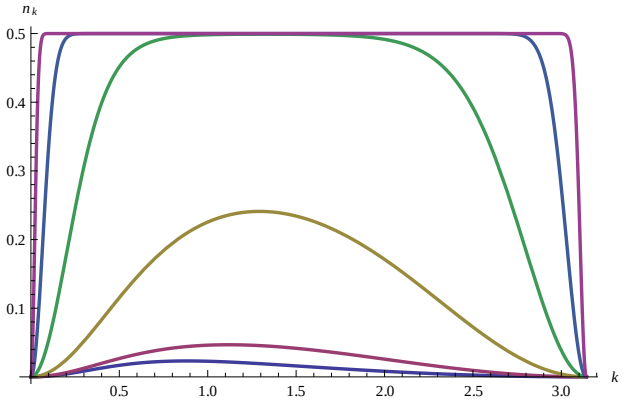

Figure 4.3: Populations, $n_k = \langle \gamma_k^\dagger \gamma_k \rangle$ *vs* wave vector k at different times: from bottom to up, $\Gamma t = 0.1, 1, 10, 10^2, 10^3, 10^4$ ($g_0 = 2$, $g = 4$).

4.4.1 Energy absorbed by the QIC

Let us start considering the energy absorbed by the system during the noisy protocol:

$$E(t) = \langle \psi(t) | H(g(t)) | \psi(t) \rangle, \tag{4.49}$$

where $|\psi(t)\rangle$ is the state at time t. Substituting the expression for the hamiltonian (2.28), we get

$$\begin{aligned} E(t) =& \langle \psi(t) | \Big(H_0(g) + \delta g(t) \sum_i \sigma_i^z \Big) | \psi(t) \rangle = \\ =& \langle \psi(t) | H_0(g) | \psi(t) \rangle + \delta g(t) \langle \psi(t) | \sum_i \sigma_i^z | \psi(t) \rangle. \end{aligned} \tag{4.50}$$

Let us now assume that at the time τ and onwards the noise is turned off. Therefore the total energy acquired at time τ by the system is

$$E(\tau) = N \int_0^\pi \frac{dk}{2\pi} E_k(g) (\langle \gamma_k^\dagger(\tau) \gamma_k(\tau) \rangle - \langle \gamma_{-k}(\tau) \gamma_{-k}^\dagger(\tau) \rangle). \tag{4.51}$$

We can now use the expectation values for the two-point functions of the Bogolyubov fermions derived in the previous section to evaluate this expression as a function of τ. For times $\Gamma\tau \ll 1$, the energy is equal to the energy injected in an ordinary quench E_{Quench} plus small corrections

$$E(\tau) = E_{Quench} + N \int_0^\pi \frac{dk}{2\pi} \epsilon_k \cos(2\Delta\theta_k) \sin^2(2\theta_k) \Gamma\tau, \tag{4.52}$$

where $E_{Quench} = -\frac{N}{2\pi} \int_0^\pi dk \epsilon_k \cos(2\Delta\theta_k)$ is the energy injected in the system by a sudden quench.

At longer times, $\Gamma t \gg 1$, the energy saturates towards its asympotic limit, zero with our choice of the vacuum energy, with an asymptotic power

law behaviour $\frac{1}{\sqrt{\Gamma t}}$, which is the signature of the slow relaxation of $k \simeq 0, \pi$ modes [4]. In particular, (4.51) can be written as

$$\begin{aligned} E(t) &= \frac{N}{2\pi}\int_0^\pi 2E_k \delta f_k = \\ &= -\frac{N}{2\pi}\int_0^\pi dk E_k \cos 2\Delta\theta_k e^{-\Gamma t \sin^2 2\theta_k} \end{aligned} \tag{4.53}$$

and for $\Gamma t \gg 1$ this quantity is dominated by the modes with smallest relaxation rate, $k \simeq 0, \pi$, with the final result

$$E(t)_{\Gamma t \gtrsim 1} - \frac{N}{2\sqrt{\pi}}\frac{g^2+1}{\sqrt{\Gamma t}}. \tag{4.54}$$

4.4.2 Evolution of the number of kinks

Let us now turn our attention to a more interesting quantity to highlight the dynamics of thermalization: the density of the number of kinks, defined as

$$n_{kink} \equiv \frac{1}{2N}\sum_i \langle (1 - \sigma_i^x \sigma_{i+1}^x)\rangle. \tag{4.55}$$

Simple algebraic manipulations yield

$$\begin{aligned} n_{kink}(t) &= \frac{1}{2N}\sum_k (1 + 2\langle \gamma_k^\dagger(g=0)\gamma_k(g=0)\rangle) = \\ &= \frac{1}{2N}\sum_k \Big(2 + 2\delta f_k(t)\cos 2\Delta\alpha_k^* + 2y_k(t)\sin 2\Delta\alpha_k^*\Big). \end{aligned} \tag{4.56}$$

This result has been obtained by expressing Bogoliubov fermions at $g = 0$ in terms of fermions diagonalizing the chain at finite g, consequently $\Delta\alpha_k^* = \theta_k(g=0) - \theta_k(g)$ is the difference between the two angles. It is clear from this expression that the number of kinks can be written as the sum of two terms, $n_{kink}(t) \equiv n_{drift}(t) + \Delta n(t)$, the first due to populations (plus the constant term) and describing the heating of the system towards the asymptotic steady state and the second one responsible for dephasing and exclusively due to coherences, which is at the origin of an intermediate stage of the dynamics of n_{kink}, which we shall relate to *prethermalization*.
Thermalization dynamics of $n_{kink}(t)$ can be divided in three stages as summarized in Fig. 4.4:

1. first of all, the system relaxes towards the asymptotic steady state of the QIC after a quench of the transverse field without noise, which is

[4] The saddle-point method efficiently approximates the value of the integral in the $\Gamma t \gg 1$ limit, if $\Gamma t \gg (g+1)^2$.

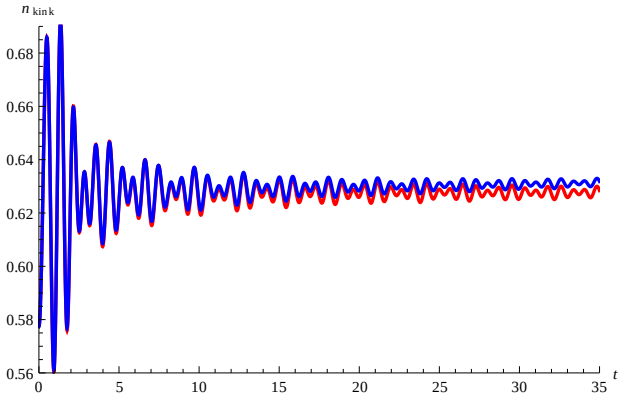

Figure 4.4: The density of kinks vs. time for a quench with $\Gamma = 0.01$, $g_0 = 1.1$, $g = 4$. While the red line shows the value attained by n_{kink} without perturbation and predicted by the GGE, the full time evolution (blue line) shows first a saturation towards the GGE value and later a runaway towards the infinite temperature state.

the GGE of the QIC, accounting for the conserved quantities of the theory, i.e. the occupation number of the fermions $n_k = \gamma_k^\dagger \gamma_k$. This happens through the usual inhomogeneous dephasing [47], arising from the overlap of a continuum of frequencies in (4.56) and leading to a $\frac{1}{(Jt)^{3/2}}$ decay in the $Jt \gg 1$ limit. This result can be easily derived applying a stationary phase argument to Eq.(4.56) in the $Jt \gg 1$ limit and in the temporal frame when the noise is not effective $\Gamma t \ll 1$. Though the term *prethermalization* has been introduced for closed quantum many body systems driven out of equilibrium, the appearance of an intermediate stage of the dynamics observed here is very similar to what have been found in closed systems [5], suggesting to use this term also in this context.

2. The second stage consists in a noise induced dephasing, where coherences are suppressed exponentially by the noise for $\Gamma t \gg 1$, as the leading $e^{-\Gamma t}$ behaviour discussed before suggests.

3. The third stage corresponds to populations heating up. This drives the number of kinks towards the final stage of the dynamics, i.e an infinite temperature state. This happens following the same $\frac{1}{\sqrt{\Gamma t}}$ behaviour of the energy, and it is due again to the presence of slow relaxing modes dominating thermalization dynamics.

This scenario can be better understood by looking separately at n_{drift} and Δn_{kink}. In Fig. 4.5, n_{drift} is plotted as a function of time (red line), showing that this term is responsible for the deviation of n_{kink} from the GGE expectation value (blue line), while Δn_{kink}, plotted in Fig. 4.6, first decays

following a power law, while for times $\Gamma t \gg 1$ it starts decaying exponentially fast, departing clearly from the values attained in the usual sudden quench protocol (blue line).

As a last remark in this Section, it should be noticed that the appearance of prethermalization stage strictly depends on the different behaviour of the populations and coherences during the dynamics. This implies that whether an observable will show *prethermalization* or not will depend crucially on its expression in the Bogolyubov basis. This is the reason beneath the absence of a similar behaviour in the dynamics of $E(t)$.

4.4.3 On-site transverse magnetization

A *pre-thermal* plateau would be also observed in the thermalization dynamics of the on-site transverse magnetization, $\langle \sigma_i^z(t) \rangle$, which posses a similar expression to (4.56) in the Bogolyubov basis

$$m^z \equiv \langle \sigma_i^z \rangle = \int_0^\pi dk \frac{2}{\pi} \Big(\delta f_k(t) \cos 2\theta_k - \sin 2\theta_k y_k(t) \Big). \tag{4.57}$$

The pre-thermal plateau is in correspondence of the expectation value of σ_i^z evaluated in the GGE of the QIC without noise

$$\langle \sigma_i^z \rangle_{GGE} \simeq - \int_0^\pi dk \frac{1}{\pi} \cos 2\Delta\theta_k \cos 2\theta_k \tag{4.58}$$

and it is approached with a power law, $\frac{1}{(Jt)^{3/2}}$, in the limit $Jt \gg 1$, as in a quenched QIC [37]. On the other hand, the on-site transverse magnetization will approach its infinite temperature expectation value ($\langle \sigma_i^z \rangle_{T=\infty} = 0$) as a power law, $\frac{1}{\Gamma t}$, for $\Gamma t \gg 1$, when quantum coherent effects have been already exponentially suppressed by the noise. Hence the non-equilibrium dynamics of this observable is exactly the same observed for the number of kinks. In the next section we are going to consider two-points functions of the transverse magnetization looking for new physics behind the interplay of noise and quench.

4.4.4 Transverse magnetization correlator

A similar scenario can be also observed in the equal-time transverse magnetization correlation function, computed at different spin sites $\rho^{zz}(r,t) = \langle \sigma_{i+r}^z(t) \sigma_i^z(t) \rangle$. Similarly to what we have done for n_{kink}, the expression for $\rho^{zz}(r,t)$ can be written as a sum of three terms

$$\rho^{zz}(r,t) = \langle \sigma_r(t)\sigma_0(t) \rangle_{pop.} + \langle \sigma_r(t)\sigma_0(t) \rangle_{coh.} + \langle \sigma_r(t)\sigma_0(t) \rangle_{mix.} \tag{4.59}$$

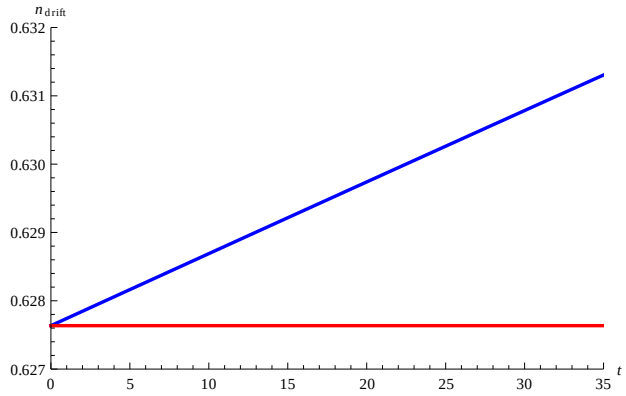

Figure 4.5: Red line: populations contribution, n_{drift}, for the case of a quantum quench ($\Gamma = 0$). Blue line: populations contribution in the case of a quench with noise ($\Gamma = 0.01$). $g_0 = 1.1$, $g = 4$.

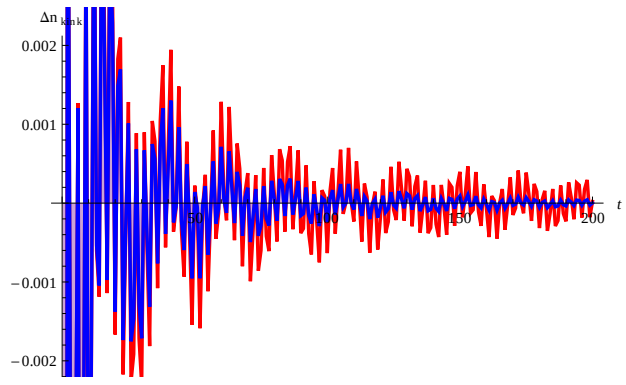

Figure 4.6: Red line: coherences contribution, Δn_{kink}, for the case of a quantum quench ($\Gamma = 0$). Blue line: coherences contribution in the case of a quench with noise ($\Gamma = 0.01$). $g_0 = 1.1$, $g = 4$.

where

$$\begin{aligned}\langle\sigma_r(t)\sigma_0(t)\rangle_{pop.} &= 4\int_{-\pi}^{\pi}\frac{dk}{2\pi}\int_{-\pi}^{\pi}\frac{dk'}{2\pi}e^{i(k-k')r}\times\\ &\times\Big[\sin 2\theta_k\sin 2\theta_{k'}\delta f_k(t)\delta f_{k'}(t)+\\ &+\Big(\frac{1}{2}+\cos 2\theta_{k'}\delta f_{k'}(t)\Big)\Big(\frac{1}{2}-\cos 2\theta_k\delta f_k(t)\Big)\Big],\end{aligned} \tag{4.60}$$

$$\begin{aligned}\langle\sigma_r(t)\sigma_0(t)\rangle_{coh.} &= 4\int_{-\pi}^{\pi}\frac{dk}{2\pi}\int_{-\pi}^{\pi}\frac{dk'}{2\pi}e^{i(k-k')r}\times\\ &\times\Big[-\sin 2\theta_k\sin 2\theta_{k'}y_k(t)y_{k'}(t)+(x_k(t)+iy_k(t)\cos 2\theta_k)\times\\ &\times(x_{k'}(t)-iy_{k'}(t)\cos 2\theta_{k'})\Big],\end{aligned} \tag{4.61}$$

$$\begin{aligned}\langle\sigma_r(t)\sigma_0(t)\rangle_{mix.} &= 4\int_{-\pi}^{\pi}\frac{dk}{2\pi}\int_{-\pi}^{\pi}\frac{dk'}{2\pi}e^{i(k-k')r}\times\\ &\times\Big[i\delta f_k(t)\sin 2\theta_k(x_{k'}(t)-y_{k'}(t)\cos 2\theta_{k'})+\\ &-i\delta f_{k'}(t)\sin 2\theta_{k'}(x_k(t)+y_k(t)\cos 2\theta_k)+\\ &+\sin 2\theta_k\delta f_{k'}(t)y_k(t)\cos 2\theta_{k'}+\sin 2\theta_{k'}\delta f_k(t)y_{k'}(t)\cos 2\theta_k\Big].\end{aligned} \tag{4.62}$$

Looking the expression of the coherences (4.45), it should be clear that we can extract from the integrals in (4.61) and (4.62) a purely time dependent exponential decay prefactor, which allow us to neglect these terms in the $\Gamma t \gg 1$ limit

$$\begin{aligned}\langle\sigma_r(t)\sigma_0(t)\rangle_{coh.} &\propto e^{-2\Gamma t}\\ \langle\sigma_r(t)\sigma_0(t)\rangle_{mix.} &\propto e^{-\Gamma t}.\end{aligned} \tag{4.63}$$

In order to discriminate the separate physical associated to noise and to the ordinary quench dynamics, we start our analysis considering the case in which the QIC is driven out of equilibrium only by the noise, $g_0 = g$, and later we will consider the more involved case of the interplay between quench and noise. out of equilibrium only by the noise, $g_0 = g$, and later we will consider the more involved case of the interplay between quench and noise.

Noise without quench

Let us assume to be in the long time limit $\Gamma t \gg 1$, and let us restrict our attention to a protocol without quench ($g_0 = g$).

The dynamics is dominated by modes near to $k = 0, \pm\pi$ which have the slowest relaxation. We can thus at long times evaluate the correlator ρ^{zz} as

$$\rho^{zz} \simeq \rho_0^{zz} + \rho_\pi^{zz} + \rho_{-\pi}^{zz} \tag{4.64}$$

where the first contribution (which is also the only one that would survive in the scaling limit if taken from the outset) comes from modes close to $k \sim 0$, the second and the third one come from modes close to $k \sim \pm\pi$. Let us then consider first ρ_0^{zz}.

Equation (4.60) for large enough times $\Gamma t \gg 1$ becomes

$$\begin{aligned}\rho_0^{zz}(r,t) \simeq 4 \int_{-\infty}^{\infty} \frac{dk}{2\pi} \int_{-\infty}^{\infty} \frac{dk'}{2\pi} e^{i(k-k')r} \\ \Big(\frac{1}{4} + \frac{k}{E_k}\delta f_k(t)\frac{k'}{E'_k}\delta f_{k'}(t) - \frac{\Delta^2}{E_k E_{k'}}\delta f_k(t)\delta f_{k'}(t)\Big),\end{aligned} \tag{4.65}$$

where the time dependence of $\rho_0^{zz}(r,t)$ is going to be fully determined by the slowest mode $k \simeq 0$, and where the small k behaviour of δf_k is taken

$$\delta f_k(t)_{\underset{k\simeq 0}{=}} - \frac{1}{2} e^{-\Gamma t \frac{k^2}{\Delta^2}}. \tag{4.66}$$

The correlator can thus be derived by computing the following integral

$$I = \int_{-\infty}^{\infty} \frac{dk}{2\pi} \frac{e^{ikr}}{E_k} e^{-\Gamma t \frac{k^2}{\Delta^2}}. \tag{4.67}$$

First of all, we make the substitution $k = \Delta q$

$$I = \int_{-\infty}^{\infty} \frac{dq}{2\pi} \frac{e^{iq\Delta r}}{\sqrt{q^2+1}} e^{-\Gamma t q^2}. \tag{4.68}$$

From Eq. (4.68) it is clear that the exponential decay induced by the noise gives a natural cut-off which enforces the convergence of the integral; in particular, it is clear that the largest contribution to the integral comes from the modes $q \ll \frac{1}{\sqrt{\Gamma t}}$; in other words, recalling that $\Gamma t \gg 1$, we can expand the denominator of the integrand for small q. To first order we get

$$\begin{aligned} I = \int_{-\infty}^{\infty} dq e^{iq\Delta r} e^{-\Gamma t q^2} (1 - \frac{1}{2}q^2 + ...) = \\ = \sqrt{\frac{\pi}{\Gamma t}} e^{-\frac{(\Delta r)^2}{4\Gamma t}} + O\Big(\frac{\Delta r}{\Gamma t}\Big)\end{aligned} \tag{4.69}$$

and so, substituing in (4.65), for the transverse magnetization correlator we get

$$\rho_0^{zz}(r,t) = -\frac{1}{\pi}\frac{\Delta^2}{4}\frac{1}{\Gamma t} e^{-\frac{(\Delta r)^2}{2\Gamma t}} \tag{4.70}$$

Concerning the computation in the $\Delta r \gg \Gamma t$ regime, we observe first of all that

$$\frac{1}{(q^2+1)^{1/2}} = \frac{1}{\Gamma(\frac{1}{2})}\int_0^\infty da a^{-1/2} e^{-a(q^2+1)} \tag{4.71}$$

where $\Gamma(\frac{1}{2})$ is the Euler Gamma function. Inserting (4.71) in (4.68), we have

$$\begin{aligned}
&\int_{-\infty}^{\infty} dq \frac{e^{iq\Delta r - \Gamma t q^2}}{\sqrt{q^2+1}} = \int_{-\infty}^{\infty} dq \int_0^\infty \frac{da}{\Gamma(1/2)} a^{-1/2} e^{-iqmr - \Gamma t q^2 - a(q^2+1)} = \\
&\int_0^\infty da a^{-1/2} e^{-\frac{m^2 r^2}{4(a+\Gamma t)} - a} \frac{1}{\sqrt{a+\Gamma t}} \overset{=}{a+\Gamma t \equiv b} \int_{\Gamma t}^\infty \frac{db}{\sqrt{b-\Gamma t}} \frac{e^{-\frac{m^2 r^2}{4b} - b + \Gamma t}}{\sqrt{b}} \overset{=}{b \equiv \frac{mr}{2} c} \\
&= e^{\Gamma t} \int_{2\frac{\Gamma t}{mr}}^\infty dc \frac{\sqrt{\frac{mr}{2}}}{\sqrt{\frac{mrc}{2} - \Gamma t}} \frac{1}{\sqrt{c}} e^{-mr(c+\frac{1}{c})} = 2e^{\alpha^2\beta} \int_\alpha^\infty dx \frac{1}{\sqrt{x^2-\alpha^2}} e^{-\beta\left(x^2 + \frac{1}{x^2}\right)}
\end{aligned} \tag{4.72}$$

where in the last equality we defined $c = x^2$, $\alpha^2 = \frac{2\Gamma t}{\Delta r}$ and $\beta = \frac{\Delta r}{2}$. The last integral in Eq. (4.72) can be evaluated with a saddle point approximation around $x \simeq 1$, in the limit $\alpha \ll 1$, $\beta \gg 1$

$$\begin{aligned}
&2e^{\alpha^2\beta} \int_\alpha^\infty dx \frac{1}{\sqrt{x^2-\alpha^2}} e^{-\beta\left(x^2+\frac{1}{x^2}\right)} \simeq 2e^{\alpha^2\beta} \frac{e^{-2\beta}}{\sqrt{1-\alpha^2}} \int_0^\infty dx e^{-4\beta(x-1)^2} \overset{\simeq}{\beta \gg 1} \\
&\simeq \frac{2e^{\alpha^2\beta - 2\beta}}{\sqrt{1-\alpha^2}} \frac{\sqrt{\pi}}{2\sqrt{\beta}} = \sqrt{\frac{2\pi}{\Delta r}} \frac{e^{-\Delta r + \Gamma t}}{\sqrt{1 - \frac{2\Gamma t}{\Delta r}}} \overset{\propto}{\frac{\Delta r}{\Gamma t} \gg 1} \frac{e^{-\Delta r}}{\sqrt{\Delta r}}.
\end{aligned} \tag{4.73}$$

where we kept the gaussian fluctuations around the saddle point $x \simeq 1$.

This expression allows to find the correlation function in the $\Delta r \gg \Gamma t$ limit, after some straightforward algebra on Eq.(4.65)

$$\rho_0^{zz}(r,t) \simeq \frac{e^{-2\Delta r}}{2\pi r^2}. \tag{4.74}$$

It should be clear from these expressions that the diffusive behaviour found for the correlator (4.70) in the $\Delta r \ll \Gamma t$ limit and indicating the continuous heating of the system towards the infinite temperature state, travels with a wavefront speed $\gamma = \frac{\Gamma}{\Delta}$, which means that points with $\Delta r \gg \Gamma t$ do not present any signature of the noise and their correlation function is the same of σ_i^z in the QIC without noise and quench (see eq. (4.74) and for comparison [48]).

Before considering the combined signature of the noise and the quench on the on-site magnetization correlation function, let us restore lattice corrections originating from $k \simeq \pm\pi$ modes in Eq. (4.60); for $\rho^{zz}(r,t)$, in the $\frac{\Delta r}{\Gamma t} \ll 1$ limit, we get (assuming the lattice spacing $a = 1$)

$$\rho^{zz}(r,t) = -\frac{1}{\pi}\frac{\Delta^2}{4}\frac{1}{\Gamma t} e^{-\frac{(\Delta r)^2}{2\Gamma t}} \left(1 + \frac{g+1}{g-1}\cos(\pi r) e^{-\frac{gr^2}{\Gamma t}}\right)^2. \tag{4.75}$$

In the space-time region defined by $\sqrt{\frac{\Gamma t}{g}} \ll r \ll \frac{\Gamma t}{\Delta}$, lattice corrections are completely negligible, on the other hand, in the limit $r \ll \sqrt{\frac{\Gamma t}{g}}$ the signature of the noise is still diffusive. Therefore, we can conclude that the qualitative behaviour of the on-site magnetization correlation function is diffusive.

Effect of the quench

Now we are interested in studying the interplay between quench and noise in the spreading of quantum correlations in $\rho^{zz}(r,t)$. We use the expressions for populations and coherences, (4.44), (4.45), and look for the different spatio-temporal regimes emerging during the time evolution of this observable.

The dynamics is characterized by the propagation of two "wave" fronts: at earlier times, $\Gamma t \ll 1$, a first front appears at $r \simeq Jt$, controlled by the velocity of quasiparticles emitted after a quench ($v \simeq J$), which separates unconnected space-time regions, $r \gg Jt$, where σ_i^z correlations behave as in the QIC without quench, from a region of space-time connected points $r \ll t$, where the stationary correlation function is the same of a quenched QIC [37]. This is consistent with the Lieb-Robinson limit [63], as already found for other systems [64] and by many authors for the sudden quench of the QIC [46, 37, 47]. The effects of the noise are hardly relevant at early times as observed for the evolution of n_{kink}.

On the other side, taking the long time limit, $\Gamma t \gg 1$, for $\Delta r \ll \Gamma t$ we find again a diffusive spreading of correlations, while for unconnected spacetime points ($\Delta r \gg \Gamma t$) the stationary correlation function crosses over to the asymptotic expression of the correlation function in a quenched QIC without noise [37].

This scenario can be summarized in the following expressions for the correlation function

$$\rho^{zz}(r,t) \simeq_{\Gamma t \ll 1} \begin{cases} \frac{1}{2\pi r^2} \exp[-2\Delta_0 r] & r \gg vt \\ \\ \frac{1}{r^\alpha} \exp[-r/\xi_z] & r \ll vt \end{cases} \tag{4.76}$$

where ξ_z is the correlation length associated to a simple *quantum quench* of the transverse field and α a constant, computed in [37]. In the large-times regime, $\Gamma t \gg 1$, the noise becomes relevant and the second crossover, between quenched QIC correlation functions and *diffusive* behavior emerges

$$\rho^{zz}(r,t) \simeq_{\Gamma t \gg 1} \begin{cases} \frac{1}{r^\alpha} \exp[-r/\xi_z] & \gamma t \ll r \ll vt \\ \\ -\frac{1}{\pi} \frac{\Delta^2}{4} \frac{1}{\Gamma t} \exp\left[-\frac{(\Delta r)^2}{2\Gamma t}\right] & r \ll \gamma t \end{cases} \tag{4.77}$$

where $\gamma = \frac{\Gamma}{\Delta}$ is the small parameter, which controls the self-consistent Born

approximation used to resum the Dyson series [5].

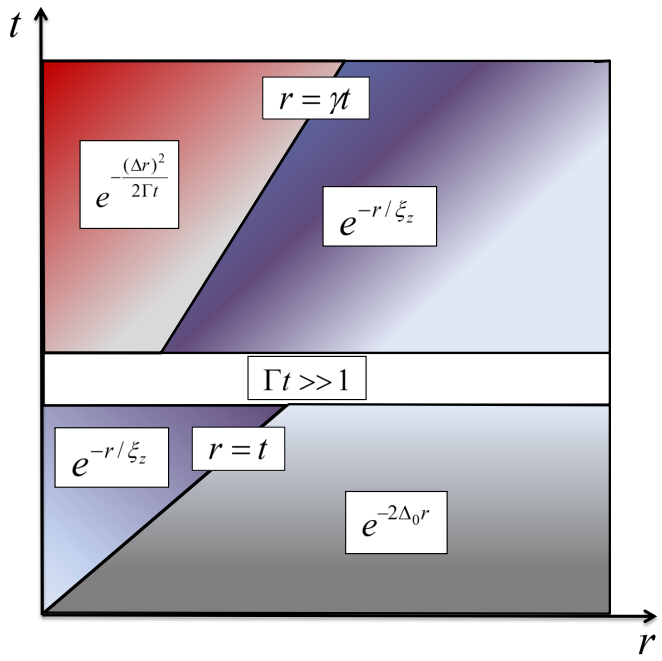

Figure 4.7: The spreading of quantum and thermal correlations in the noisy Quantum Ising Model ($J = 1$): the transverse field correlator has a first crossover when ballistic quasi-particles, carrying quantum correlations, propagate at the distance r. Thermal correlations propagate at a second stage, leading to a crossover to a diffusive form, consistent with thermal dynamics.

This type of light-cone spreading of correlations has been observed experimentally (without noise) in the quench dynamics of the Bose-Hubbard model [65] and in the coherent split of 1D Bose gases, characterizing the wave front associated to the pre-thermal state [66].

4.4.5 Order Parameter correlations

This last subsection is devoted to study whether the diffusive behaviour observed before is a general signature of the effect of the noise in correlation functions; in order to answer to this question, it is sufficient to compute the equal-time order parameter correlation functions, ρ^{xx}_{lm} for a QIC perturbed by the noise without adding the effect of a quench in the transverse field.

The usual way to perform this computation in the ground as in a thermal state is to recast ρ^{xx}_{lm} in a Toepltiz determinant form and to evaluate the large-spin separation limit $l - m = n \to \infty$, using Fisher-Hartwig conjecture [68].

[5] For $\Gamma/\Delta \ll 1$ vertex corrections entering the self energies as well as the correlation functions can be neglected.

For a quantum quench the situation is in general much more complicated [37]. Hence, we will therefore restrict our attention to the dynamics in the presence of the noise at long-times where the coherences have been suppressed and only populations evolve. In this case we may proceed with standard methods.

Let introduce the operators

$$A_i \equiv c_i^\dagger + c_i \quad B_i \equiv c_i^\dagger - c_i \tag{4.78}$$

where c_i is the Jordan-Wigner fermion on the lattice; from (4.78) it follows [67] that

$$\rho^x_{ml} = \langle \sigma^x_m \sigma^x_l \rangle = \langle B_l A_{l+1} B_{l+1} ... A_{m-1} B_{m-1} A_m \rangle \tag{4.79}$$

We can factorize this expression, using Wick theorem, and, noticing that $\langle A_l A_m \rangle = 0$ and $\langle B_l B_m \rangle = 0$, we only need to compute $\langle B_l A_m \rangle$:

$$\langle B_l A_m \rangle = \int_{-\pi}^{\pi} \frac{dk}{2\pi} e^{-ikR} e^{i2\theta_k} 2\delta f_k \equiv s(R) \tag{4.80}$$

where $R = l - m$ and $\delta f_k = -\frac{1}{2} e^{-\Gamma \sin^2 2\theta_1 t}$.

It is possible to show [67] that the order parameter correlator can be cast in the form of a $n+1 \times n+1$ *Toeplitz determinant*

$$det(T_n) = det|s(j-k)|^n_{j,k=0} = D_n[f] \tag{4.81}$$

where T_n is a Toeplitz matrix

$$T_n = \begin{pmatrix} s(0) & s(-1) & s(-2) & ... & s(-n) \\ s(1) & s(0) & s(-1) & ... & s(1-n) \\ s(2) & s(1) & s(0) & ... & s(2-n) \\ ... & ... & ... & ... & ... \\ s(n) & s(n-1) & s(n-2) & ... & s(0) \end{pmatrix} \tag{4.82}$$

It is convenient to write

$$s(R) = \int_{-\pi}^{\pi} \frac{dk}{2\pi} e^{-iRk} f(k) \tag{4.83}$$

where $f(k)$ is a periodic complex function $f(k) = f(k + 2\pi)$, called the *generating function*.

Let us now compute the order parameter correlator (Eq. (4.79)) in the large R limit, using the large n expansion of a Toeplitz determinant (Eq. (4.81)) which can be extracted using the Fisher-Hartwig conjecture [68]. The latter states that, if $f(k)$ can be cast in the form

$$f(k) = f_0(k) \prod_r \exp\left[ib_r(k - k_r - \pi sign(k - k_r))\right](2 - 2\cos(k - k_r))^{a_r} \tag{4.84}$$

where $k \in (0, 2\pi)$, k_r are singularities (jumps, zeros or poles) of $f(k)$, $f_0(k)$ is an infinitely differentiable function in $k \in (0, 2\pi)$ and a_r, b_r are two complex numbers, then the asymptotic expansion of the Toeplitz determinant, for large n, is

$$T_n \underset{n\to\infty}{\sim} e^{l_0 n} n^{\sum_r (a_r^2 - b_r^2)}, \tag{4.85}$$

where $l_0 = \int_{-\pi}^{\pi} \frac{dk}{2\pi} \log f_0(k)$.

First of all, we are briefly going to set the notation, computing the order parameter correlator of the QIC at equilibrium, and then we will move to the case of interest for this Section.

Order Parameter Correlations in the QIC

Consider the Quantum Ising Model

$$H_0 = -\sum_i \sigma_i^x \sigma_{i+1}^x + g\sigma_i^z \tag{4.86}$$

in the paramagnetic phase $g > 1$.

In this case (see note [6])

$$\begin{aligned} &\langle B_l A_m \rangle = s(R) = \\ &= \int_{-\pi}^{\pi} \frac{dk}{2\pi} e^{ikR} e^{-ik} \frac{\cos k - g + i \sin k}{\sqrt{(\cos k - g)^2 + \sin^2 k}} \end{aligned} \tag{4.87}$$

and $f(k)$ can be rewritten, making the change of variable $z = e^{ik}$, as a function in the complex plane ($\lambda \equiv 1/g$)

$$f(z) = z^{-1/2} \frac{(z-g)^{1/2}}{(zg-1)^{1/2}} = z^{-1} \frac{(\lambda z - 1)^{1/2}}{(\lambda z^{-1} - 1)^{1/2}}, \tag{4.88}$$

which has four branch points $z = 0$, $1/g$, g, ∞. We choose the two branch cuts in the following way: the first linking $z = 0$ with $z = 1/g$, and the second one linking $z = g$ with $z = \infty$.

It is not immediate to apply the Fisher-Hartwig conjecture on Eq.(4.88); in this case, some additional manipulations on the generating function are required, following Ref. [69], we note that

$$\frac{1}{2\pi} \int_{-\pi}^{\pi} dk f(k) e^{-ikR} = \int_C f(z) z^{-R} \frac{dz}{2\pi i z} \tag{4.89}$$

[6] In order to make $\rho_{xx}(R)$ identically equal to the Toeplitz determinant, T_n, it is necessary to shift $\rho_{xx}(R)$ from R to $R+1$ and this causes the appearance of a factor e^{-ik} in the expression of $s(R)$.

where C is a closed contour encircling the origin in the aulus $1/g < |z| < g$, where $f(z)$ is analytic with our choices of branch cuts. The integral involed in the Toeplitz Determinant is defined over a circle of radius 1, encircling the origin, (4.89), but applying Cauhy's theorem inside the anulus $1/g < |z| < g$ we can move the integration from the circle of radius 1 to the circle of radius $g = 1/\lambda$; this is equivalent to make the substituion $z \to z/\lambda$ in (4.89), and to keep the integration over the circle $|z| = 1$, as shown in [69] (for a technical remark on this point see [7]).

Following this procedure it is possible to rewrite Eq. (4.88) in this form

$$f(z) = \frac{\lambda}{z} \frac{(1-z)^{1/2}}{\left(1 - \frac{\lambda^2}{z}\right)^{1/2}}, \tag{4.90}$$

where the Fisher-Hartwig formula can be immediately applied; re-substituting again $z = e^{ik}$, we get the following Fisher-Hartwig decomposition (4.84)

$$f(k) \sim f_0(k) e^{-\frac{3}{4}ik} (1 - \cos k)^{1/4}, \tag{4.91}$$

where

$$f_0(k) = \frac{\lambda}{(1 - \lambda^2 e^{-ik})^{1/2}}. \tag{4.92}$$

It is now easy to show that

$$l_0 = \int_{-\pi}^{\pi} \frac{dk}{2\pi} \log \frac{\lambda}{(1 - \lambda^2 e^{-ik})^{1/2}} = \log \lambda, \tag{4.93}$$

which gives for the correlation function $\rho^{xx}(R)$, according to (4.85), the following result

$$\rho^{xx}(R) \underset{R \to \infty}{\sim} R^{-1/2} e^{-R/\xi_{eq}} \tag{4.94}$$

where $\xi_{eq} = (\log g)^{-1}$.

Order Parameter correlations in a noisy QIC

We are now ready to derive the main result of this section, adding to the QIC the usual noisy time dependent perturbation. Recalling (4.80), we get in this case for the generating function $f(k)$

$$f(k) = e^{-\Gamma t \sin^2 2\theta_k} f^{eq}(k), \tag{4.95}$$

[7] Changing the integration circle from unitary radius to radius $1/\lambda$, we get $c_p = \int_{-\pi}^{\pi} \frac{d\theta}{2\pi} f(\theta) e^{-ip\theta} = \lambda^p \int_{-\pi}^{\pi} f(\frac{e^{i\theta}}{\lambda}) e^{-ip\theta} \frac{d\theta}{2\pi}$. For the asymptotics of the Toeplitz determinant, we are interested in $l_p = \int_{-\pi}^{\pi} \log f(\theta) e^{-ip\theta} \frac{d\theta}{2\pi} = \oint_{|z|=1} \log f(z) z^{-p} \frac{dz}{2\pi i z} = \oint_{|z|=1/\lambda} \log f(z) z^{-p} \frac{dz}{2\pi i z} \underset{z'=z\lambda}{=} \oint_{|z'|=1} \log f\left(\frac{z'}{\lambda}\right) \frac{z'^{-p}}{\lambda^{-p}} \frac{dz'}{2\pi i z'} = \int_{-\pi}^{\pi} \log \left(\frac{e^{i\theta}}{\lambda}\right) \frac{e^{-ip\theta}}{\lambda^{-p}} \frac{d\theta}{2\pi}$, where in the last passage we used $z' = e^{i\theta}$ and so $l_0 = \int_{-\pi}^{\pi} \log \frac{e^{i\theta}}{\lambda} \frac{d\theta}{2\pi}$ (see also [69]).

where $f^{eq}(k)$ is the static generating function for the Toeplitz determinant in the QIC at equilibrium, presented in the previous subsection. The function $e^{-\Gamma t \sin^2 2\theta_k}$ is non zero and smooth in $(0, 2\pi)$, so our only task is to make the change of variable in the complex plane $z \to z/\lambda$ as before, necessary to apply the Fisher Hartwig conjecture.

The correlation function, using Fisher-Hartwig conjecture, takes the form

$$\rho^{xx}(R,t) \underset{R\to\infty}{\sim} R^{-1/2} e^{-R/\xi(t)}, \tag{4.96}$$

where

$$\frac{1}{\xi(t)} = \frac{1}{\xi_{eq.}} + \frac{1}{\xi(t)_{noise}} \tag{4.97}$$

and

$$\frac{1}{\xi(t)_{noise}} = \Gamma t \int_{-\pi}^{\pi} \frac{dk}{2\pi} a(k); \tag{4.98}$$

$\xi_{eq.}$ is the exponent coming from the regular part of the generating function at equilibrium (see Eq. (4.94)), while $a(k)$ has the following form

$$a(k) \equiv \sin^2 2\theta_k = \frac{(e^{ik} - e^{-ik})^2}{(e^{ik} - e^{-ik})^2 - (2g - e^{ik} - e^{-ik})^2}. \tag{4.99}$$

The integral

$$\int_{-\pi}^{\pi} \frac{dk}{2\pi} a(k) \tag{4.100}$$

can be written in the complex plane ($z = e^{ik}$) as

$$\oint_{|z|=1} \frac{dz}{2\pi i z} a(z), \tag{4.101}$$

where

$$a(z) \equiv \frac{1}{1 - \left(\frac{(z-1-\sqrt{1-\frac{1}{g^2}})(z-1+\sqrt{1+\frac{1}{g^2}})}{(z-\frac{1}{g})(z+\frac{1}{g})} \right)^2} \tag{4.102}$$

has poles in $z = 0, \frac{1}{g^2}, 1$.

Considering we move from the circle of radius 1 to the one of radius $\frac{1}{\lambda}$, where $f_{eq}(k)$ has a branch cut, we need to regularize the integral (4.101), deforming the integration contour from inside in order to avoid $z = 1$; in other words, we consider the circle of radius $1 - \epsilon$, taking the limit $\epsilon \to 0^+$.

Applying the residue theorem to (4.101) we get

$$\frac{1}{\xi(t)_{noise}} = \frac{\Gamma t}{2g^2} \tag{4.103}$$

This result can be checked numerically, studying the asymptotic behaviour of a Toeplitz determinant, whose entries are generated by (4.95).

For a quench without dissipation the stationary correlation function has in general an exponential form $\rho^{xx}(R,t) \sim \exp[-R/\xi]$, with a correlation length ξ dictated by the non-thermal distribution function of quasi-particles and predicted by the Generalized Gibbs ensemble [37]. Turning on the noise, the signatures of the crossover observed for the transverse magnetization are expected in this case to be different; indeed, the same exponential form persists and the spreading of quantum and thermal correlations will not result in a diffusive form, but rather modify just the specifics of the correlation length which at later times shrinks as $1/\Gamma t$ for large times.

The different signatures observed in the transverse and longitudinal magnetization are consistent with analogous phenomenology observed elsewhere for quenches in the QIC [46].

4.5 Appendix: Time-dependent Bogolyubov transformation and Statistics of the Work

In this Appendix we derive a formula for the characteristic function, $G(u)$, introduced in Eq. (4.7). We use a generalization of Bogolyubov transformations for time-dependent protocols, and then in Section 4.2 we specialize these results for a time-dependent noisy perturbation.

We consider a QIC in the transverse field g_0 and we prepare the system in the ground state of the paramagnetic phase, $|\psi(g_0)\rangle$; we perform a generic time-dependent protocol, $g(t)$, with these boundary conditions: $g(t=0) = g_i > 1$ and $g(t=\tau) = g_f > 1$, in general $g_i, g_f \neq g_0$. For instance, the sudden quench case is recovered from our expressions when $\dot{g}(t) = 0$, hence $g_i = g_f$.

Our goal is to compute

$$G(u) = \langle \psi(g_0) | e^{iuH^H_{\tau,\tau_0}} | \psi(g_0) \rangle, \tag{4.104}$$

where $H^H_{\tau,\tau_0} = U^\dagger(\tau,\tau_0) H_{\tau,\tau_0} U(\tau,\tau_0)$ denotes the Hamiltonian used in the measurement process; the superscript H indicates that operators are taken in the Heisenberg picture. In Eq. (4.104) we dropped the inessential global phase prefactor present in Eq. (4.7). We can rewrite $G(u)$ in Schrodinger representation, absorbing the evolution in the wavefunction

$$|\psi(\tau)\rangle = U(\tau,\tau_0)|\psi(g_0)\rangle, \tag{4.105}$$

we get

$$G(u) = \langle \psi(\tau) | e^{iuH_\tau} | \psi(\tau) \rangle. \tag{4.106}$$

In order to compute this quantity, we make the central *ansatz* of our method, that consists in introducing an operator $\widetilde{\gamma}_k(t)$, which annihilates the state at time t

$$\widetilde{\gamma}_k(t)|\psi(t)\rangle = 0, \tag{4.107}$$

which means that $|\psi(t)\rangle$ is a *Bogolyubov vacuum* at each time, for a certain operator, $\widetilde{\gamma}_k(t)$. The choice of the initial state implies $\widetilde{\gamma}_k(0) = \gamma_k(g_0)$. From our ansatz, it follows that

$$\begin{aligned} 0 = i\frac{d}{dt}(\widetilde{\gamma}_k(t)|\psi(t)\rangle) = \Big(i\frac{\partial}{\partial t}\widetilde{\gamma}_k(t)\Big)|\psi(t)\rangle + \widetilde{\gamma}_k(t)\Big(i\frac{\partial}{\partial t}|\psi(t)\rangle\Big) = \\ = \Big(i\frac{\partial}{\partial t}\widetilde{\gamma}_k(t) + \widetilde{\gamma}_k(t)H(t) - H(t)\widetilde{\gamma}_k(t)\Big)|\psi(t)\rangle \end{aligned} \tag{4.108}$$

and this implies

$$i\frac{\partial}{\partial t}\widetilde{\gamma}_k(t) = -[\widetilde{\gamma}_k(t), H(t)]. \tag{4.109}$$

At a certain time t, $H(t)$ is diagonalized by a set of Bogolyubov operators $\gamma_k(t)$, which are related in the usual way to the Jordan-Wigner fermions, $c_k = u_k(t)\gamma_k(t) - iv_k(t)\gamma^\dagger_{-k}(t)$, where $u_k(t) = \cos\theta_k(t)$, $v_k(t) = \sin\theta_k(t)$; the Bogolyubov angle, $\theta_k(t)$, depends on the time protocol $g(t)$ and the Hamiltonian is diagonalized as usual,

$$H(t) = \sum_{k>0} E_k(t)(\gamma^\dagger_k(t)\gamma_k(t) - \gamma_{-k}(t)\gamma^\dagger_{-k}(t)). \tag{4.110}$$

Now, we looks for two time-dependent coefficients $a_k(t)$ and $b_k(t)$, which unitarly relate $\widetilde{\gamma}_k(t)$ to $\gamma_k(t)$, through the following rotation

$$\widetilde{\gamma}_k(t) = a_k(t)\gamma_k(t) - ib_k(t)^*\gamma^\dagger_{-k}(t). \tag{4.111}$$

At $t = 0$ this equation becomes with our boundary conditions

$$\widetilde{\gamma}_k(g_0) = a_k(t=0)\gamma_k(g_i) - ib_k(t=0)^*\gamma_{-k}(g_i)^\dagger, \tag{4.112}$$

which is the usual Bogolyubov rotation in the case of a sudden quench in the QIC (see, for instance, [59]), with initial conditions, $a_k(t=0) = \cos\Delta\theta_k$ and $b_k(t=0) = \sin\Delta\theta_k$. We are now ready to substitute (4.110) and (4.111) in (4.109), where we need $\dot{u}_k = -v_k(t)\dot{\theta}_k(t)$ and $\dot{v}_k = u_k(t)\dot{\theta}_k(t)$; after straightforward algebra we get two coupled first order differential equations for $a_k(t)$ and $b_k(t)$

$$\begin{aligned} i\dot{a_k} &= -E_k(t)a_k - ib^*_k\dot{\theta}_k(t) \\ i\dot{b^*_k} &= i\dot{\theta}_k(t)a_k + b^*_k E_k(t). \end{aligned} \tag{4.113}$$

Defining $q_k(t) \equiv \frac{b^*_k(t)}{a_k(t)}$, it is possible to write the following differential equation

$$i\dot{q}_k = i\dot{\theta}_k(t) + 2q_k E_k(t) + iq^2_k\dot{\theta}_k(t). \tag{4.114}$$

In the following we will need the small k expansion of q_k, so we solve (4.114), expanding q_k in series, $q_k(t) = \sum_{n=0}^{\infty} c_n(t)k^n$.

The zeroth order solution is null

$$\begin{aligned} i\dot{c}_0 &= 2c_0\Delta(t) \\ c_0(t=0) &= 0, \end{aligned} \tag{4.115}$$

because $q_k(t=0) = \tan\Delta\theta_k \sim_{k\sim 0} \frac{1}{2}k\frac{\Delta_0-\Delta_i}{\Delta_0\Delta_i}$ has a vanishing zero order in the k expansion.
For the first order solution we have

$$\begin{aligned} i\dot{c}_1(t) &= -\frac{i}{2\Delta(t)^2}\dot{g}(t) + 2\Delta(t)c_1(t) \\ c_1(t=0) &= \frac{1}{2}k\frac{\Delta_0-\Delta_i}{\Delta_0\Delta_i}. \end{aligned} \tag{4.116}$$

Using the method of separation of arbitrary constants and taking into account that $c_0(t) = 0$, $\forall t$, we find

$$c_1(t) = e^{-2i\int_0^t \Delta(t')dt'}\Big(c_1(0) - \int_0^t \frac{e^{2i\int_0^{t'}\Delta(t'')dt''}}{2\Delta(t')^2}\dot{\Delta}(t')dt'\Big) \tag{4.117}$$

If we now come back to the original problem, we see that (4.111) and the ansatz $\widetilde{\gamma_k}(t)|\psi(t)\rangle = 0$ allows us to write the state at time $t = \tau$ as a BCS-state, similarly to what is usually done for a sudden quench in the QIC (see for instance [46, 37, 59] or Eq. (4.4)):

$$|\psi(\tau)\rangle = \exp\Big[i\sum_{k>0}\frac{b_k(\tau)^*}{a_k(\tau)}\gamma_k^\dagger(\tau)\gamma_{-k}^\dagger(\tau)\Big]|0\rangle_\tau, \tag{4.118}$$

where $|0\rangle_\tau$ is the vacuum of the QIC at time τ and $\gamma_k^\dagger(\tau)$, the Bogolyubov operators diagonalizing the Hamiltonian at time $t = \tau$. Following the same procedure of [59], it is possible to write the characteristic function, $G(u)$, of the statistics of the work as

$$G(u) \sim \frac{\exp\Big(N\int_0^\pi \frac{dp}{\pi}\log(1+|q_p(\tau)|^2 e^{2iuE_p(g_f)})\Big)}{\exp\Big(N\int_0^\pi \frac{dp}{\pi}\log(1+|q_p(\tau)|^2)\Big)} \tag{4.119}$$

where $g_f = g(t=\tau)$.

Considering that $G(u)$ is the Fourier transform of $P(\omega)$, and since we are interested in the low energy behaviour of $P(\omega)$, it is sufficient to compute $G(u)$ for large values of u. In the limit $Ju \gg 1$ we can use a stationary phase argument and consider only the small p contribution of $|q_p(\tau)|^2$ to the integrals in Eq. (4.119). The small p expansion of $|q_p(\tau)|^2$ can be straightforwardly computed from Eq. (4.117). This computation differs from the sudden quench case [59] only in the expression of $q_p(\tau)$; while in the latter

$q_p(\tau)$ is time-independent, in this case it is a complicated expression depending on the details of the protocol. On the other hand, the square-root singularity at $2\Delta_f$ is left unchanged. Apart from this important difference, the computation of $P(\omega)$ follows a standard procedure, see for instance [59]. We mention that a similar technique has been developed in [60] to compute the statistics of the work done by globally changing in time the mass in a free bosonic field theory with relativistic dispersion and for generic time variations of the transverse field in a Quantum Ising Chain.

Chapter 5

Pre-Thermalization in a Non-Integrable Spin Chain

In the previous chapter we have shown that pre-thermalization can emerge in a simple quantum many body system when the combined effect of a time-dependent noise and an integrable quantum quench are considered.

Making progress in the original framework where pre-thermalization has been introduced, i.e. closed non-integrable quantum many body systems is not a trivial task. By definition it is impossible to solve a non-integrable system, hence in order to deepen our physical insight into pre-thermalization, it could be useful to resort to some non-perturbative techniques which allow to study -under certain approximations- the out-of-equilibrium dynamics of a closed system, at least up to time scales where pre-thermal effects may emerge.

In [8], we introduce a simple, prototypical model for studying thermalization and pre-thermalization: a quantum Ising chain (QIC) perturbed away from integrability by a long-range spin-spin interaction. Even if many of the conservation laws of the QIC are violated by this long-range interaction, we show that the model maps into one of hard-core bosons hopping on a lattice. Within the latter, pre-thermalization occurs naturally for small quenches: as long as the quasi-particle density remains sufficiently low, the hard-core constraint is not effective and the model can be solved numerically up to quite a large size, distinctively showing pre-thermal plateaux in the dynamics of physically relevant observables. The associated quasi-stationary values are typically approached algebraically in time. At longer times, the hard-core constraint generates inelastic scattering processes, which, leading the dynamics away from this substantially integrable scenario, are expected to cause the asymptotic thermalization of the system. In order to study the late dynamics of the model, where the above mentioned effective low density description breaks down, we resort to a diagrammatic study of the quench dynamics. We disregard tadpoles diagrams, which are expected to give just a renormalization of the free theory (as shown by Cardy in [71]), and we focus

on the effects of the sunset diagrams on the non-equilibrium dynamics of the system. We first study their contribution to the life-time of a quasi-particle injected by the initial quench at the perturbative level and then we show how the inelastic processes described by the sunsets are necessary in order to have thermalization in this model. Within this diagrammatic approach, the expected long-time behavior of the model is investigated via a self-consistent re-summation of self-energy diagrams.

5.1 The model

We consider the effect of an integrability-breaking perturbation on the dynamics of the QIC,

$$H_0(g) = -\sum_{i=1}^{N}(\sigma_i^x\sigma_{i+1}^x + g\sigma_i^z), \tag{5.1}$$

where $\sigma^{(x,y,z)}$ are Pauli matrices, N is the total number of spins, and g the strength of the transverse field. This model, which undergoes a prototypical quantum phase transition between a paramagnetic ($g > 1$) and a ferromagnetic ($g < 1$) phase, has been extensively studied both in and out of equilibrium, taking advantage of its integrability as we discussed in Section 2.5. After a Jordan-Wigner transformation followed by a Bogolyubov rotation, H_0 becomes $H_0 = \sum_{k>0}\epsilon_k\psi_k^\dagger\sigma^z\psi_k$ in terms of spinors $\psi_k \equiv \binom{\gamma_k}{\gamma_{-k}^\dagger}$ where γ_k are fermionic operators, and $\epsilon_k \equiv \sqrt{1+g^2-2g\cos k}$ is the energy of the quasi-particles. The dynamics after a quench of the transverse field $g_0 \to g$ has been thoroughly investigated both numerically and analytically as we discussed in the previous chapters.

Focusing for simplicity on quenches within the same phase (say $g_0, g > 1$), the integrability of H_0 makes the dynamics trivial in the quasi-particle representation: the ground state $|0\rangle_{g_0}$ of $H_0(g_0)$, in fact, can be represented as a BCS state $|0\rangle_{g_0} \propto \exp\{-\sum_k B_{g_0\to g}(k)b_k^\dagger\}|0\rangle_g$, in terms of the ground state $|0\rangle_g$ of $H_0(g)$ and of the *pair* operators $b_k^\dagger = \gamma_k^\dagger\gamma_{-k}^\dagger$ of its quasi-particles γ_k, as we discussed in the introductory paragraphs. The initial distribution of these *zero-momentum* fermionic pairs, determined by $B_{g_0\to g}$ is not modified by the time evolution and therefore it affects the asymptotic values of local observables, described consequently by a GGE.

The peculiar structure of the initial state and of the subsequent dynamics is generically spoiled by breaking the integrability of the model, which is expected to cause scattering not only of pairs, but also of individual quasi-particle modes γ_k; as a consequence, the energy initially injected into the system gets redistributed among the various modes, eventually leading to thermalization. In order to make progress in understanding thermalization and pre-thermalization it is particularly valuable to have at hand a simple

enough model in which the breaking of integrability is amenable to both analytic and numerical analysis in a controlled and physically transparent way. Such an instance is provided by a quantum chain with Hamiltonian $H_0 + V$, where H_0 is given by Eq.(5.1) and the interaction

$$V = \frac{\lambda}{N}\Big(\sum_i \sigma_i^z\Big)^2 \tag{5.2}$$

is proportional to the squared global transverse magnetization. Instead of (5.2), in the following we are going to study H_0 perturbed by

$$V = \frac{\lambda}{N}(M_z - \overline{M_z})^2, \tag{5.3}$$

where $M_z = \sum_i \sigma_i^z$ is the global transverse magnetization and $\overline{M_z}$ its long-time temporal average (as an operator) in the absence of perturbation $\lambda = 0$. This subtraction eliminates the constants of motion $\hat{n}_k = \gamma_k^\dagger \gamma_k$ present in the definition of M_z (see Eq.(5.6) below) and is made in order to recover the cluster property of transverse magnetization's expectations in the long-time limit. In order to clarify better this point, consider a quenched ($g_0 \to g$) QIC ($\lambda = 0$) and let us compute the two-times correlation function of M_z. In the long-time limit, the stationary properties of the connected correlation function are not recovered, since

$$\lim_{t\to\infty}\Big(\langle M_z(t+\tau)M_z(t)\rangle - \langle M_z(t+\tau)\rangle\langle M_z(t)\rangle\Big) \tag{5.4}$$

contains a constant term (apart from stationary oscillating terms)

$$\begin{aligned} C = &\sum_{kk'} \cos 2\theta_k \cos 2\theta_{k'} \langle 0|(\gamma_k^\dagger\gamma_k - \gamma_{-k}\gamma_{-k}^\dagger)(\gamma_{k'}^\dagger\gamma_{k'} - \gamma_{-k'}\gamma_{-k'}^\dagger)|0\rangle + \\ &- \sum_{kk'} \cos 2\theta_k \cos 2\theta_{k'} \langle 0|(\gamma_k^\dagger\gamma_k - \gamma_{-k}\gamma_{-k}^\dagger)|0\rangle\langle 0|(\gamma_{k'}^\dagger\gamma_{k'} - \gamma_{-k'}\gamma_{-k'}^\dagger)|0\rangle \end{aligned} \tag{5.5}$$

which spoils the time clustering property (the second term in (5.5) stands for the subtraction of the unconnected component of the stationary correlation function and $|0\rangle$ is the pre-quench ground state). This constant is of order $\sim L$ and it is non zero because of pre-existent correlation between modes of opposite momenta, $\langle \gamma_k^\dagger \gamma_{-k}^\dagger \rangle \neq 0$ and $\langle \gamma_{-k}\gamma_k \rangle \neq 0$, in the initial state. This term is also present in correlation functions of local operators, like the on-site transverse magnetization, σ_i^z, but in that case it is suppressed in the the thermodynamic limit, since it is of order $\propto O(\frac{1}{L})$. For this reason, we subtract *ab initio* the stationary value of the global transverse magnetization $\overline{M_z}$, intended as an operator, which cancels out these pathological terms due to the global nature of the interaction. It should be stressed that

without this subtraction the diagrammatic treatment of this model would suffer some unpleasant pathologies, coming from the inclusion in the perturbative expansion of a macroscopic number, $O(L)$, of terms in the interaction which are essentially integrable; for instance, they would be at the origin of a bunch of delta singularities in the perturbative treatment of the model. To summarize the out-of-equilibrium protocol considered, we quench $H_0(g_0)$ to $H \equiv H_0(g) + V$ at $t > 0$; V effectively breaks the integrability of $H_0(g)$ in terms of its Bogolyubov fermions γ_k and introduces scattering among *zero-momentum pairs* in the fermionic representation.

5.2 The mapping

The spin chain described by H can be conveniently mapped onto a quadratic (yet non-diagonal) Hamiltonian of hardcore bosons, as we show here. First of all, we take advantage of the fermionic representation of $H_0(g_0)$ in order to understand better the effect of breaking the integrability. In fact, in terms of γ_k, V becomes

$$V = \frac{\lambda}{N}\Big[\sum_{k>0} \sin(2\theta_k)\ \psi_k^\dagger \sigma^y \psi_k\Big]^2, \tag{5.6}$$

where $\theta_k(g)$ is the Bogolyubov angle with $\tan(2\theta_k) = (\sin k)/(g - \cos k)$. Note that $I_k = \hat{n}_k - \hat{n}_{-k}$ commutes with $H_0(g)$ for all $k > 0$ and therefore $\{I_k\}_k$ is a set of $N/2$ constants of motion [44]. The eigenvalues of I_k are 0 and ± 1, corresponding to states in which two quasi-particles with momenta $\pm k$ are either simultaneously present or absent, and to states in which only one of the two is present, respectively. Accordingly, the configuration space is split in eigensectors characterized by the string of the $N/2$ possible eigenvalues of $\{I_k\}_k$, with dimension 2^{N_0}, N_0 being the number of 0s present in the corresponding string. These sectors are closed under the action of two-fermion operators such as the number operator $\hat{n}_k$, and the pair creation $b_k^\dagger$ and annihilation b_k operators, in terms of which H becomes

$$\begin{aligned} H &= \sum_{l,k>0} \left[\epsilon_k - (\lambda/N)\sin^2(2\theta_k)\right]\left(I_k^2 - 1\right) + H', \\ H' &= \sum_{l,k>0} \left[2\beta_{kq} b_k^\dagger b_q - \alpha_{kq}(b_k^\dagger b_q^\dagger + b_k b_q)\right], \end{aligned} \tag{5.7}$$

where $\alpha_{kq} = (\lambda/N)(1 - \delta_{kq})\sin(2\theta_k)\sin(2\theta_q)$ and $\beta_{kq} = \epsilon_k \delta_{kq} + \alpha_{kq}$. The Hamiltonian can be written as $B_i M_{ij} B_j$, where $\vec{B} = (b_1, b_2, \ldots, b_1^\dagger, b_2^\dagger, \ldots)$ are generalized vectors and M_{ij} is a symmetric matrix which is expressed in terms of the matrices $\alpha_{i,j}$ and $\beta_{i,j}$ appearing above. M_{ij} contains the whole information on the one-particle spectrum of the theory and it can be diagonalized by numerical methods. The "b" operators commute at different momenta and anti-commute at equal ones, except for $\{b_k, b_k^\dagger\} = 1 - I_k^2$, and

thus they behave almost as hard-core bosons. On the other hand, it is useful to notice that, in a sector with $I_k = \pm 1$, both b_k and $b_k^\dagger$ act as the null operator and can be effectively expunged from H', leaving behind only those corresponding to momenta q for which $I_q = 0$, which can be treated instead as bona-fide hard-core bosons. Summarizing, within a sector characterized by having $N/2 - N_0$ unpaired quasi-particles, H describes a fully-connected model of hard-core bosons on a lattice with N_0 sites.

5.3 Prethermalization

The representation introduced in the previous section allows a consistent description of pre-thermalization and thermalization based on standard approximations. Note that, although H' is quadratic in the pair operators, it cannot be trivially integrated via a Jordan-Wigner transformation and/or a Bogoliubov rotation, for that could not preserve the mixed (anti)commutation relations. Some progress can be made, instead, by re-expressing H in terms of bosonic operators a_k with $[a_k, a_q^\dagger] = \delta_{kq}$, via a Holstein-Primakoff transformation [70] $b_k = (1 - a_k^\dagger a_k)^{1/2}\, a_k$, $b_k^\dagger = a_k^\dagger (1 - a_k^\dagger a_k)^{1/2}$. Assuming a low density of excitations (i.e., a small quench), one can expand the square roots to lowest order $b_k \simeq a_k$, $b_k^\dagger \simeq a_k^\dagger$ and H becomes a Hamiltonian of free bosons (whose dynamics describes pre-thermalization), while higher-order terms introduce the interactions which are expected to lead to thermalization. For this approximation to be valid, the mean bosonic populations have to remain small during the evolution. More precisely, $b_k^\dagger b_k = 2a_k^\dagger a_k - (a_k^\dagger a_k)^2$, but in the sector of physical interest[1], $n_k \equiv n_k n_{-k}$, so considering that $n_k n_{-k} = b_k^\dagger b_k$, we have $n_k \equiv 2N_k - N_k^2 = N_k$, where $N_k = a_k^\dagger a_k$. The heuristic condition of validity for the truncation of Holstein-Primakoff transformation at the lowest order is $\langle N_k \rangle \ll 1$, which implies $\langle n_k \rangle \ll 1$. As heuristically expected, this occurs the smaller the energy injected at $t = 0$ is, i.e., the smaller the amplitude $|g - g_0|$ of the quench is and the further g is from the critical value $g_c = 1$. Actually, for small values of λ, this approximation turns out to be rather accurate in a significantly wider range of parameters: for example, we verified that the dynamics of $n_{k=\pi/2}$ obtained from this method for $\lambda = 0.1$, $g_0 = 8$ and $g = 1.01$ agrees with the one obtained via an exact numerical diagonalization of the fermionic model for $N = 20$ spins within 2% up to time scales $t \simeq 10^3$. Beyond the time range of validity of the low-density approximation, higher-order terms in the Holstein-Primakoff transformation are eventually expected to make the system thermalize, analogously to what is experimentally observed in bosons in 1D (see Fig. 5.1 and Fig. 5.2).

[1] Each state in the sector of physical interest can be expressed as a linear combination of states $|S_n^{(k)}\rangle$, which do not contain the pair $(k, -k)$ and $|C_n^{(k)}\rangle$, which contain the pair $(k, -k)$. The action of n_k and $n_k n_{-k}$ is the same on states given by such linear combinations.

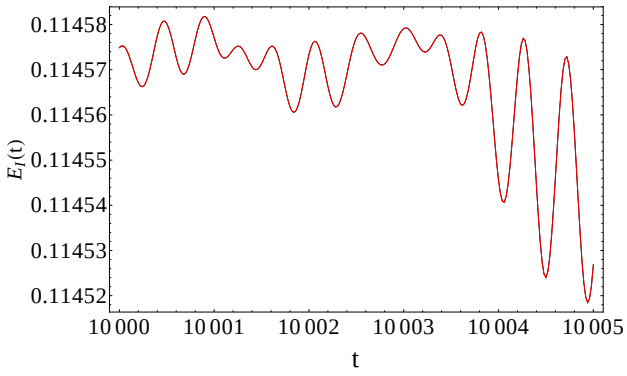

Figure 5.1: Comparison between the fermionic model and the effective low-density bosonic description ($\lambda = 0.1$, $N = 20$, $g_0 = 8$, $g = 3.5$). The red line (effective bosonic description) is indistinguishable from the black line (fermionic model).

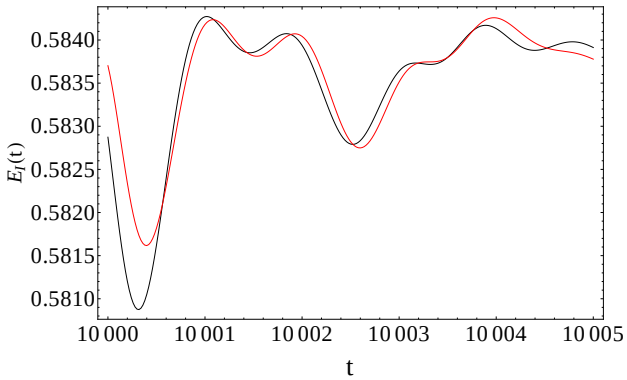

Figure 5.2: Comparison between the fermionic model (black line) and the effective bosonic description (red line), when the low density approximation breaks, i.e. for quenches near to the critical point ($\lambda = 0.1$, $N = 20$, $g_0 = 8$, $g = 1.5$).

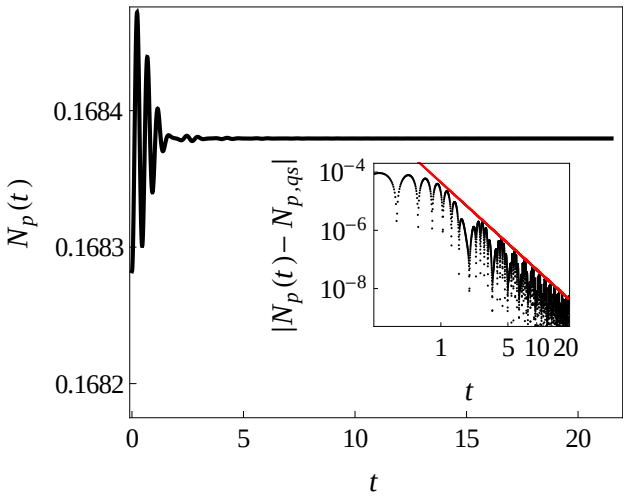

Figure 5.3: Time evolution of the total number of quasi-particles $N_p(t)$ for $N = 100$, $g_0 = 8$, $g = 3.5$, and $\lambda = 0.1$. N_p attains a quasi-stationary value $N_{p,qs}$ before recurrence occurs at $t_R \simeq 25$. We remark that for $\lambda = 0$ this quantity would remain constant at the initial value $N_p(0) \approx 1.68282$. For small enough λ, the difference $N_{p,qs} - N_p(0)$ is proportional to λN, as is the amplitude of the oscillations around $N_{p,qs}$. The inset shows $|N_p(t) - N_{p,qs}|$ in double logarithmic scale and highlights the algebraic approach $\propto t^{-\alpha}$ of N_p to $N_{p,qs}$; the straight line corresponds to $\alpha = 3$.

The main advantage of the mapping is that the diagonalization of H within each sector is of polynomial complexity. Although the total number of sectors grows exponentially with N, as long as one can restrict the analysis to just a few of them, a numerical approach becomes effective for quite large systems, and this is generically the case for our choice: the initial state $|0\rangle_{g_0}$, in fact, contains all possible pairs of Ising quasi-particles with opposite momenta such that $I_k = 0$, $\forall\, k$, and therefore $N_0 = N/2$. Before going on with our analysis, it should be stressed that the usual diagonalization method, which consists in replacing b_k with some new degrees of freedom d_k, related by a linear transformation (summation over repeated indices is understood)

$$\begin{aligned} b_k &= A_{kq} d_q + B_{kq} d_q^\dagger \\ b_k^\dagger &= A_{kq}^* d_q^\dagger + B_{kq}^* d_q \end{aligned} \tag{5.8}$$

should be handled with care, since in order to ensure that the standard commutation relation $[d_k, d_q^\dagger] = 1$ holds, the transformation must be simplectic which requires the use of Williamson theorem.[2] [73]

The evolution of any quantity which does not connect this particular sector with the others can be therefore computed quite easily. In particular, the operators n_k, b_k and $b_k^\dagger$ can be expressed as sums of terms oscillating in time with frequencies $|E_n - E_m|$ and $E_n + E_m$ (referred to as "slow" and "fast", respectively), where $\{E_n\}_n$ is the bosonic single-particle spectrum. For small λ the spectrum of H_0 is weakly perturbed, thus we can substitute E_n with the energy $2\epsilon_n$, of a pair of quasi-particles; this implies that the slow frequencies range approximately from 0 to 4, whereas the fast ones from $4(g-1)$ to $4(g+1)$, which justifies this notion for $g > 2$. Our numerical analysis shows that the fermion numbers $\langle \hat{n}_k \rangle$ — which are also equal to the numbers of pairs if $I_k = 0$ — display weak relaxation of the fast modes. It is therefore more convenient to study, instead, an observable such as the total number of quasi-particles $N_p(t) = \sum_{k>0} \langle \hat{n}_k(t) \rangle$ which displays a marked plateau as in Fig. 5.3, as a consequence of an application of the stationary phase approximation in the long time limit. The time evolution of this quantity can be determined, recalling that $n_k \equiv 2N_k - N_k^2$ and using the low density approximation, which allow to express $\langle n_k(t) \rangle \simeq \langle a_k^\dagger(t) a_k(t) \rangle \simeq \langle b_k^\dagger(t) b_k(t) \rangle$, in terms

[2] *Williamson theorem.* If V is a $2N$ dimensional real matrix, symmetric and positive definite, then there exists a matrix $S \in S_p(2N, \mathbb{R})$ which diagonalizes V: $S^T V S = D^2 \equiv (d_1, ..., d_N, d_1, ..., d_N) > 0$. The proof shows how to explicitly construct S. First of all, define $M \equiv V^{-1/2} J V^{-1/2}$, with $J = \begin{pmatrix} 0 & \mathbf{1}_N \\ -\mathbf{1}_N & 0 \end{pmatrix}$, then it is possible to find a matrix $R \in O(2N, \mathbb{R})$ such that $R^T M R = \begin{pmatrix} 0 & \Omega \\ -\Omega & 0 \end{pmatrix}$, with Ω diagonal and positive; the matrix S, diagonalizing V, is given by $S \equiv V^{-1/2} R D$ (for further details see the complete proof of the theorem in [73]). Using S, it was possible to diagonalize numerically the effective bosonic hamiltonian discussed in this Section.

of the bosons. The expectation value of $\langle b_k^\dagger(t) b_k(t)\rangle$ can be easily expressed in terms of the bosonic degrees of freedom, which diagonalize the theory

$$\begin{aligned}\langle b_k^\dagger(t) b_k(t)\rangle = \sum_{q_1 q_2} \{ & A^*_{kq_1} A_{kq_2} \langle d^\dagger_{q_1} d_{q_2}\rangle e^{i(E_{q_1}-E_{q_2})t} + \\ & + A^*_{kq_1} B_{kq_2} \langle d^\dagger_{q_1} d^\dagger_{q_2}\rangle e^{i(E_{q_1}+E_{q_2})t} + B^*_{kq_1} A_{kq_2} \langle d_{q_1} d_{q_2}\rangle e^{-i(E_{q_1}+E_{q_2})t} + \\ & + B^*_{kq_1} B_{kq_2} \langle d_{q_1} d^\dagger_{q_2}\rangle e^{i(E_{q_2}-E_{q_1})t} \}\end{aligned} \tag{5.9}$$

As mentioned above, however, the dynamics of observables such as N_p is characterized by a finite collection of frequencies; at any finite size N, the system can count at most on the $2N^2$ different frequencies mentioned above for the dynamics of quadratic operators. Consequently, its behavior is bound to display quasi-periodic features. Furthermore, a destructive interference, such as the one which brings forth the quasi-stationary behavior we have found, cannot last forever. There must be a time at which the oscillations amplitudes start growing again. We have called it recurrence time, t_R, since it is intimately related to the quasi-periodic nature of the system. Thus, the destructive interference required to give rise to a plateau (such as the one in Fig. 5.3) cannot last indefinitely at any finite size N and, in fact, we have verified that oscillations start to grow again after a recurrence time $t_R \approx N/4$, as can be see in Fig. 5.4.

The formalism developed here is therefore able to capture the relaxation of N_p towards a *pre-thermal* quasi-stationary state which, up to quantum oscillations, is approached as $\propto t^{-\alpha}$ with $\alpha \simeq 3$ (see the inset of Fig. 5.3). This same algebraic relaxation has also been observed in the average of the unperturbed hamiltonian $\langle H_0\rangle$ and is actually expected to characterize every generic observable which can be expressed as linear combinations of the fermion numbers $\langle \hat{n}_k\rangle$ or of the number of pairs — with possible exceptions depending on specific choices of the coefficients of these combinations. Furthermore, it is independent of the specific values of N and λ, provided that the former is large enough and the latter small enough. Finally, we have been able to check that the amplitude of the oscillations grow as λN, as it is shown in Fig. 5.4.

5.4 Diagrammatic approach

At long times higher-order terms will allow the redistribution of energy among the degrees of freedom of this system leading to full thermalization. As stated above, inelastic effects cannot be disregarded anymore in this regime, which therefore cannot be captured by our numerical approach. Hence, in this Section we switch to a complementary study of the mechanism leading to relaxation and eventually to thermalization in the late dynamics of this model. In order to see this it is convenient first to study pre-thermalization within a diagrammatic, perturbative approach at the second order in λ. For

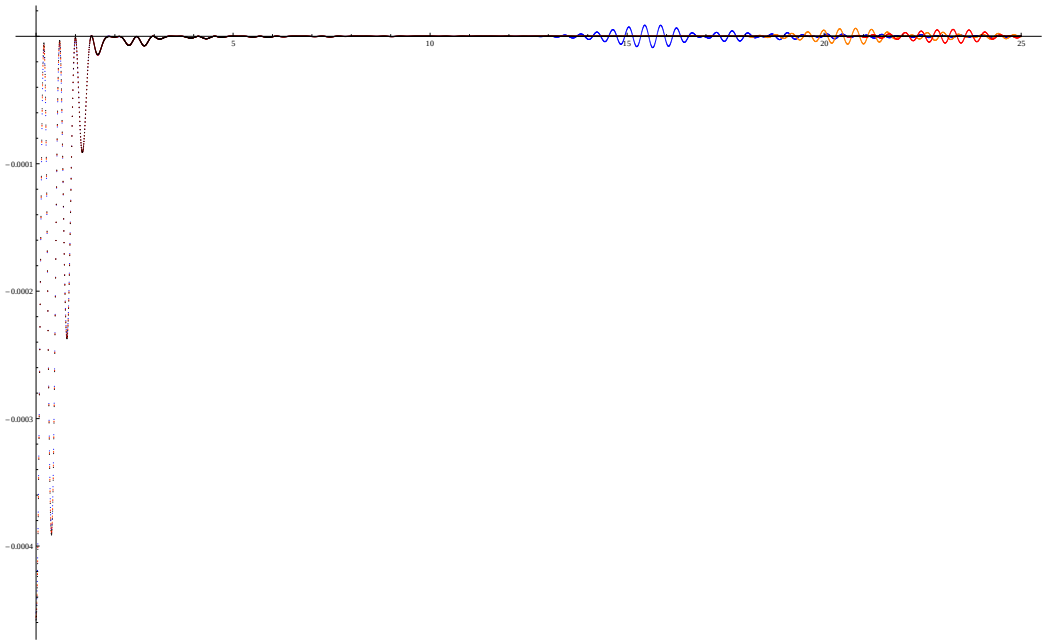

Figure 5.4: This picture shows different plots of $N_p(t)/N$ for different sizes of the system $N = 60, 80, 90, 120$ ($g_0 = 9$, $g = 4$, $\lambda = 0.1$). The collapse of the various curves for different values of N shows that oscillations are of the order λN. A similar plot (not shown here) for fixed N and different values of λ corroborates this fact. At longer times oscillations start again signaling the recurrent nature of the dynamics at finite size; this recurrence time appears earlier for smaller N.

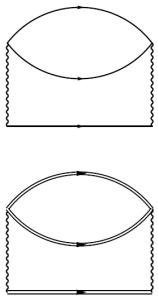

Figure 5.5: The sunset diagram at the perturbative level (upper figure) and in the self-consistent approximation (lower figure), see Section 5.5.

this purpose, we employ the Dyson equation for the Green function ordered on the Keldysh contour [62]. In [71] a composite quench of mass and interaction in a ϕ^4 model has been studied within a self-consistent diagrammatic approach, which included only the tadpoles diagrams. Using this approximation the authors of [71] fond that the two point correlation function long after the quench is of the same form as the free correlation function but with a different renormalized mass that has to be determined self-consistently. This means that nothing really changes in terms of the relaxation of the system, since tadpoles ignore the effect of collisions between quasiparticles with different momenta that can induce a mixing of the different modes and possibly thermalization. So in the remaining part of this Chapter we are going to consider the first non-trivial diagram which can redistribute energy among the elementary degrees of freedom of the model, i.e. the sunset diagram, and in order to focus on its effects on the relaxation dynamics of the model, we are going to assume that the self-energy is only due to sunsets (see 5.5).

Among the quantities one can study within this diagrammatic approach, the simplest is the distribution of the quasi-stationary populations

$$n_k = \lim_{T\to\infty} \frac{1}{T} \int_0^T dt \langle \hat{n}_k(t) \rangle = \int_{-\infty}^{\infty} \frac{d\omega}{2\pi} F_k(\omega) A_k(\omega), \tag{5.10}$$

expressed in terms of the spectral density $A_k(\omega)$ and of the statistical function $F_k(\omega)$, where the limit is intended to hold up to the time scales of validity of perturbation theory. For a quenched QIC ($\lambda = 0$, $g \neq g_0$), $A_k(\omega) = 2\pi i \delta(\omega - \epsilon_k)$ whereas F_k corresponds to a Fermi-Dirac distribution function $f_{GGE,k}(\omega) \equiv (\mathrm{e}^{\beta_k \omega} + 1)^{-1}$ for the GGE, with a mode-dependent inverse temperature $\beta_k = 2\,\mathrm{th}^{-1}(\cos\Delta\theta_k)/\epsilon_k$, where $\Delta\theta_k = 2[\theta_k(g) - \theta_k(g_0)]$. This clearly highlights the role of integrability: the absence of inelastic processes prevents the QIC from redistributing the energy among the quasi-

particles, and therefore thermalization as a whole.

In order to compute quantities like (5.10), we write down the Dyson equation for the statistical Green function on the Keldysh contour (see [62] or the Appendix)

$$G^c = -i\langle T_c \psi_{ki}(\tau)\psi^\dagger_{kj}(\tau')\rangle, \tag{5.11}$$

where T_c is the time ordering operator on the Keldysh contour, τ and i and j are indices in the Nambu space and $\widehat{\psi}_k$ is the Nambu spinor $\binom{\gamma_k}{\gamma^\dagger_{-k}}$; we define the lesser Green function as

$$G^<(t,t') = \left[G^<_k(t,t')\right]_{i,j} = i\langle \psi^\dagger_{k,j}(t')\psi_{k,i}(t)\rangle, \tag{5.12}$$

which is a matrix in the Nambu space (here t and t' are real times). For the unperturbed problem ($\lambda = 0$), the lesser Green's function is

$$G^<_0(t,t') = \begin{pmatrix} \sin^2(\Delta\theta_k)e^{-i\epsilon_k\tau} & i\frac{\sin(2\Delta\theta_k)}{2}e^{-i\epsilon_k T} \\ -i\frac{\sin(2\Delta\theta_k)}{2}e^{i\epsilon_k T} & \cos^2(\Delta\theta_k)e^{i\epsilon_k\tau} \end{pmatrix} \tag{5.13}$$

where $\tau = t - t'$ and $T = \frac{t+t'}{2}$. Using the standard approach [62], we first write the equation for the statistical Green function with the self energy computed at the perturbative level, i.e. replacing the full Green's functions by the unperturbed ones (see Fig. 5.6)

$$G^c_{\tau,\tau'} = G^c_{0_{\tau,\tau'}} + G^c_{0_{\tau,\tau''}} \otimes \Sigma^c_{0_{\tau'',\tau'''}} \otimes G^c_{\tau''',\tau'} \tag{5.14}$$

where $G^c_{0_{\tau,\tau'}}$ is the unperturbed Green function and $\Sigma^c_{0_{\tau'',\tau'''}}$ is the self energy evaluated at the second order in perturbation theory and including only the sunset diagram; in right hand side the symbol $\otimes$ is understood as a convolution product, all the quantities are evaluated along the Keldysh contour.

The analytic expression for the self-energy is

$$\begin{aligned} \Sigma^k_{t_1,t_2} &= \lambda^2 \widetilde{\sigma_z} G^c_k(t_1,t_2)\widetilde{\sigma_z}\Pi(t_1,t_2), \\ \Pi(t_1,t_2) &= \sum_{p>0} tr\left\{G^c_p(t_1,t_2)\sigma_z G^c_p(t_2,t_1)\sigma_z\right\}, \\ \widetilde{\sigma_z} &= \cos 2\theta_k \sigma_z + \sin 2\theta_k \sigma_y. \end{aligned} \tag{5.15}$$

It is easy to show that the lesser component of $\Pi^>_0(t_1,t_2)$ (i.e. $\Pi^>(t_1,t_2)$ at the perturbative level) is the two-times correlation function of the global transverse magnetization of the QIC after a quench of the transverse field. Hence, roughly speaking, the out-of-equilibrium dynamics of the model is initiated by the out-of-equilibrium fluctuations of the global transverse magnetization after a quench of the transverse field. Moreover, from (5.15) it should be easy to realize that the system acts as its own bath: a single excitation carrying momentum k, represented by the Green's function $G_k(t_1,t_2)$, can effectively

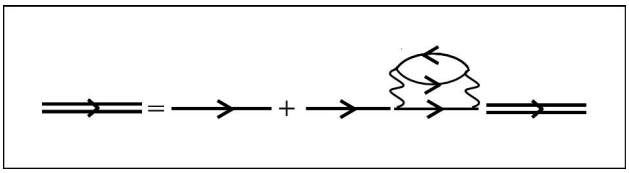

Figure 5.6: The perturbative Dyson equation at the second order in perturbation theory. Full lines stand for the dressed Green's function, while single lines are the unperturbed ones.

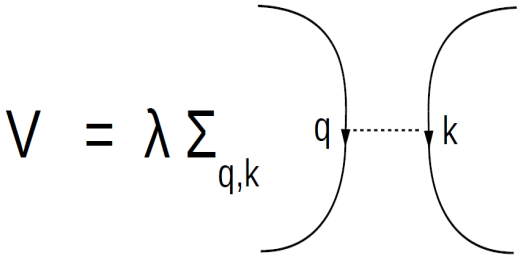

Figure 5.7: The vertex contributing to the sunset diagram of Fig. 5.5; each line conserves separately momentum.

exchange energy with the whole set of fermionic modes and this feature is encoded mathematically in $\Pi(t_1, t_2)$. From Eq.(5.15) we can have even a more clear insight into the collision processes responsible for relaxation; because of the peculiar nature of the interaction, vertexes exchange only energy but not momentum: momentum is super-conserved in each vertex, in the sense that each line conserves separately momentum, as Fig. 5.7 should clarify.

When V is turned on, we expect that the single quasi-particle peak, $\delta(\omega - \epsilon_k)$, in the spectral density, A_k will broaden into a Lorentzian with a frequency-dependent inverse life time

$$\begin{aligned}\Gamma_k(\omega) = &\frac{2\lambda^2}{N^2}\sin^2(2\theta_k)\times \\ &\times\Big[f_{GGE,k}(\epsilon_k)\Pi^{>}(\omega+\epsilon_k) + f_{GGE,k}(-\epsilon_k)\Pi^{>}(-\omega-\epsilon_k)\Big].\end{aligned} \tag{5.16}$$

which can be computed solving in second-order perturbation theory the retarder Dyson equation. $\Pi^{>}(\omega)$, calculated in second-order perturbation theory, describes effective absorption and emission of a pair of fermions γ_k:

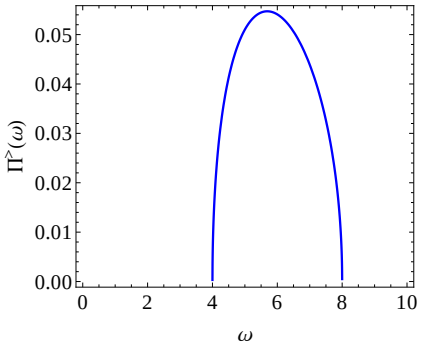

Figure 5.8: The emission component of $\Pi^>(w)$ for $g_0 = 2$, $g = 3$.

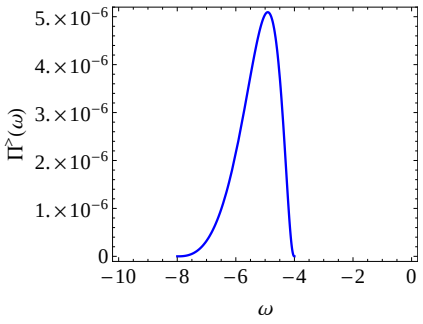

Figure 5.9: The absorption component of $\Pi^>(w)$ for $g_0 = 2$, $g = 3$.

$$\Pi^>(\omega) = \sum_{k>0} \sin^2 2\theta_k \Big(\delta(\omega - 2\epsilon_k) f_{GGE,k}\Big(-\frac{\omega}{2}\Big)^2 + \delta(\omega + 2\epsilon_k) f_{GGE,k}\Big(-\frac{\omega}{2}\Big)^2 \Big). \tag{5.17}$$

The absorption processes occur for $\omega \in [2(g-1), 2(g+1)]$ (see 5.8), while emission has support in $[-2(g+1), -2(g-1)]$ (see 5.9), respectively; this is easy to understand since the unperturbed spectrum ϵ_k of each fermion ranges from $g-1$ to $g+1$.

$\Gamma_k(\omega)$ quantifies the spreading of the Ising quasi-particles over the new interacting eigenmodes; close to the pronounced peak at $\omega = \epsilon_k$ (energy level shifts are disregarded here), Γ_k determines the effective width of the Lorentzian, given by

$$\Gamma_k(\epsilon_k) = \frac{\lambda^2}{4Ng} \sin^3(2\theta_k) f_{GGE,k}(\epsilon_k) f_{GGE,k}(-\epsilon_k). \tag{5.18}$$

Analogously, the statistical distribution function F_k gets a correction to

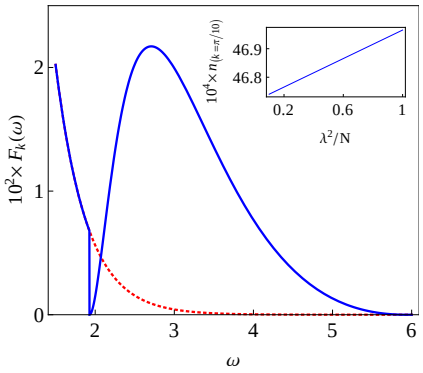

Figure 5.10: Distribution functions in the pre-thermal stage of dynamics, with $k = \pi/10$, $g_0 = 2$, and $g = 3$. The red dotted line corresponds to the GGE distribution $f_{k=\pi/10}(\omega)$ for $\lambda = 0$, while the blue solid line is the corresponding distribution function $F_{k=\pi/10}(\omega)$ for $\lambda \neq 0$.

the aforementioned GGE distribution function $f_{GGE,k}(\omega)$,

$$F_k(\omega) = f_{GGE,k}(\omega) + \frac{\lambda^2}{N^2}\sin^2(2\theta_k)\times \\ \times \frac{f_{GGE,k}(-\epsilon_k)f_{GGE,k}(-\omega)\Pi^{>}(-\omega-\epsilon_k) - f_{GGE,k}(\epsilon_k)f_{GGE,k}(\omega)\Pi^{>}(\omega+\epsilon_k)}{2\Gamma_k(\omega)}, \tag{5.19}$$

which is actually independent of λ [see Eq.(5.16)]. This computation can be done solving at the perturbative level the Dyson equation for the lesser Green's function (this is the so called Keldysh equation, see Appendix for more details). This distribution function is *neither* thermal *nor* GGE-like [see Eq.(5.19)] and causes perturbative corrections — characteristic of a *pre-thermal* state — to appear in the occupation number f_k, upon integrating Eq.(5.10) (see Fig. 5.10). The apparent puzzle of a perturbative correction to observables, despite a pre-thermal distribution function independent of λ, is resolved by realizing that $F_k = f_k$ for $\omega = \epsilon_k$, hence the first non-zero correction is proportional to λ^2/N.

Even if the sunset contribution to the pre-thermal plateau in Fig. 5.3 describes just higher order corrections, we expect it will be crucial at longer times in order to capture full thermalization, since the sunset is the first diagram contributing to the imaginary part of the self energy, which is necessary in order to have relaxation and eventually thermalization.

5.5 Thermalization

First of all, we rewrite the Dyson equation in the form of the celebrated Kadanov-Baym equation (disregarding terms which describe renormalization

effects see [62])

$$i\partial_T G_k^< - [H_0, G_k^<] = \frac{1}{2}(\{\Sigma_k^>, G_k^<\} - \{G_k^>, \Sigma_k^<\}) \tag{5.20}$$

where the products in the right hand side are intended as convolution products. Our aim in this section is to show that the thermal distribution is the unique solution of this equation when the broadening which accounts for inelastic scattering is taken into account. In order to do so, we shall assume that $G_k^<$ is diagonal and that the matricial structure of $G_k^<$ is all encoded in the spectral density, in the following way

$$G_k^<(\omega) = iF_k(\omega)A_k(\omega) \tag{5.21}$$

where $F_k(\omega)$ is the stationary distribution function attained in the long time limit and $A_k(\omega)$ is a diagonal matrix whose entries are Lorentzian with a frequency ω and wave-vector k dependent life-time $\Gamma_k(\omega)$. The diagonal approximation is valid in limit $\frac{\frac{\lambda^2}{N}}{\Delta} \ll 1$, beacause the off-diagonal elements are of order $O(\frac{\frac{\lambda^4}{N^2}}{\Delta^2})$, as we are going to show in the following.

Let us start with the more general form of the retarded self-energy

$$\Sigma_k^R(\omega) \equiv \begin{pmatrix} -i\Gamma_k(\omega) & N_k(\omega) \\ N_k(-\omega)^* & -i\Gamma_k(-\omega) \end{pmatrix} \tag{5.22}$$

where we neglected the real part of the self energy since it is expected to shift only the unperturbed eigenvalues and $N_k(\omega)$ are the off-diagonal matrix elements, which we would like to neglect in the small interaction limit.

Introducing an effective hamiltonian, $\omega - H_{eff} \equiv (G_0^R)^{-1} - \Sigma^R$, and diagonalizing $\omega - H_{eff}$, we get for the eigenvalues

$$\lambda_{eff} = \frac{2\omega + i(\Gamma_k(\omega) + \Gamma_k(-\omega))}{2} \pm \sqrt{\Big(\frac{-2\epsilon_k + i(\Gamma_k(\omega) - \Gamma_k(-\omega))}{2}\Big)^2 + I} \tag{5.23}$$

where $I \equiv N_k(\omega)N_k(-\omega)^*$ and from which it is clear that, since $\Gamma_k(\omega)$, $N_k(\omega)$ are of order $\sim \frac{\lambda^2}{N}$, the second term in square root is subleading with respect to the first one provided that $\frac{\frac{\lambda^2}{N}}{\Delta} \ll 1$, where Δ is the gap of the unperturbed QIC.

Within the diagonal approximation, $[H_0, G_k^<] = 0$, since also H_0 is diagonal, and the right hand side of the Kadanov-Baym is just given by the so-called *collision kernel*. Recalling the expression for the self-energy (Eq. (5.15)), and assuming it is given only by the dressed sunset diagrams (see

Fig. 5.5), we find that

$$\begin{aligned}
\Sigma_k^<(\omega) &= \frac{\lambda^2}{N^2}\int \frac{d\omega' d\omega''}{(2\pi)^2}\widetilde{\sigma}_k^z G_k^<(\omega-\omega'-\omega'')\widetilde{\sigma}_k^z \Pi^<(\omega',\omega'') \\
\Sigma_k^>(\omega) &= \frac{\lambda^2}{N^2}\int \frac{d\omega' d\omega''}{(2\pi)^2}\widetilde{\sigma}_k^z G_k^>(\omega-\omega'-\omega'')\widetilde{\sigma}_k^z \Pi^>(\omega',\omega'') \\
\Pi^<(\omega',\omega'') &= \sum_q Tr\{\widetilde{\sigma}_k^q G_q^<(\omega')\widetilde{\sigma}_k^q G_q^>(-\omega'')\} \\
\Pi^>(\omega',\omega'') &= \sum_q Tr\{\widetilde{\sigma}_k^q G_q^>(\omega')\widetilde{\sigma}_k^q G_q^<(-\omega'')\}.
\end{aligned} \tag{5.24}$$

Substituting these expressions in (5.20), we find for the *collision kernel*

$$\begin{aligned}
&\{\Sigma_k^>, G_k^<\} - \{G_k^>, \Sigma_k^<\} = \\
&\int \frac{d\omega' d\omega''}{(2\pi)^2}\sum_q \Big[F_k(\omega)F_k(-\omega+\omega'+\omega'')F_q(-\omega')F_q(-\omega'')- \\
&+F_k(-\omega)F_k(\omega-\omega'-\omega'')F_q(\omega')F_q(\omega'')\Big]\mathcal{D}_{kq}(\omega,\omega',\omega''),
\end{aligned} \tag{5.25}$$

where

$$\mathcal{D}_{kq}(\omega,\omega',\omega'') = 2Tr\{\widetilde{\sigma}_q^z A_q(\omega')\widetilde{\sigma}_q^z A_q(-\omega'')\}(\widetilde{\sigma}_k^z A_k(\omega-\omega'-\omega'')\widetilde{\sigma}_k^z)_{1,1}A_k(\omega)_{1,1}\Big]. \tag{5.26}$$

This expression for the *collision kernel*, even if quite involved is the core of this Section. First of all, with a straightforward calculation it is easy to show that if $A_k(\omega)_{(1,1)} \propto \delta(\omega-\epsilon_k)$ (and $A_k(\omega)_{(2,2)} \propto \delta(\omega+\epsilon_k)$), then the *collision kernel* identically vanishes for each $f_k(\omega)$ satisfying the basic symmetries of the theory. When a broadening ($\Gamma_k \neq 0$) is generated by the the inelastic collisions, the quantity in square bracket in Eq. (5.25) is zero only for $F_k(\omega) = \frac{1}{e^{\beta\omega}+1}$, i.e. the Boltzmann distribution function. β is the inverse temperature and it can be in principle determined by imposing the conservation of energy during the time evolution $\langle H\rangle = Tr[\rho_{thermal}(\beta)H)]$.

Notice that a distribution function with frequency-dependent inverse temperature β_k, like the GGE distribution function, would not make the *collision kernel* vanish, corroborating the idea that in the long-time limit the system would reach a fully thermalized state. An approximate expression for the broadening $\Gamma_k(\omega)$ can be determined solving self-consistently the retarded Dyson equation; it is a long and cumbersome computation that will be reported in an extended version [72] of [8]. We are currently carrying on a study on the stability of the thermal solution, perturbing the thermal state with a small displacement $\delta f_k(\omega, T)$ in order to have some conclusive statement about the thermalization of this model.

Chapter 6

Conclusions and future perspectives

In this PhD Thesis we focused on *Pre-Thermalization*, an important topic in the domain of non-equilibrium quantum many body physics. The appearance of long-lived non-equilibrium quasi-steady states has been observed in 2011 in the coherent split of 1D Bose gases and their theoretical explanation in terms of an effective integrable theory describing the intermediate states of dynamics has been suggested in the same year (see Chapter 3). Despite the few numerical and analytical cases studied, the problem is of paramount importance, because it is a novel feature of quantum non-equilibrium dynamics, the first step to understand how to solve the puzzle of thermalization in a quantum many body system (see Chapter 2). For this reason, we decided to study extensively pre-thermalization in the out-of-equilibrium dynamics of a QIC perturbed by time dependent and time independent interactions, benefiting of the full control achieved in the past years on quench dynamics of the QIC, which is also the simplest exactly solvable model in condensed matter physics. Our aim was two-fold: first, to generalize the notion of pre-thermalization to open noisy quantum many body systems, and secondly, to deepen our physical intuition of the mechanism governing pre-thermalization and thermalization in closed non-integrable quantum many body systems, which is the usual framework where these concepts have been developed first.

In Chapter 4 we showed as a QIC perturbed by a time dependent noise displays pre-thermalization plateaux in a broad class of physically relevant observables. We considered the combined effect of the noise and the usual quench of the transverse field and we realized that noise and quench affect differently populations and coherences of the underlying Bogolyubov fermions, which diagonalize the Ising Chain. In particular, while coherences are damped for intermediate time scales by the usual dephasing mechanism peculiar of a quenched integrable model, at late times, when noise is relevant, this first slow algebraic dephasing is suppressed in an exponential way,

and at the same time populations start heating, leading the system towards the final thermal state. This system is amenable to analytic computations within the Keldysh technique, hence it could be very interesting to test in this framework many tantalizing modern issues in the domain of quantum quenches. The noise considered in our work is homogeneous in space; in order to make progress in the analytical study of pre-thermalization in quantum many body systems, an interesting generalization could consist in considering a lattice-site dependent noise, which closely resemble what happens in the integrability breaking of a quantum spin chain, where the perturbation in general affects in a different way each single site. It is conceivable to think that pre-thermal plateaux will occur as well in this case, since they are essentially determined by the underlying integrable model, while we expect a different scenario for the departure from the pre-thermal state and the approach towards the new asymptotic steady state, attained in such a system. Another possibility could be to study how fluctuation-dissipation relations set up in a quenched system. While it is widely known that a system at equilibrium satisfy the fluctuation-dissipation theorem, it is not clear how these relations establish starting from a quantum out-of-equilibrium state. A first step in this direction has been made the last year by F. Essler and collaborators [76], showing that the GGE attained in the long-time dynamics satisfy a generalized version of the fluctuation-dissipation relations with the usual mode-dependent temperature, replacing the canonical temperature of the canonical thermal state. In the noisy QIC it is possible to compute unequal times correlation functions which are the essential tool to explore such a problem and which could be extremely useful in order to approach the tantalizing problem of universality out-of-equilibrium.

In Chapter 5 we considered a non-integrable version of the QIC subject to a composite quench of mass and interactions. Using a mapping into an effective bosonic theory valid in the limit of small quenches, we showed the appearance of a pre-thermal behavior in a class of observables. We started to study the interesting problem of how inelastic scattering affects thermalization dynamics and leads to the asymptotic thermal state within a diagrammatic approach. Focusing on the sunset diagrams, which are expected to give the leading contribution towards thermalization, we derived some features of the pre-thermal state, such as the effect of inelastic processes on the distribution function and on the imaginary part of the self energy, which governs the spreading of the original eigenmodes on the new ones. The same features can derived in a self-consistent formalism which is able to capture some properties of the asymptotic steady state, showing that inelastic processes and a finite life-time are essential in order to have a thermal distribution in the late time dynamics. The approach developed in this Chapter opens many interesting problems: first of all, the possibility to describe how and whether the system departs from the pre-thermal state towards the thermal state using higher

order corrections to the integrable effective bosonic description and/or the diagrammatic framework. Another issue could consist in applying the ideas developed in this Chapter to more experimentally relevant models, such as out-of-equilibrium perturbations of the Luttinger Liquid model (see for a first attempt in this direction the paper by Tavora and Mitra [75]).

A comprehensive understanding of pre-thermalization in quenched quantum systems is the key to understand the mechanism behind quantum thermalization. At the core of this problem, there is the unsolved question of the existence of a RG description of quantum dynamics, i.e. whether there exists a finite threshold of the integrability breaking strength for pre-thermalization to disappear, and to have, instead, a smooth decay towards the thermal state, looking at pre-thermal and thermal states as basins of attraction of the out-of-equilibrium dynamics, potentially influenced also by the choice of the initial state. Pre-thermalization could become also an useful source for quantum technology, since the possibility of trapping experimentally a system in such an a-thermal quasi-steady state could be used to explore states of matter with completely new and undiscovered features; for instance, pre-thermalization could be used to realize non-ergodic quantum heat engines able to exceed the equilibrium Carnot bound (see about this topic Ref. [77]). Finally, the surprising emergence of pre-thermalization in a broad variety of contexts, like cosmology, heavy ions collisions, coherently splitted one dimensional bose gases, and all the other models discussed in this PhD Thesis, open the intriguing question of a unified an universal description of out-of-equilibrium dynamics embracing all the domains of Physics.

We hope this PhD Thesis helped extending our current understanding of pre-thermalization and to open new interesting questions in this fascinating and modern research field.

Chapter 7

Appendix: The Keldysh Formalism

In this Appendix we summarize the basics of the Keldysh formalism, which is the main analytical tool used in this PhD Thesis for the computations outlined in Chapter 4 and 5.
The exposition closely follows Jahuo's book [62] and the review by J. Maciejko [74], to which we refer for further details.

7.1 Contour Ordered Green Functions

Let us consider a system described by the time-independent Hamiltonian:

$$H = H_0 + H_I, \tag{7.1}$$

where H_0 is the free part (usually exactly solvable) and H_I the time independent interaction term. We assume that the system is in thermal equilibrium and so it is described by the thermodynamical equilibrium density matrix:

$$\rho(H) = \frac{e^{-\beta H}}{Tr\left[e^{-\beta H}\right]}. \tag{7.2}$$

At time t_0 we perturb our system by adding a time dependent Hamiltonian $H'(t)$. The total Hamiltonian is then:

$$\mathcal{H}(t) = H_0 + H_I + H'(t) \tag{7.3}$$

where the operators are intended in Heisenberg picture and obey the evolution equation:

$$i\frac{d}{dt}\mathcal{O}_{\mathcal{H}}(t) = \left[\mathcal{O}_{\mathcal{H}}(t), \mathcal{H}(t)\right]. \tag{7.4}$$

Before we switch on the perturbation, $H'(t)$, our system is in thermal equilibrium. If we assume that our observation times are much smaller than the

time scales for the evolution of the thermodynamical degrees of freedom, we can compute thermodynamical averages with (7.2): the thermodynamics is frozen in the initial equilibrium state, while the dynamics is sensible to the perturbation and evolve with the full Hamiltonian (7.3), hence

$$\langle \mathcal{O}_{\mathcal{H}}(t) \rangle = Tr\left[\rho(H)\mathcal{O}_{\mathcal{H}}(t)\right]. \tag{7.5}$$

Let us now give some proper definition for the Green's functions. The contour ordered Green's function is [1]:

$$G(1,2) = -i\langle T_C\left(\psi_{\mathcal{H}}(1)\psi^{\dagger}_{\mathcal{H}}(2)\right)\rangle \tag{7.6}$$

where $\psi_{\mathcal{H}}$ is a Bose or Fermi field in the Heisenberg picture. C is the contour represented in Figure (7.1) in the complex plane that starts and ends at t_0 (the time at which we turn on the perturbation): it runs along the real axis and passes through t_1 and t_2 once. At a first look this choice can seem weird, but it can be justified by the following argument. In conventional equilibrium diagrammatic theory we adiabatically switch on and off the interaction and consequently we can assume that the state in the asymptotic past and in the asymptotic future differs only by a phase, as follows straightforwardly from the adiabatic theorem. Such an argument is unjustified out-of-equilibrium, since the final state will strongly differs from the initial one, hence it is necessary to employ the Schwinger-Keldysh contour technique, in order to avoid any reference to the state in the asymptotic future.

The contour ordering operator, T_C, orders the operators according to the position on the contour of their time arguments: the operators with time labels that occur later on the contour have to stand left to operators with earlier time labels,

$$T_C\left(\psi_{\mathcal{H}}(1)\psi^{\dagger}_{\mathcal{H}}(2)\right) = \begin{cases} \psi_{\mathcal{H}}(1)\psi^{\dagger}_{\mathcal{H}}(2) & \text{if } t_1 \underset{C}{\geq} t_2 \\ \pm\psi^{\dagger}_{\mathcal{H}}(2)\psi_{\mathcal{H}}(1) & \text{if } t_1 \underset{C}{<} t_2 \end{cases}, \tag{7.7}$$

where the upper sign holds for boson and the lower for fermions. The contour ordered Green's function plays an analogous role in non equilibrium theory as the time ordered Green's function plays in equilibrium theory: as we will show in this section, it possesses a perturbation theory based on Wick's theorem. However, since the time labels lie on the contour with two branches, we must keep track of which branch we are considering. With two time labels, which can be located on either of the two branches of the contour, there are four distinct possibilities. If we call C_1 the branch that starts in t_0 and C_2 the

[1] We use the abbreviation $1 = (t_1, \mathbf{x}_1)$. $\mathbf{x}$ denotes the spatial variable, which can be generalized to include spin and others degrees of freedom.

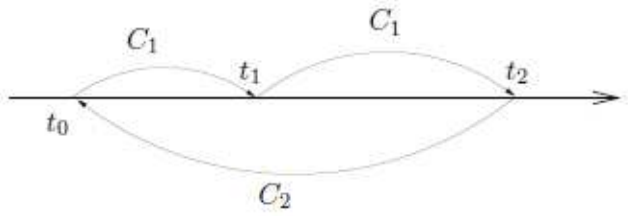

Figure 7.1: The Schwinger-Keldysh contour starting at t_0, ending at t_2 and passing through t_1 just once.

branch that ends in t_0, these possibilities are:

$$G(1,2) = \begin{cases} G_T(1,2) & t_1,\, t_2 \in C_1 \\ G^{>}(1,2) & t_1 \in C_2,\, t_2 \in C_1 \\ G^{<}(1,2) & t_1 \in C_1,\, t_2 \in C_2 \\ G_{\tilde{T}}(1,2) & t_1,\, t_2 \in C_2 \end{cases} \tag{7.8}$$

Here we have introduced the time ordered Green function G_T :

$$G_T(1,2) = -i\langle T(\psi_{\mathcal{H}}(1)\psi^{\dagger}_{\mathcal{H}}(2))\rangle, \tag{7.9}$$

the greater Green function $G^{>}$:

$$G^{>}(1,2) = -i < \psi_{\mathcal{H}}(1)\psi^{\dagger}_{\mathcal{H}}(2) >, \tag{7.10}$$

the lesser Green function $G^{<}$:

$$G^{<}(1,2) = \mp i < \psi^{\dagger}_{\mathcal{H}}(1)\psi_{\mathcal{H}}(2) >, \tag{7.11}$$

and the anti-time ordered Green function $G_{\tilde{T}}$:

$$G_{\widetilde{T}}(1,2) = -i\langle \widetilde{T}\psi_{\mathcal{H}}(1)\psi^{\dagger}_{\mathcal{H}}(2)\rangle. \tag{7.12}$$

Since $G_T + G_{\tilde{T}} = G^{<} + G^{>}$ there are only three linearly independent functions. This freedom of choice reflects itself in the literature, where a number

of different conventions can be found. For our purposes the most suitable functions are the greater and the lesser function $G^{>,<}$, and the advanced and the retarded functions defined as:

$$G^A(1,2) = i\theta(t_2 - t_1) < [\psi_{\mathcal{H}}(1),\, \psi^\dagger_{\mathcal{H}}(2)]_\mp > = \tag{7.13}$$
$$= \theta(t_2 - t_1)\,[G^>(1,2) - G^<(1,2)] \tag{7.14}$$

and:

$$G^R(1,2) = -i\theta(t_1 - t_2) < [\psi_{\mathcal{H}}(1),\, \psi^\dagger_{\mathcal{H}}(2)]_\mp > = \tag{7.15}$$
$$= \theta(t_1 - t_2)\,[G^>(1,2) - G^<(1,2)] \tag{7.16}$$

We also note that

$$G^R - G^A = G^> - G^< \tag{7.17}$$

which is usually an helpful relation when computations are performed in practice.
After all these definitions, we would like to comment on the physical meaning of all these Green's functions. Like in equilibrium, the retarded and the advanced Green's functions contain information about spectral properties of the system, like the shift or the broadening of energy levels, while the lesser and the greater Green's functions usually enter in the computation of observables like the occupation number of Ising quasiparticles or the correlation functions of spins after a quench, just to mention some quantities we computed in this PhD Thesis.

We now prove one of the main statement of this Appendix, i.e. the perturbative expansion of the contour ordered Green function.
The first step is to switch from the Heisenberg to the interaction picture with respect to H. We know that, for any operator

$$\mathcal{O}_{\mathcal{H}}(t) = u^\dagger(t, t_0)\mathcal{O}_H(t)u(t, t_0), \tag{7.18}$$

where

$$u(t, t_0) = T \exp\left[-i \int_{t_0}^{t} dt' H'_H(t')\right] \tag{7.19}$$

and $H'_H(t)$ represents the operator $H'(t)$ in the interaction picture with respect to H. We can obviously re-express (7.18) as:

$$\mathcal{O}_{\mathcal{H}}(t) = T_{C_t}\left[\exp\left[-i \int_{C_t} d\tau H'_H(\tau)\right] O_H(t)\right], \tag{7.20}$$

where the contour C_t runs from t_0 to t and than back gain to t_0.

Using this transformation we can write the contour ordered Green function in the interaction picture with respect to H as:

$$G(1,2) = -i < T_C\left(S^H_C \psi_H(1)\psi^\dagger_H(2)\right) > \tag{7.21}$$

where:

$$S_C^H = \exp\left[-i\int_C d\tau H'_H(\tau)\right]. \tag{7.22}$$

Since we would like to employ Wick's theorem, we must transform to the interaction picture with respect to the free-particle Hamiltonian H_0, which is quadratic in the field operators. Using the relation

$$\exp(-\beta H) = \exp(-\beta H_0)v(t_0 - i\beta, t_0), \tag{7.23}$$

where

$$v(t, t_0) = T\exp\left[-i\int_{t_0}^{t} dt' H^I_{H_0}(t')\right] \tag{7.24}$$

with $H^I_{H_0}(t)$ being the operator H^I in the interaction picture with respect to the Hamiltonian H_0, we finally obtain:

$$G(1,2) = -i\frac{Tr\left\{\rho_0 T_{C_v}\left[S^I_{C_v} S'_C \psi_{H_0}(1)\psi^\dagger_{H_0}(2)\right]\right\}}{Tr\left\{\rho_0 T_{C_v}\left[S^I_{C_v} S'_C\right]\right\}}, \tag{7.25}$$

where ρ_0 is the free particle density matrix:

$$\rho_0 = \frac{e^{-\beta H_0}}{Tr\left[e^{-\beta H_0}\right]} \tag{7.26}$$

and:

$$S'_C = \exp\left[-i\int_C d\tau H'_{H_0}(\tau)\right], \tag{7.27}$$

$$S^I_{C_v} = \exp\left[-i\int_{C_v} d\tau H^I_{H_0}(\tau)\right]. \tag{7.28}$$

The contour C_v is shown in figure (7.2).

In equation (7.25) we can use Wick's theorem to get a perturbative expansion for G. As in the equilibrium case, the denominator cancels the contribution arising from the disconnected diagrams. The equilibrium and the non equilibrium theory are structurally equivalent: the only difference is the replacement of the real axis integrals by contour integrals. A simplification occurs if we can set $t_0 \to -\infty$. In fact, in this way the contribution from the $[t_0, t_0 - i\beta]$ piece vanishes and the contour C and C_v are now identical: they both start and end at $-\infty$. It has been shown (see [62]) that discarding this part of the contour corresponds to neglect initial correlations. It appears plausible that in many physical situations, for example in the long time limit after a quench, when the thermal state is approached, the initial correlations have been washed out by the interactions.
From now on we will consider the limit $t_0 \to -\infty$, and so we will use the Keldysh contour represented in figure 7.3.

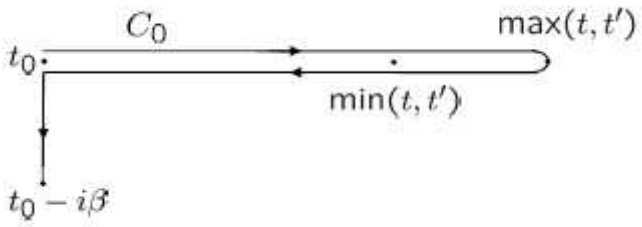

Figure 7.2: The contour C_v

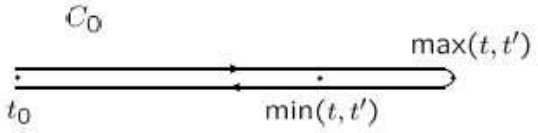

Figure 7.3: The Keldysh contour usually employed for an out-of-equilibrium diagrammatic expansion.

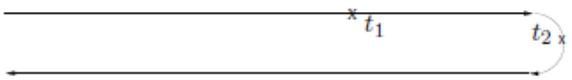

Figure 7.4: t_1 is on the first branch of $\mathcal{K}$ while t_2 is on the second one.

7.2 Langreth Theorem

The contour ordered Green's functions are the building block of the theory, since they possess a perturbative expansion in Feynman diagrams. However, studying this expansion we will face time integral on the Keldysh contour $\mathcal{K}$ (fig. 7.3) and we prefer to avoid integral in the complex plain. In this section we will study an analytic continuation technique, the Langreth Theorem, that will allow us to convert all the integral in the complex plane in integral on the real axis. In doing so, we will have to convert the contour ordered Green's functions in the retarded, advanced and lesser ones: instead to calculate one Green's function we will have to calculate three of them.
Studying the perturbative expansion of the contour ordered Green's function we will face terms like

$$C(t_1, t_2) = \int_{\mathcal{K}} d\tau A(t_1, \tau) B(\tau, t_2) \tag{7.29}$$

and their generalizations. Now, for definiteness let us assume that t_1 is on the first branch of C and t_2 is on the second one: we are thus analyzing a lesser function (fig. 7.4).

Now, since we can deform the contour as we prefer. So we deform it as in figure (7.5). Thus (7.29) becomes:

$$C^{<}(t_1,\, t_2) = \int_{\mathcal{K}_1} d\tau A(t_1,\, \tau)\; B(\tau,\, t_2) + \int_{\mathcal{K}_2} d\tau A(t_1,\, \tau)\; B(\tau,\, t_2) \tag{7.30}$$

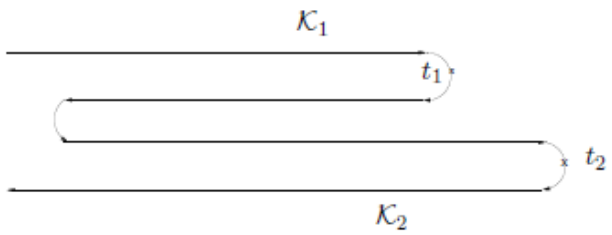

Figure 7.5: The deformation of the contour. K_1 is the upper half, while K_2 is the the lower half.

We notice that, as long as the integration variable τ is confined in the contour $\mathcal{K}_1$, it is less (on the contour) than t_2 and so $B(\tau, t_2) = B^<(\tau, t_2)$. In the same way, when τ is on $\mathcal{K}_2$, t_1 is greater than τ, so $A(t_1, \tau) = A^>(t_1, \tau)$. So, we can rewrite (7.30) as:

$$C^<(t_1, t_2) = \int_{\mathcal{K}_1} d\tau A(t_1, \tau)\, B^<(\tau, t_2) + \int_{\mathcal{K}_2} d\tau A^<(t_1, \tau)\, B(\tau, t_2). \quad (7.31)$$

Now, let us consider the first term of (7.31) :

$$\begin{aligned}
&\int_{\mathcal{K}_1} d\tau A(t_1, \tau) B^<(\tau, t_2) = \\
&= \int_{-\infty}^{t_1} dt\, A(t_1, t)\, B^<(t, t_2) + \int_{t_1}^{-\infty} dt\, A(t_1, t)\, B^<(t, t_2) = \\
&= \int_{-\infty}^{t_1} dt\, A^>(t_1, t)\, B^<(t, t_2) + \int_{t_1}^{-\infty} dt\, A^<(t_1, t)\, B^<(t, t_2) = \\
&= \int_{-\infty}^{+\infty} dt\, A^R(t_1, t) B^<(t, t_2). \qquad (7.32)
\end{aligned}$$

In the last line we used the definition of retarded function (7.16). A similar analysis can be applied to the second term involving contour $\mathcal{K}_2$, where the advanced Green's function appears. Putting the two terms together we have

the first of the Langreth's results:

$$C^<(t_1,\, t_2) = \int_{-\infty}^{+\infty} dt \left[A^R(t_1,\, t)\, B^<(t,\, t_2) + A^<(t_1,\, t) B^A(t,\, t_2)\right]. \qquad (7.33)$$

The same results applies for the greater function: we have only to replace all $<$' with $>$'s. This result can also be straightforwardly generalized to the integral of three functions (see Table below).
Often we need to evaluate the retarded or the advanced component of a structure like (7.29). This can be done using the rules for the greater and lesser functions we have just proved. So:

$$\begin{aligned}
&C^R(t_1,t_2) = \theta(t_1-t_2)\,[C^>(t_1,\, t_2) - C^<(t_1,\, t_2)] = \\
&= \theta(t_1-t_2) \int_{-\infty}^{+\infty} dt\, \left\{\left[A^R\, B^> + A^>\, B^A\right] - \left[A^R\, B^< + A^<\, B^A\right]\right\} = \\
&= \theta(t_1-t_2)\Big[\int_{-\infty}^{t_1} dt\, (A^> - A^<)\, (B^> - B^<) + \\
&+ \int_{-\infty}^{t_2} dt\, (A^> - A^<)\, (B^< - B^>)\Big) = \\
&= \int_{t_2}^{t_1} dt\, A^R(t_1\, t)\, B^R(t,t_2) \qquad (7.34)
\end{aligned}$$

We will not prove all the analytic continuation rules of the Langreth theorem (their proofs are very similar to the previous one), we merely state them in the following table.

Contour	Real Axis
C=$\int_{\mathcal{K}_a} AB$	$C^< = \int [A^R B^< + A^< B^A]$ $C^R = \int A^R B^R$
D=$\int_{\mathcal{K}_a} ABC$	$D^< = \int A^R B^R C^< + A^R B^< C^A + A^< B^A C^A$ $D^R = \int A^R B^R C^R$
$C(\tau,\tau') = A(\tau,\tau')B(\tau,\tau')$	$C^<(t,t') = A^<(t,t')B^<(t,t')$ $C^R(t,t') = A^< B^R + A^R B^< + A^R B^R$
$D(\tau,\tau') = A(\tau,\tau')B(\tau',\tau)$	$D^<(t,t') = A^<(t,t')B^>(t',t)$ $D^R(t,t') = A^< B^A + A^R B^<$

Rules for greater Green function are equal to rules for the lesser one with all $<$'s replaced with $>$'s and vice versa.

7.3 Kinetic Equations

In this Section, we want to write the analogous of the Dyson equation for the two-points out-of-equilibrium Green's functions. Since the non-equilibrium theory is structurally equivalent to the equilibrium one, we know that for the contour ordered Green's function holds the same Dyson equation that holds for two- points equilibrium time ordered Green function, with contour integral in place of real axis integral, i.e.:

$$G(1,1') = G_0(1,1') + \int d^3x_2 \int d^3x_3 \int_{\mathcal{K}} d\tau_2 \int_{\mathcal{K}} d\tau_3 G_0(1,2)\,\Sigma(2,3)\,G(3,1'), \tag{7.35}$$

where G_0 is the free two-point Green function and Σ is the contour ordered self-energy.
In this section it is convenient to use a notation where the product of two terms is interpreted as a matrix product of the internal variables (space, time[2], spin, etc.) .
Applying Langreth theorem to Eq.(7.35), we can easily conclude that G^R and G^A obey Dyson equation with the appropriate self energy, and so:

$$G^{R,A} = G_0^{R,A} + G_0^{R,A}\,\Sigma^{R,A}\,G^{R,A} \tag{7.36}$$

The equation for $G^<$ is a bit more complicated.
Applying the analytic continuation rules to (7.35) we obtain:

$$G^< = G_0^< + G_0^R\,\Sigma^R\,G^< + G_0^R\,\Sigma^<\,G^A + G_0^<\,\Sigma^A\,G^A \tag{7.37}$$

Now we proceed by iteration on $G^<$. Iterating once we get:

$$\begin{aligned} G^< \;=& \big(1 + G_0^R\,\Sigma^R\big)\; G_0^<\; \big(1 + \Sigma^A G^A\big) + \\ &+ \big(G_0^R + G_0^R\,\Sigma^R\,G_0^R\big)\; \Sigma^<\,G^A + G_0^R\,\Sigma^R\,G_0^R\,\Sigma^R\,G^<, \end{aligned} \tag{7.38}$$

and so, the infinite order iterate is :

$$G^< = \big(1 + G^R\Sigma^R\big)\,G_0^<\,\big(1 + G^A\Sigma^A\big) + G^R\Sigma^<G^A \tag{7.39}$$

which is the celebrated *Keldysh equation*.
Applying the resolvent G_0^{-1} to equation (7.35), with respect to t_1 and $t_{1'}$, and summing the two resulting equations, we get the *Kadanov-Baym* equation, which is the integro-differential version of the *Keldysh equation*,

$$i\partial_T G^<(\tau,T) - [H_0, G^<] - [\mathrm{Re}\,\Sigma, G^<] - [\Sigma^<, \mathrm{Re}\,G] = \frac{1}{2}(\{\Sigma^>, G^<\} - \{G^>, \Sigma^<\}), \tag{7.40}$$

where $\mathrm{Re}\,\Sigma = \frac{1}{2}(\Sigma^R + \Sigma^A)$ and $\mathrm{Re}\,G = \frac{1}{2}(G^R + G^A)$ are the so-called renormalization terms.

[2]Time integrals are over the real axis.

Bibliography

[1] T. Kinoshita, T. Wenger and D. Weiss, A quantum Newton's cradle, Nature 440, 900 (2006).

[2] A. Polkovnikov, K. Sengupta, A. Silva, and M. Vengalattore, Nonequilibrium dynamics of closed interacting quantum systems, Rev. Mod. Phys. 83, 863883 (2011).

[3] M. Gring, M. Kuhnert, T. Langen, T. Kitagawa, B. Rauer, M. Schreitl, I. Mazets, D. A. Smith, E. Demler, J. Schmiedmayer, Relaxation and Pre-thermalization in an Isolated Quantum System, Science, Vol. 337 no. 6100 pp. 1318-1322 (2012).

[4] J. Berges, S. Borsanyi, C. Wetterich, Prethermalization, Phys.Rev.Lett. 93, 142002 (2004).

[5] M. Kollar, F. A. Wolf, M. Eckstein, Generalized Gibbs ensemble prediction of prethermalization plateaus and their relation to nonthermal steady states in integrable systems, Phys. Rev. B 84, 054304 (2011).

[6] J. Marino, A. Silva, Phys. Rev. B 86, 060408 (2012).

[7] J. Marino, A. Silva, arXiv:1309.7595 (submitted to Phys. Rev. B) (2013).

[8] M. Marcuzzi, J.Marino, A. Gambassi, A. Silva, arXiv:1307.3738 (submitted to Phys. Rev. Lett.) (2013).

[9] J. von Neumann, Proof of the Ergodic Theorem and the H-Theorem in Quantum Mechanics, Z. Phys. 57, 30 (1929).

[10] M. Fagotti, F. H. L. Essler, Reduced Density Matrix after a Quantum Quench, Phys. Rev. B 87, 245107 (2013).

[11] M. Rigol, V. Dunjko, V. Yurovsky, M. Olshanii, Relaxation in a Completely Integrable Many-Body Quantum System: An Ab Initio Study of the Dynamics of the Highly Excited States of Lattice Hard-Core Bosons, Phys. Rev. Lett. 98, 050405 (2007).

[12] E. T. Jaynes, Information Theory and Statistical Mechanics, Phys. Rev. 106, 620 (1957); Phys. Rev. 108, 171 (1957).

[13] I. Bloch, J. Dalibard, W. Zwerger, Many-body physics with ultracold gases, Rev. of Mod. Physics, Vol. 80 (2008).

[14] M. Greiner, O. Mandel, T. Esslinger, T. W. Hansch, and I. Bloch, Collapse and revival of the matter wave field of the Bose-Einstein condensate, Nature 415, 39 (2002).

[15] L. E. Sadler, J. M. Higbie, S. R. Leslie, M. Vengalattore, and D. M. Stamper-Kurn, Spontaneous symmetry breaking in a quenched ferromagnetic spinor Bose condensate, Nature 443, 312 (2006).

[16] C. Chin, R. Grimm, P. Julienne, E. Tiesinga, Feshbach Resonances in Ultracold Gases, Rev. of Mod. Physics, Vol. 80 (2008).

[17] D. Jaksch, C. Bruder, J.I. Cirac, C.W. Gardiner, P. Zoller, Cold bosonic atoms in optical lattices, Phys. Rev. Lett. 81, 3108 (1998).

[18] E. H. Lieb and W. Liniger, Phys. Rev. 130, 1605 (1963); E. H. Lieb, Phys. Rev. 130, 1616 (1963).

[19] M. Cheneau, P. Barmettler, D. Poletti, M. Endres, P. Schau, T. Fukuhara, C. Gross, I. Bloch, C. Kollath, S. Kuhr, Light-cone-like spreading of correlations in a quantum many-body system, Nature 481, 484487 (2012).

[20] E. Lieb, D. W. Robinson, The finite group velocity of quantum spin systems, Commun. Math. Phys. 28, 251257 (1972).

[21] P. Calabrese, J. Cardy, Time dependence of correlation functions following a quantum quench, Phys. Rev. Lett. 96, 136801 (2006).

[22] S. Trotzky, Y. Chen, A. Flesch, I. P. McCulloch, U. Schollwck, J. Eisert, I. Bloch, Nature Physics 8, 325 (2012).

[23] F. Meinert, M. J. Mark, E. Kirilov, K. Lauber, P. Weinmann, A. J. Daley, H. C. Ngerl, Quantum quench in an atomic one-dimensional Ising chain, Phys. Rev. Lett. 111, 053003 (2013).

[24] J. Simon, W. S. Bakr, R. Ma, M. E. Tai, P. M. Preiss, and M. Greiner, Quantum Simulation of Antiferromagnetic Spin Chains in an Optical Lattice, Nature 472, 307 (2011).

[25] S. Sachdev, K. Sengupta, and S. M. Girvin, Mott insulators in strong electric fields, Phys. Rev. B 66, 075128 (2002).

[26] M. Srednicki, Chaos and quantum thermalization. Phys. Rev. E 50, 888901 (1994).

[27] J. M. Deutsch, Quantum statistical mechanics in a closed system, Phys. Rev. A 43, 20462049 (1991).

[28] M. Rigol, V. Dunjko, and M. Olshanii, Thermalization and its mechanism for generic isolated quantum systems, Nature, Vol 452 (2008).

[29] C. Kollath, A. Laeuchli, E. Altman, Quench dynamics and non equilibrium phase diagram of the Bose-Hubbard model, Phys. Rev. Lett. 98, 180601 (2007).

[30] M. C. Bauls, J. I. Cirac, M. B. Hastings, Strong and weak thermalization of infinite non-integrable quantum systems, Phys. Rev. Lett. 106, 050405 (2011)

[31] E. Canovi, D. Rossini, R. Fazio, G. E. Santoro, A. Silva, Quantum Quenches, Thermalization and Many-Body Localization, Phys. Rev. B 83, 094431 (2011).

[32] M. Olshanii and V. Yurovsky, Memory of the Initial Conditions in an Incompletely-Chaotic Quantum System: Universal Predictions and an Application to Cold Atoms, Phys. Rev. Lett. 106, 025303 (2011).

[33] J. Caux and J. Mossel, Remarks on the notion of quantum integrability, JSTAT P02023 (2011).

[34] B. Sutherland, Beautiful models: 70 years of exactly solved quantum many-body problems (World Scientific, Pub Co Inc, 2004).

[35] A. Lamacraft, Diffractive scattering of three particles in one dimension: a simple result for weak violations of the Yang-Baxter equation, arXiv:1211.4110 (2012).

[36] G. Mussardo, Statistical Field Theory: An Introduction to Exactly Solved Models in Statistical Physics. (Oxford, 2010).

[37] P. Calabrese, F.H.L. Essler, and M. Fagotti, Phys. Rev. Lett. 106, 227203 (2011); P. Calabrese, F.H.L. Essler, and M. Fagotti, J. Stat. Mech. P07016 (2012); P. Calabrese, F.H.L. Essler, and M. Fagotti, J. Stat. Mech. P07022 (2012).

[38] M. Fagotti, F. H. L. Essler, Reduced Density Matrix after a Quantum Quench, Phys. Rev. B 87, 245107 (2013).

[39] D. Fioretto, G. Mussardo, Quantum Quenches in Integrable Field Theories, New J.Phys.12:055015, (2010).

[40] M. Cazalilla, The Luttinger model following a sudden interaction switch-on, Phys. Rev. Lett. 97, 156403 (2006).

[41] M. Fagotti, F. H. L. Essler, Stationary behaviour of observables after a quantum quench in the spin-1/2 Heisenberg XXZ chain, J. Stat. Mech. (2013) P07012.

[42] T. Barthel, U. Schollwock, Dephasing and steady state in a quantum many-particle system, , Phys. Rev. Lett. 100, 100601 (2008).

[43] D. M. Gangardt, M. Pustilnik, Correlations in an expanding gas of hard-core bosons, Phys. Rev. A 77, 041604(R) (2008).

[44] M. Fagotti, Finite-size corrections vs. relaxation after a sudden quench, Phys. Rev. B 87, 165106 (2013).

[45] M. Kormos, M. Collura, P. Calabrese, Analytic results for a quantum quench from free to hard-core one dimensional bosons, arXiv:1307.2142 (2013).

[46] D. Rossini, A. Silva, G. Mussardo, and G. Santoro, Phys. Rev. Lett. 102, 127204 (2009); D. Rossini, S. Suzuki, G. Mussardo, G. E. Santoro, and A. Silva, Phys. Rev. B 82, 144302 (2010).

[47] H. Rieger and F. Igloi, Phys. Rev. B. 84, 165117 (2011); F. Igloi and H. Rieger, Phys. Rev. Lett. 106, 035701 (2011); L. Foini, L. F. Cugliandolo, and A. Gambassi, J. Stat. Mech.: Th. Exp. P09011 (2012).

[48] S. Sachdev, *Quantum Phase Transitions* (Cambridge University Press, Cambridge, 1999).

[49] Ghoshal, S., and A. B. Zamolodchikov, Boundary S-Matrix and Boundary State in Two-Dimensional Integrable Quantum Field Theory, Int. J. Mod. Phys. A 9, 3841 (1994).

[50] M. Moeckel, S. Kehrein, Interaction Quench in the Hubbard model, Phys. Rev. Lett. 100, 175702 (2008).

[51] S. Kehrein, The Flow Equation Approach to Many- Particle Systems (Springer, Berlin, 2006).

[52] M. Stark, M. Kollar, Kinetic description of thermalization dynamics in weakly interacting quantum systems, arXiv:1308.1610 (2013).

[53] M. Eckstein, M. Kollar, P. Werner, Dynamical phase transition in correlated fermionic lattice systems, Phys. Rev. Lett. 103, 056403 (2009).

[54] J. Berges, *Far from equilibrium quantum fields in particle physics and cosmology*, Les Houches Summer School 2012 Lectures Notes.

[55] R. Barnett, A. Polkovnikov, M. Vengalattore, Prethermalization in quenched spinor condensates, Phys. Rev. A 84, 023606 (2011).

[56] A. Mitra, Correlation functions in the prethermalized regime after a quantum quench of a spin-chain, Phys. Rev. B 87, 205109 (2013).

[57] T. Giamarchi, Quantum Physics in One Dimension (Oxford University Press, 2004).

[58] M. Campisi, P. Hanggi and P. Talkner, Rev. Mod. Phys. **83** 771 (2011).

[59] A. Silva, Phys. Rev. Lett. 101, 120603 (2008); A. Gambassi, A. Silva, arXiv:1106.2671 (2011).

[60] P. Smacchia, A. Silva, arXiv:1305.2822 (2013).

[61] S. Sotiriadis, A. Gambassi, A. Silva, Phys. Rev. E 87, 052129 (2013).

[62] H. Haug and A.-P. Jauho, Quantum Kinetics in Transport and Optics of Semiconductors (Springer, Berlin, 1996).

[63] E. H. Lieb and D. W. Robinson, Commun. Math. Phys., 28, 251 (1972).

[64] P. Calabrese, J. Cardy, Phys.Rev.Lett. 96, 136801 (2006); P. Calabrese, J. Cardy, J.Stat.Mech.0706:P06008 (2007); L. Mathey, A. Polkovnikov, Phys. Rev. A 81, 033605 (2010).

[65] M. Cheneau, P. Barmettler, D. Poletti, M. Endres, P. Schauss, T. Fukuhara, C. Gross, I. Bloch, C. Kollath, S. Kuhr, Nature 481, 484487 (2012).

[66] T. Langen, R. Geiger, M. Kuhnert, B. Rauer, J. Schmiedmayer, Local emergence of thermal correlations in an isolated quantum many-body system, arXiv:1305.3708 (2013).

[67] E. Barouch and B. McCoy, Phys. Rev. A 3, 786 (1971).

[68] M. E. Fisher, R. E. Hartwig, Adv. Chem. Phys. 15 (1968) 333.

[69] P. J. Forrester, N. E. Frankel, arXiv:math-ph/0401011 (2004).

[70] T. Holstein and H. Primakoff, Phys. Rev. **58**, 1098 (1940).

[71] S. Sotiriadis and J. Cardy, Phys. Rev. B **81**, 134305 (2010).

[72] M. Marcuzzi, J. Marino, A. Gambassi, and A. Silva, in preparation (2013).

[73] J. Williamson, On the algebraic problem concerning the normal forms of linear dynamical systems. Am. J. Math. 58, 141-163 (1936). Zbl. 13, 284.

[74] J. Maciejko, An Introduction to Nonequilibrium Many-Body Theory (2007).

[75] M. Tavora, A. Mitra, Quench dynamics of one-dimensional bosons in a commensurate periodic potential: A quantum kinetic equation approach, arXiv:1306.6121 (2013).

[76] F. H. L. Essler, S. Evangelisti, M. Fagotti, Dynamical Correlations after a Quantum Quench, Phys. Rev. Lett. 109, 247206 (2012).

[77] P. Mehta, A. Polkovnikov, Efficiency bounds for nonequilibrium heat engines, Annals Phys. 332, 110-126 (2013).